# Theoretical Evaluation of Electron Delocalization in Aromatic Molecules by Means of Atoms in Molecules (AIM) and Electron Localization Function (ELF) Topological Approaches

Jordi Poater,[‡] Miquel Duran,[‡] Miquel Solà,*[,‡] and Bernard Silvi*[,§]

*Institut de Química Computacional and Departament de Química, Universitat de Girona, 17071 Girona, Catalonia, Spain, and Laboratoire de Chimie Théorique, Université Pierre et Marie Curie, UMR-CNRS 7616, 4 place Jussieu, 75252 Paris Cedex 05, France*

*Received December 28, 2004*

## *Contents*



* Authors to whom correspondence should be addressed (telephone +34-972-418912; fax +34-972-418356; e-mail miquel.sola@udg.es or silvi@lct.jussieu.fr).
‡ Universitat de Girona.
§ Université Pierre et Marie Curie.

## *1. Introduction*

Benzene is the emblematic example of an aromatic molecule, and the problem of its structure has given rise to a chemical serial story running over several decades. The epistemological digest of this story written by Stephen G. Brush[1,2] shows how this problem has been at the root of important concepts such as those of mesomery and resonance. Before the advent of quantum mechanics, chemists had thought of the benzene structures in terms of two center bonds attempting to preserve the valence of the carbon atom and to explain its chemical properties. Kekulé's theory of the structure of the benzene molecule[3] invokes the oscillatory hypothesis in which "the fourth valence of each carbon oscillates between its neighbors, synchronously with all the other fourth valences, so that the structure switches rapidly between the two structures",[1] whereas Claus proposed a diagonal hypothesis[4] in which the fourth valence of each carbon is directed toward the carbon in the para position. The latter hypothesis has been rejected because it enables only two derivatives, and it has been revised to remove this inconsistency: instead of forming a bond, the fourth valence stops near the center of the ring in the Armstrong−Baeyer formula,[5] or there is only one bridging bond as in the Dewar's bridged benzene formula.[6] In Thiele's partial valence model,[7] the adjacent carbon−carbon bonds are considered as intermediate between single and double bonds. These formulas were later considered by K. C. Ingold to set up his intra-annular tautomerism,[8] which appears to be the generalization of Kekulé's oscillatory hypothesis. Ingold's tautomerism hypothesis was later called mesomerism.[9] The mesomery is an important concept in chemistry, which implicitly introduces the electron delocalization in the context of the prequantum electronic theory. The first applications of quantum chemistry to the benzene problem led on the molecular orbital (MO) side Erich Hückel to propose his famous $4n + 2$ rule[10] and on the valence bond (VB) side Pauling and Wheland to identify resonance with Ingold's mesomerism.[11,12] An enlighting contribution of modern VB theory on the benzene structure has been brought by Shaik et al.,[13] who have shown that the hexagonal symmetry of benzene is due to the $\sigma$-system because the $\pi$ component is distortive along a Kekulean distortion.

10.1021/cr030085x CCC: $53.50 
Published on Web 07/13/2005

Jordi Poater was born in Banyoles, Catalonia, Spain, in 1977. He received his bachelor's degree in chemistry in 1999 at the University of Girona. At the same university, in 2003 he obtained his Ph.D. in computational and theoretical chemistry, under the supervision of Profs. Miquel Solà and Miquel Duran. His thesis was based on the application of the delocalization index (DI), derived from the bielectronic density, to the analysis of and applications in molecular structure, chemical reactivity, and aromaticity. In particular, his most relevant works are based on the introduction of a new aromaticity criterion based on electron delocalization (PDI). At this time he is carrying out postdoctoral research with the group of Dr. F. Matthias Bickelhaupt (Vrije Universiteit Amsterdam, The Netherlands), in the quantum biological field.

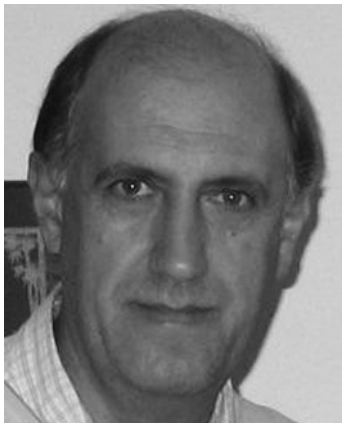

Miquel Duran was born in Catalonia, Spain, in 1957 and was educated at the Universitat Autònoma de Barcelona (UAB), where he received his Ph.D. in 1984. After pursuing postdoctoral work with Prof. H. F. Schaefer at the University of California, Berkeley, he became first assistant professor at UAB and later in 1992 full professor at the University of Girona. His primary research interests lie in the development of methodology for the study of nonlinear optical effects, intermolecular interactions, and molecular electron density.

Miquel Solà was born in Fonteta, Catalonia, Spain, in 1964. He received his diploma of chemistry at the University Autonomous of Barcelona in 1986 and his Ph.D. from the same university in 1991, both with academic honors. His doctoral research on the carbonic anhydrase enzymatic catalysis under the direction of Joan Bertran and Agustí Lledós was awarded the Catalan Saint Albert Prize. After several months as a consultant with a private company, in 1993 he moved to the University of Girona (UdG) as assistant researcher. In 1994 he did postdoctoral research in Amsterdam with Evert Jan Baerends and in 1995 in Calgary with Tom Ziegler. He was appointed assistant professor at UdG in 1997. In 2001, he was awarded the Distinguished University Research Promotion of the Generalitat de Catalunya. Since 2003, he has held a permanent position as full professor with UdG. He has published about 120 papers on theoretical studies of organic and organometallic reaction mechanisms, the use of quantum molecular similarity measures, the development of conceptual density functional theory, and the analysis of electron delocalization and aromaticity.

Bernard Silvi (1946) is full professor at the University Pierre et Marie Curie in Paris. He is the director of the Laboratoire de Chimie Théorique (UMR7616), a joint University–CNRS research group involved in both methodological and applied quantum chemistry. He is author or coauthor of about 150 publications in scientific journals. His research activity has been successively devoted to vibrational spectroscopy, intermolecular interactions, modeling of minerals, and silicated materials and in the past 10 years to the topological approaches of chemical bonding.

The concepts of electron localization and delocalization emerging from the analysis of the electronic structure of benzene are relevant not only for understanding the molecular structure in aromatic molecules[14] but also for general modern chemistry. Thus, delocalization of $\pi$-electrons has been long invoked to rationalize the molecular structure, stability, magnetic properties, and chemical reactivity of $\pi$-conjugated molecules. Electron localization is also essential for descriptive chemistry because in this field one needs to know where local groups of electrons such as core or valence electrons, electron pairs, bonding pairs, unpaired electrons, or $\pi$-electron subsystems are placed. In particular, appropriate auxiliary tools allowing electron pair localization[15,16] have been long pursued in quantum chemistry to explain the nature of the chemical bond[17−19] and with the aim of establishing a link between the rigorous but abstract wave function and the classical chemical concepts based on the Lewis theory[20,21] and the valence shell electron pair repulsion (VSEPR) model of molecular geometry.[22,23] Electronic localization/delocalization plays also a key role in the analysis of electronic fluctuation and electron correlation effects[16,24−27] and, therefore, this concept is relevant in the development of new density functionals.[28−30] A simple search on the Science Citation Index of the ISI Web of Knowlegde[31] gives about 2500 entries for

the use of the "electron* localization" or "electron* delocalization" expressions in titles, keywords, or abstracts of articles from 1990 to 2004, showing the relevance of this topic in current chemistry.

Due to the intrinsic wave nature of electrons and their indistinguishability, it is not possible to follow precisely the movements of electrons. However, recent advances in laser technology have opened entirely new possibilities for studying and controlling the dynamics of electronic processes in atoms and molecules.[32] Application of ultrashort attosecond or intense femtosecond laser pulses results in localized electron wave packets, the motion of which can be experimentally detected, thus leading to measurement of the electron motion in molecules on the attosecond time scale.

Although these pioneering attochemistry experiments allow the dynamics of electrons to be followed, the wave picture of the electron implies an always present delocalization. This electronic delocalization is not observable, and therefore there is no experimental property that allows its direct measurement. However, electronic delocalization reveals itself in several chemical phenomena that can be experimentally interrogated to have a measure of the degree of electron delocalization in our system.[33] Probably, the most widely used methodologies to analyze electronic delocalization are those based on the magnetic properties of molecules. Thus, the exaltation and the anisotropy of magnetic susceptibility[34] and the NMR chemical shifts[35] of the protons or other atoms such as $^3$He,[36−38] which are used as a probe for the magnetic shielding in a given point of space, are common magnetic properties used for the evaluation of electron delocalization in aromatic and $\pi$-conjugated molecules. Other experimental properties such as magnetic coupling constants,[39] NMR spin−spin coupling constants, or the Fermi contact terms[40−42] also depend on the extent of molecular electron delocalization, whereas high-energy UV spectra and large symmetry in infrared or Raman spectra have been found in some cases to be indicative of extensive electronic delocalization.[43] From an energetic point of view, delocalization of $\pi$-electrons in conjugated $\pi$-systems has been frequently associated with more electronically stable systems.[44,45] Finally, bond length equalization between single and double bonds in $\pi$-conjugated molecules is also usually connected to electron delocalization.[46−48]

As far as the theoretical definition of electron localization/delocalization is concerned, the fact that it is not observable implies that there is not a unique and generally accepted measure of this property. Several attempts to put this concept on a theoretically sound quantum mechanical basis have been developed. Some authors have made use of the VB theory to describe electron localization/delocalization by analyzing the weights of the most relevant resonance structures.[49] Within the framework of the MO theory, techniques for the localization of MOs have been used to determine the regions of molecular space where electron pairs are located. The localized orbitals are nothing but a unitary transformation of the MOs that leaves the electron density and the total energy unchanged. Two principal criteria have been used to compute localized MOs from the delocalized canonical molecular orbital wave functions, energetic "decoupling"[50] and direct spatial separation.[51] One obvious limit of these techniques is that localization of electron pairs is not perfect, and large fractions of localized MOs occupy common regions of molecular space.[52] Nowadays, the preferred technique for MO localization is probably the natural bond orbital (NBO) method developed by Weinhold and co-workers,[53] which has a somewhat different philosophy from the previous described methods. This approach is based not on a unitary transformation of the occupied MOs but on a mixing of the occupied and virtual spaces that localize bonds and lone pairs as basic units of the molecular structure. The NBO analysis offers a way to quantify delocalization energies from second-order orbital interaction energies.[54] In addition, several measures of delocalization based on the NBO procedure have been devised for the study of delocalization and aromaticity in heteroaromatic compounds.[55] Despite being a powerful technique for studying hybridization and molecular bonding, this methodology has the drawback that the NBO determinantal wave function containing the NBOs with the highest occupation number gives a significantly lower energy than the wave function constructed from the original MOs.[56]

Finally, there is a group of theoretical methods that analyze density functions which are extracted in the majority of cases from a MO wave function, although they could also, in principle, be applied to densities obtained from VB wave functions. The loge theory by Daudel and collaborators[15,17,57] is historically the first method that localizes electrons in certain regions of the atomic and molecular space using density functions. A loge is defined as a part of the space in which there is a high probability to find a given number of electrons with a selected organization of their spins. The molecular space is divided into loges, the best loges being those that represent the most probable division of the space of a system into localized groups of electrons. The decomposition of space in loges gives a rigorous mathematical definition of regions corresponding to core, valence, bonding, or lone pair electrons. In this sense, it must be noted that, very recently, Savin and co-workers have derived efficient formulas for computing the probability of finding a certain number of electrons in a given volume.[58] It is also worth mentioning the work by Ziesche,[26,59] Fulde,[60] and Dolg,[61,62] who, with their collaborators, have analyzed for small molecules the probability distribution function for finding $N$ particles in a given region of space and simultaneously the rest of the particles in the complementary space. The Laplacian of the one-electron density $[\nabla^2\rho(\mathbf{r})]$ is another electron density-based function that has been used to denote electronic localization. It has been demonstrated that electronic charge is locally concentrated within a molecular system in regions where $\nabla^2\rho(\mathbf{r}) < 0$. Indeed, local maxima of the negative of this quantity $[-\nabla^2\rho(\mathbf{r})]$ denote spatial domains where local electron pairing takes place, providing a physical link with the Lewis and VSEPR models.[63−70] In

addition, some authors have used the ellipticity profile along the bond path to discuss delocalization from the one-electron density.[71,72] The ellipticity ($\epsilon$) is a measure of the cylindricity of the charge distribution, and it is calculated as $\epsilon = (\lambda_1/\lambda_2) - 1$ (with $\lambda_1 < \lambda_2 < 0$), $\lambda_i$ being the eigenvalues of the corresponding eigenvectors of the Hessian matrix of $\rho(\mathbf{r})$ at the bond critical point (BCP) perpendicular to the bond path. Values of $\epsilon > 0$ usually indicate partial $\pi$-character in a bond.[72]

However, because the electron pair formation[73] depends on the probability of finding two electrons simultaneously at two positions close in space, most methods used to determine electronic localization/delocalization are based on the two-electron density or pair density,[74−76] which is the simplest quantity that describes the pair behavior, and related functions such as the exchange correlation density, the Fermi hole, or the conditional pair probability.[27,29,30,70,77−80] One of these functions is the Fermi hole density, which is a distribution function for an electron of given spin that determines, compared with an uncorrelated pair density, the decrease in the probability of finding another electron with the same spin relative to the fixed position of the electron of reference. Bader and Stephens[16,24] showed that the extent of localization or delocalization of an electron of reference is determined by the corresponding localization of its Fermi hole.[73] Accordingly, Fermi hole density maps have been employed to discuss electronic delocalization.[27,30,81,82] Moreover, on the basis of the fact that localization of the Fermi hole density results in a minimization of the pair fluctuation,[16,24] Julg and Julg[83] and Ponec and Carbó-Dorca[84,85] proposed to identify chemical bonds with the regions of minimum fluctuation of the electron pair. Other related quantities are the localization and delocalization indices defined by Bader and coworkers[16,21,86] within the framework of the atoms in molecules (AIM) theory.[64−67,87] These indices are obtained by the double integration of the exchange correlation density (the Fermi hole density weighted by the density of the reference electron)[74,75] over the atomic basins defined in the AIM theory. Single instead of double integration of the exchange correlation density in a given domain gives rise to the domain-averaged Fermi holes, also called atomic hole density functions,[88] which have been used by Ponec and others to locate electron pairs, visualize the chemical bond, and analyze its nature.[18,19,89−93] Finally, some authors have employed the conditional pair probability to locate electron pairs. Thus, within the AIM theory, Bader et al.[80,94] have proposed to analyze the topology of the conditional pair probability for same-spin electrons to discuss localization. The authors named this function the Lennard-Jones function after the scientist who carried out seminal work in this field.[95] In addition, Becke and Edgecombe made use of the leading term in the Taylor series expansion of the spherically averaged same-spin conditional pair probability to introduce another frequently used measure of localization, the so-called electron localization function (ELF).[96,97] As shown by Savin et al.,[98] ELF measures the excess of kinetic energy density due to the Pauli repulsion. In the region of space where the Pauli repulsion is strong (single electron or opposite spin-pair behavior) ELF is close to 1, whereas where the probability of finding the same-spin electrons close together is high, ELF tends to 0. Regions in which the value of ELF is close to 1 correspond to well-localized electrons and may be identified with atomic shells, chemical bonds, and lone electron pairs. More recently, Silvi,[99] Kohout,[100] and Scemama, Chaquin, and Caffarel[101] have proposed other measures of electron localizability that bear some similarities with ELF.

As seen above, most localization methods that use density functions and related quantities to analyze electronic localization require the division of space into regions (usually atomic domains) the boundaries of which are found following different criteria. Examples are the Wigner−Seitz cells,[77,102] the muffin-tin spheres,[103] the Voronoi cells,[104,105] the loges of Daudel and co-workers,[17,57] the atomic basins of Bader,[64−66] the basins derived from a topological analysis of the electrostatic potential,[106] and the basins of ELF.[98,107] Electronic population is calculated within these regions, and the fluctuation of electronic charge from one region to another can also be discussed. A satisfying property of these methodologies is that the results are unaffected by a unitary transformation of the MO set.

The aim of the present review is to illustrate with some representative examples the scope of electron localization/delocalization methods for the description of chemical structure, molecular bonding, and reactivity, with strong emphasis on their use for the quantitative analysis of aromaticity. Coverage is extensive, but not exhaustive. It is not our intention to review all of the theoretical work done in the area of electronic localization/delocalization, for which a bulky literature exists. Rather, we confine our considerations to developments and applications based on the AIM theory and the ELF function, which are probably those that have been most widely employed in the literature to discuss electron localization/delocalization and aromaticity.

The format of our presentation is divided into two major topical sections: section 2 covers the definitions of electron localization/delocalization and their applications to describe molecular structure and reactivity, and section 3 comments on the application of delocalization measures to the analysis of aromatic compounds. We have further split each section into several parts. Thus, section 2 starts with the general aspects (2.1) and then continues with the applications that are based on the AIM theory (2.2) and, finally, those that use the ELF function (2.3). Section 3 covers the applications of electron delocalization to the study of aromaticity within the AIM theory (3.1) and using the ELF function (3.2). Finally, in section 4 the most outstanding findings are briefly summarized.

Throughout, it will be evident to the reader that electron localization techniques have become a powerful, must-have tool for penetrating the complexities of molecular bonding and aromaticity. Most applications discussed in this review have been carried out

in the past five years, so this is a very active area in quantum chemistry that will certainly show dramatic advances in the coming years. It is our wish that this review will help to define more clearly the present situation of this field and become a source of inspiration for designing novel procedures and applications soon.

## 2. Electron Delocalization

As commented in the previous section, this paper reviews the most important contributions to the study of electron localization/delocalization carried out using the AIM theory and the ELF function. In the first part of the present section, we provide a summary of the general aspects and main definitions common to both approaches. In the second and third parts, we discuss the most relevant applications of the AIM and ELF electron localization/delocalization analyses to the study of the electronic structure and chemical bond.

### 2.1. General Aspects

In this section, the main similarities and differences between the ELF and AIM approaches to treat the problem of electron delocalization are examined. First, we discuss how the molecular space is partitioned in these two methodologies; second, the analysis of variances and covariances common to both methods is commented; and, finally, the spin pair composition of the AIM and ELF techniques is analyzed.

#### 2.1.1. Partition of Molecular Space

The partition of the molecular space into subsystems (basins) of attractors allows the calculation of several properties by integration over these basins. The two methodologies more commonly used in recent years to partition the molecular space are the AIM theory[64,65] and the ELF function,[96] although other partitions, such as the Mulliken-like partitioning[108] in the Hilbert space spanned by the basis functions, are also possible. In the AIM and ELF approaches, basins are defined in terms of the vector field of the gradient of the function involved. Thus, in the AIM theory, the basins are defined as a region in the Euclidean space bounded by a zero-flux surface in the gradient vectors of the one-electron density, $\rho(\mathbf{r})$, or by infinity. In this way, a molecule is split into its constituent atoms (atomic basins) using only the one-electron density distribution. Such a division of the topological space is exhaustive, so that many properties, for example, energy and electron populations, can be written as the sum of atomic contributions. A different partition of the space is performed using ELF,[96] a local scalar function denoted $\eta(\mathbf{r})$. As ELF is a scalar function, the analysis of its gradient field can be carried out to locate its attractors (local maxima) and the corresponding basins. For an $N$-electron single determinantal closed-shell wave function built from Hartree−Fock (HF) or Kohn−Sham (KS) orbitals, $\phi_j$, the ELF function is given by[109]

$$\eta(\vec{r}) = \frac{1}{1 + \left[\frac{D(\vec{r})}{D_h(\vec{r})}\right]^2} \tag{1}$$

where

$$D(\vec{r}) = \frac{1}{2}\sum_{j=1}^{N}|\nabla\phi_j(\vec{r})|^2 - \frac{1}{8}\frac{|\nabla\rho(\vec{r})|^2}{\rho(\vec{r})} \tag{2}$$

$$D_h(\vec{r}) = \frac{3}{10}(3\pi^2)^{2/3}\rho(\vec{r})^{5/3} \tag{3}$$

$$\rho(\vec{r}) = \sum_{j=1}^{N}|\phi_j(\vec{r})|^2 \tag{4}$$

and $N$ is the number of electrons.

The gradient vector field of ELF, $\nabla\eta(\vec{r})$, enables one to divide the Euclidian space in basins of attractors where electron pairs are located. These basins are either core basins surrounding a nucleus or valence basins that do not include a nucleus (except for protonated valence basins that include a proton). The number of connections of a given valence basin with core basins is called the synaptic order. A disynaptic valence basin corresponds to a two-center bond, whereas a monosynaptic one characterizes a lone pair. Multicenter bonds, such as three-center two-electron (3c−2e) bonds, are accounted for by polysynaptic basins.[110]

Basin-related properties are calculated by integrating a certain property over the volume of the basins. For instance, for a basin labeled $\Omega_A$, one can define its average population and pair populations by integrating the electron density and the pair densities as

$$\bar{N}(\Omega_A) = \int_{\Omega_A}\rho(\vec{r})\,d\vec{r}$$

$$\bar{N}^{\alpha\alpha}(\Omega_A) = \int\int_{\Omega_A}\Gamma^{\alpha\alpha}(\vec{r}_1,\vec{r}_2)\,d\vec{r}_1\,d\vec{r}_2$$

$$\bar{N}^{\beta\beta}(\Omega_A) = \int\int_{\Omega_A}\Gamma^{\beta\beta}(\vec{r}_1,\vec{r}_2)\,d\vec{r}_1\,d\vec{r}_2$$

$$\bar{N}^{\alpha\beta}(\Omega_A) = \int\int_{\Omega_A}\Gamma^{\alpha\beta}(\vec{r}_1,\vec{r}_2)\,d\vec{r}_1\,d\vec{r}_2 \tag{5}$$

where the subscript A on $\Omega$ indicates that the integration has to be carried out only through the space corresponding to the atomic basin of atom A and $\Gamma^{\alpha\alpha}(\vec{r}_1,\vec{r}_2)$, $\Gamma^{\beta\beta}(\vec{r}_1,\vec{r}_2)$, and $\Gamma^{\alpha\beta}(\vec{r}_1,\vec{r}_2)$ are the same-spin and opposite-spin components of the pair density.[75] Summation of all the atomic populations in a molecule yields the total number of electrons, $N$.

#### 2.1.2. Multivariate Analysis of Electron Densities

The multivariate analysis is a basic statistical method enabling one to reveal the correlations between different groups of data. It relies upon the construction of the covariance matrix elements defined by

$$\langle\mathrm{cov}(A,B)\rangle = \langle AB\rangle - \langle A\rangle\langle B\rangle \tag{6}$$

where $\langle A\rangle$, $\langle B\rangle$, and $\langle AB\rangle$ are the averages of the data

values and of their product. The diagonal elements of the covariance matrix are the variances

$$\sigma^2(A) = \langle A^2 \rangle - \langle A \rangle^2 \quad (7)$$

which measure the dispersion of the data among the group. The square root of the variance is the standard deviation. Finally, the correlation coefficients are the ratios of the covariance matrix elements by the corresponding standard deviation, that is, $[\mathrm{cov}(A,B)]/[\sigma(A)\sigma(B)]$. Positive and negative values of the correlation coefficients indicate that the $A$ and $B$ data are respectively correlated (they vary in the same direction) or anticorrelated (opposite direction), whereas a value close to 0 corresponds to independent behaviors. Applied to electrons distributed among a collection of adjacent regions spanning the geometrical space occupied by a molecule, the multivariate analysis provides a convenient tool to study electron delocalization. Consider such a partition in $M$ basins for an $N$ electron system. The number of electrons within each region is a quantum mechanical observable to which corresponds the population operator introduced by Diner and Claverie:[111]

$$\hat{N}(\Omega_A) = \sum_i^N \hat{y}(\vec{r}_i) \quad \text{with} \quad \hat{y}(\vec{r}_i) \begin{cases} \hat{y}(\vec{r}_i) = 1 \ \vec{r}_i \in \Omega_A \\ \hat{y}(\vec{r}_i) = 0 \ \vec{r}_i \notin \Omega_A \end{cases} \quad (8)$$

In an $N$-electron system the population operators obey the closure relation[112]

$$\sum_A \hat{N}(\Omega_A) = N \quad (9)$$

The eigenvalues of the population operators, the electron numbers $N(\Omega_A)$, are integers in the range 0, ..., $N$. As they also obey the closure relationship, the electron count in a region is not independent of those in the other regions and, therefore, these eigenvalues must be determined simultaneously. A set of eigenvalues represents an electronic structure of the partition scheme. The expectation values of the population operators

$$\bar{N}(\Omega_A) = \langle \hat{N}(\Omega_A) \rangle = \int_{\Omega_A} \rho(\vec{r}) \, d\vec{r} = \bar{N}^{\alpha}(\Omega_A) + \bar{N}^{\beta}(\Omega_A) \quad (10)$$

are real numbers and can be understood as the average of the measurements of the electron numbers $N(\Omega_A)$, and therefore they can be interpreted as arising from weighted electronic structures. Moreover, they can be written in terms of spin contributions. The closure relationship of the basin population operators enables one to carry out the multivariate statistical analysis of the basin populations through the definition of the covariance operator.[112] The expectation values of this operator

$$\langle \mathrm{cov}(\Omega_A,\Omega_B) \rangle = \int_{\Omega_A} \int_{\Omega_B} \Gamma(\vec{r}_1,\vec{r}_2) \, d\vec{r}_1 \, d\vec{r}_2 - \bar{N}(\Omega_A)\bar{N}(\Omega_B) \quad (11)$$

where $\Gamma(\vec{r}_1,\vec{r}_2)$ denotes the spinless pair density,[75] provide pieces of information about electron delocalization. In particular, the diagonal elements, the variances

$$\sigma^2(\Omega_A) = \int_{\Omega_A} \int_{\Omega_A} \Gamma(\vec{r}_1,\vec{r}_2) \, d\vec{r}_1 \, d\vec{r}_2 - [\bar{N}(\Omega_A)]^2 + \bar{N}(\Omega_A) \quad (12)$$

are a measure of the quantum mechanical uncertainty of the basin's population, namely, the degree of *fluctuation of the electron pair* (i.e., the square of the standard deviation), which can be interpreted as the dispersion of the electronic structures. According to the partition scheme, the multivariate analysis enables one to build a phenomenological classical model of the charge distribution of a molecule in terms of the superposition of weighted promolecular densities (AIM partition) or mesomeric structure (ELF partition).

The function $\Gamma(\vec{r}_1,\vec{r}_2)$ appearing in eqs 11 and 12 is the spinless second-order density or pair density.[75] This function can be interpreted as the probability density of two electrons being simultaneously at positions $\vec{r}_1$ and $\vec{r}_2$. It can be split into an uncorrelated pair density part and a part that gathers all exchange and correlation effects:

$$\Gamma(\vec{r}_1,\vec{r}_2) = \rho(\vec{r}_1)\rho(\vec{r}_2) + \Gamma_{XC}(\vec{r}_1,\vec{r}_2) \quad (13)$$

The uncorrelated component of the pair density, given by the product $\rho(\vec{r}_1)\rho(\vec{r}_2)$, provides the probability of finding simultaneously two *independent* electrons at positions $\vec{r}_1$ and $\vec{r}_2$. The difference between $\Gamma(\vec{r}_1,\vec{r}_2)$ and $\rho(\vec{r}_1)\rho(\vec{r}_2)$ is the exchange correlation density,[74,75] $\Gamma_{XC}(\vec{r}_1,\vec{r}_2)$, which is a measure of the degree to which density is excluded at $\vec{r}_2$ because of the presence of an electron at $\vec{r}_1$. Therefore, $\Gamma_{XC}(\vec{r}_1,\vec{r}_2)$ contains all necessary information for the study of electron correlation and electron pair formation.

Equation 12 can be written in terms of the exchange correlation density, $\Gamma_{XC}(\vec{r}_1,\vec{r}_2)$, as

$$\sigma^2(\Omega_A) = \int_{\Omega_A} \int_{\Omega_A} \Gamma_{XC}(\vec{r}_1,\vec{r}_2) \, d\vec{r}_1 \, d\vec{r}_2 + \bar{N}(\Omega_A) = \bar{N}(\Omega_A) - \lambda(\Omega_A) \quad (14)$$

where $\lambda(\Omega_A)$ is the so-called localization index (LI), so that, as the variance $\sigma^2(\Omega_A)$ is a measure of total electron delocalization of the basin $\Omega_A$,[113] $\lambda(\Omega_A)$ gives the number of electrons localized in basin $\Omega_A$. Besides, the relative fluctuation parameter introduced by Bader[16,24] indicates the electron charge fluctuations for a given basin $\Omega_A$ relative to its total electron population

$$\lambda_F(\Omega_A) = \frac{\sigma^2(\Omega_A)}{\bar{N}(\Omega_A)} \quad (15)$$

which is positive and expected to be $<1$ in most cases. It is important noticing the difference between this quantity and the LI in eq 14. Whereas $\lambda_F(\Omega_A)$ is a fluctuation parameter that stands for the ratio of electrons delocalized, the latter is a measure of the number of electrons localized into the basin $\Omega_A$. It is always less than the corresponding atomic popula-

tion, $N(\Omega_A)$, except for totally isolated atoms, where there is no exchange or correlation with electrons in other atoms.

The variance, $\sigma^2(\Omega_A)$, can also be spread in terms of contribution from other basins, the covariance, $\mathrm{cov}(\Omega_A,\Omega_B)$, which has a clear relationship with the so-called delocalization index (DI), $\delta(\Omega_A,\Omega_B)$:

$$\mathrm{cov}(\Omega_A,\Omega_B) = \langle N(\Omega_A)\cdot N(\Omega_B)\rangle - \langle N(\Omega_A)\rangle\langle N(\Omega_B)\rangle = \int_{\Omega_A}\int_{\Omega_B} (\Gamma(\vec{r}_1,\vec{r}_2) - \rho(\vec{r}_1)\rho(\vec{r}_2))\, d\vec{r}_1\, d\vec{r}_2 = \int_{\Omega_A}\int_{\Omega_B} \Gamma_{XC}(\vec{r}_1,\vec{r}_2)\, d\vec{r}_1\, d\vec{r}_2 = -\frac{\delta(\Omega_A,\Omega_B)}{2} \quad (16)$$

The DI, $\delta(\Omega_A,\Omega_B)$, accounts for the electrons delocalized or shared between basins $\Omega_A$ and $\Omega_B$.[21,86] As the total variance in a certain basin can be written in terms of covariance, we have

$$\sigma^2(\Omega_A) = -\sum_{B\neq A} \mathrm{cov}(\Omega_A,\Omega_B) = \sum_{B\neq A} \frac{\delta(\Omega_A,\Omega_B)}{2} \quad (17)$$

From the quantity above one can do the usual contribution analysis (CA), given usually as a percentage:

$$\mathrm{CA}(\Omega_A|\Omega_B) = \frac{\mathrm{cov}(\Omega_A,\Omega_B)}{\sum_{A\neq B}\mathrm{cov}(\Omega_A,\Omega_B)} \times 100 = -\frac{\mathrm{cov}(\Omega_A,\Omega_B)}{\sigma^2(\Omega_B)} \times 100 \quad (18)$$

The CA gives us the main contribution arising from other basins to the variance, that is, the delocalized electrons of basin $\Omega_B$ on basin $\Omega_A$, providing a measure of electron pair sharing between two regions of the molecular space.

According to eqs 14 and 16, the LI and DI can be written as

$$\lambda(\Omega_A) = -\int_{\Omega_A}\int_{\Omega_A} \Gamma_{XC}(\vec{r}_1,\vec{r}_2)\, d\vec{r}_1\, d\vec{r}_2 \quad (19)$$

$$\delta(\Omega_A,\Omega_B) = -\int_{\Omega_A}\int_{\Omega_B} \Gamma_{XC}(\vec{r}_1,\vec{r}_2)\, d\vec{r}_1\, d\vec{r}_2 - \int_{\Omega_B}\int_{\Omega_A} \Gamma_{XC}(\vec{r}_1,\vec{r}_2)\, d\vec{r}_1\, d\vec{r}_2 = -2\int_{\Omega_A}\int_{\Omega_B} \Gamma_{XC}(\vec{r}_1,\vec{r}_2)\, d\vec{r}_1\, d\vec{r}_2 \quad (20)$$

These equations are completely general and can be used at any level of theory, provided that the first and pair density functions are known. In particular, most of the current theoretical ab initio methods expand the molecular wave function in terms of MOs. Then, for a closed-shell molecule, $\lambda(A)$ and $\delta(A,B)$ can be expressed as

$$\lambda(\Omega_A) = -\sum_{i,j,k,l} D_{ijkl} S_{ij}(\Omega_A) S_{kl}(\Omega_A) + N(\Omega_A)^2 \quad (21)$$

$$\delta(\Omega_A,\Omega_B) = -2\sum_{i,j,k,l} D_{ijkl} S_{ij}(\Omega_A) S_{kl}(\Omega_B) + 2N(\Omega_A)N(\Omega_B) \quad (22)$$

respectively, where $\{D_{ijkl}\}$ are density matrix elements for the pair density matrix in MO base and $\{S_{ij}(\Omega_A)\}$ are overlaps between MOs, integrated within the basin of atom A.[21,86] [We consider here that the pair density is given by $\sum_{i,j,k,l} D_{ijkl}\phi_i^*(\vec{r}_1)\phi_j(\vec{r}_1)\phi_k^*(\vec{r}_2)\phi_l(\vec{r}_2)$.] The four-index summations in eqs 21 and 22 run over all the occupied MOs in the molecule. These equations can also be expressed in terms of basis functions.

$$\lambda(\Omega_A) = -\sum_{\mu,\nu,\lambda,\sigma} D_{\mu\nu\lambda\sigma} S_{\mu\nu}(\Omega_A) S_{\lambda\sigma}(\Omega_A) + N(\Omega_A)^2 \quad (23)$$

$$\delta(\Omega_A,\Omega_B) = -2\sum_{\mu,\nu,\lambda,\sigma} D_{\mu\nu\lambda\sigma} S_{\mu\nu}(\Omega_A) S_{\lambda\sigma}(\Omega_B) + 2N(\Omega_A)N(\Omega_B) \quad (24)$$

$\{D_{\mu\nu\lambda\sigma}\}$ are density matrix elements for the pair density matrix in the atomic orbital (AO) base, and $\{S_{\mu\nu}(\Omega_A)\}$ are overlaps between basis functions, integrated within the basin of atom A.

For closed-shell molecules and for single-determinant wave functions, eqs 21 and 22 are simplified to

$$\lambda(\Omega_A) = \sum_{k,l} [S_{kl}(\Omega_A)]^2 \quad (25)$$

$$\delta(\Omega_A,\Omega_B) = 2\sum_{k,l} S_{kl}(\Omega_A) S_{kl}(\Omega_B) \quad (26)$$

where the summations run over all the occupied molecular spin−orbitals. Finally, using eqs 14−17 it can be proved that the following relationships between LIs and DIs and variance, covariance, and average populations exist:

$$N = \sum_A \left[\lambda(\Omega_A) + \frac{1}{2}\sum_{B\neq A}\delta(\Omega_A,\Omega_B)\right] = \sum_A [(N(\Omega_A) - \sigma^2(\Omega_A)) - \sum_{B\neq A}\mathrm{cov}(\Omega_A,\Omega_B)] = \sum_A N(\Omega_A) \quad (27)$$

### 2.1.3. Spin Pair Composition

Because $\Gamma(\vec{r}_1,\vec{r}_2)$ can be partitioned in same-spin and unlike-spin electron contributions

$$\Gamma(\vec{r}_1,\vec{r}_2) = \Gamma^{\alpha\alpha}(\vec{r}_1,\vec{r}_2) + \Gamma^{\alpha\beta}(\vec{r}_1,\vec{r}_2) + \Gamma^{\beta\alpha}(\vec{r}_1,\vec{r}_2) + \Gamma^{\beta\beta}(\vec{r}_1,\vec{r}_2) \quad (28)$$

the exchange correlation density can also be separated in same-spin and unlike-spin electron contributions. Consequently, the LI and DI in AIM theory given by eqs 19 and 20 can also be partitioned in intra- and interspin components:[16]

$$\lambda(\Omega_A) = \lambda^{\alpha\alpha}(\Omega_A) + \lambda^{\beta\beta}(\Omega_A) + \lambda^{\alpha\beta}(\Omega_A) + \lambda^{\beta\alpha}(\Omega_A) \quad (29)$$

$$\delta(\Omega_A,\Omega_B) = \delta^{\alpha\alpha}(\Omega_A,\Omega_B) + \delta^{\beta\beta}(\Omega_A,\Omega_B) + \delta^{\alpha\beta}(\Omega_A,\Omega_B) + \delta^{\beta\alpha}(\Omega_A,\Omega_B) \quad (30)$$

At the HF level, only the $\alpha\alpha$ and $\beta\beta$ components are nonzero for both LI and DI.

In ELF, the spin pair composition,[99] $d(\vec{r})$, is the ratio of the numbers of parallel and antiparallel spin pairs within a sampling volume $V$ around the reference point, the size of the sampling volume is such as its population

$$q = \int_V \rho(\vec{r})\, d\vec{r} \quad (31)$$

$$d(\vec{r}) = \frac{\bar{N}_{||}}{\bar{N}_{\perp}} \quad (32)$$

where

$$\bar{N}_{||} = \int\int_V (\Gamma^{\alpha\alpha}(\vec{r}_1,\vec{r}_2) + \Gamma^{\beta\beta}(\vec{r}_1,\vec{r}_2)\, d\vec{r}_1\, d\vec{r}_2 \quad (33)$$

and

$$\bar{N}_{\perp} = 2\int\int_V \Gamma^{\alpha\beta}(\vec{r}_1,\vec{r}_2)\, d\vec{r}_1\, d\vec{r}_2 \quad (34)$$

The expression of ELF given in eq 1, where $D$ and $D_h$ represent the curvature of the pair density of electrons of identical spin for the actual system and the homogeneous electron gas of same density, can be approximated by

$$\eta(\vec{r}) = \frac{1}{1 + c_\pi^2(\vec{r})} \quad (35)$$

where $c_\pi(\vec{r})$ is the size-independent spin pair composition $c_\pi(\vec{r}) = q^{-3/2}\, d(\vec{r})$.

## 2.2. Electron Delocalization in the Framework of Atoms in Molecules Theory

This section is organized as follows. In the first part of this section, we discuss some technical aspects related to the DIs, such as its physical meaning, the partition of these indices into $\sigma$ and $\pi$ components in planar species, the basis set and electron correlation effects, and the software available to compute them. In the second part, some applications of the DIs to the analysis of chemical bond and reactivity in chemically interesting systems are briefly reviewed.

### 2.2.1. Technical Aspects

To discuss the meaning of the DIs, it is helpful to analyze the results obtained at the HF level using eqs 25 and 26 by Fradera, Austen, and Bader (FAB)[21] for the series of diatomic molecules gathered in Table 1. FAB analyzed first the $H_2$ molecule, which has a pair of electrons equally shared between the two atoms. The $D_{\infty h}$ symmetry of the system imposes the restriction that the overlap between $\sigma_g$ MOs over each atomic basin equals $^1/_2$, and thus the contribution to the LI is $2 \times {}^1/_2 \times {}^1/_2 = {}^1/_2$ (eq 25) for each atom, and the delocalization contribution is $4 \times {}^1/_2 \times {}^1/_2 = 1$ (eq 26), which completely agrees with the prediction of the Lewis model[20] for the electronic sharing in $H_2$. The authors analyzed then the $N_2$ molecule. According to the Lewis model,[20] the LI should have the contribution of 2 from the $1s^2$ core electrons, 2 from the lone pair, and 1.5 from the three shared pairs, giving $\lambda(N) = 5.5$. Moreover, these three equally shared pairs should give a DI of 3, achieving a total contribution of 14, the number of electrons. These values are similar to those reported in Table 1. The fact that $\delta(N,N') > 3$ was attributed to a slight delocalization of the nonbonded pair of a N atom onto the basin of the other N atom.[21]

**Table 1. HF/6-311++G(2d,2p) Localization and Delocalization Indices (Electrons) of Selected Diatomic Molecules Having Bonds of Diverse Degrees of Ionicity and Covalency[a]**

| molecule | atom | $N$(A) | $\lambda$(A) | $\delta$(A,B) |
|---|---|---|---|---|
| $H_2$ | H | 1.000 | 0.500 | 1.000 |
| $N_2$ | N | 7.000 | 5.479 | 3.042 |
| $F_2$ | F | 9.000 | 8.358 | 1.283 |
| LiF | Li | 2.060 | 1.971 | 0.178 |
| | F | 9.940 | 9.851 | |
| CO | C | 4.647 | 3.860 | 1.574 |
| | O | 9.354 | 8.567 | |
| $CN^-$ | C | 5.227 | 4.121 | 2.210 |
| | N | 8.773 | 7.668 | |
| $NO^+$ | N | 5.525 | 4.323 | 2.405 |
| | O | 8.475 | 7.273 | |

[a] From ref 21.

For molecular bonds with equally shared pairs such as $H_2$ or $N_2$, a simple relationship between the DI and the number of Lewis bonded pairs (formal bond order) is generally found. However, for polar molecular bonds (unequally shared pairs), FAB found that there was no longer a simple relationship between the DI and the number of Lewis bonded pairs.[21] Indeed, FAB showed that in molecules AB such as LiF, where there is an important charge transfer, the electron pair is not equally shared but partly localized on the more electronegative atom A, and as a consequence, $\lambda$(A) increases at the expense of $\delta$(A,B) and $\lambda$(B).[21] Thus, LiF presents a $\delta$(Li,F) of 0.18 and $\lambda$(F) equals 9.85 electrons. In general, a strong localization is characteristic of ionic interactions.[114] FAB remarked that the DI of LiF does not imply a Lewis bond formed from 0.18 pair of electrons; instead, it means that in LiF there is a bonded pair that is very unequally shared. This was further illustrated[21] with the isoelectronic sequence involving $N_2$, $NO^+$, $CN^-$, and CO, all triply bonded molecules the DI of which drops in the sequence 3.04, 2.41, 2.21, and 1.57 electrons, respectively. The DIs tend to decrease with the increased electronegativity difference (greater charge transfer) of the atoms involved in the bond. FAB concluded that the DI is a measure of the number of electrons that are shared or exchanged between A and B independently of the nature of the interaction, but it determines the corresponding number of contributing bonded pairs (formal bond order or bond multiplicity) only when the pairs are equally shared.

This notwithstanding, the DI between atoms A and B given by eq 20 is found to be related to most classical definitions of bond orders.[115] For instance, substitution of the exchange correlation density cor-

responding to a closed-shell monodeterminantal wave function

$$\Gamma_{XC}(\vec{r}_1,\vec{r}_2) = -\sum_{i=1}^{N}\sum_{j=1}^{N}\phi_i^*(\vec{r}_1)\phi_i(\vec{r}_2)\phi_j(\vec{r}_1)\phi_j^*(\vec{r}_2) \quad (36)$$

into eq 20, followed by expansion of the MOs as a linear combination of AOs (LCAO) and replacement of the integrations over atomic basins by a Mulliken-like partitioning of the corresponding integrals, leads to the well-known definition of the Wiberg−Mayer bond order:[116−118]

$$B_{AB}^{W} = 2\sum_{\mu\in A}\sum_{\nu\in B}(PS)_{\mu\nu}(PS)_{\nu\mu} \quad (37)$$

which was generalized some years ago by Mayer to open-shell species and correlated wave functions[117,119] and more recently to polymers[120] and "fuzzy" atoms.[121] The formula of the bond order established by Fulton[122−125] using products of terms in the one-electron density to describe the sharing of electronic charge between two centers

$$B_{AB}^{F} = 2\sum_{i,j} n_i^{1/2} n_j^{1/2} \mathrm{S}_{ij}(A)\mathrm{S}_{ij}(B) \quad (38)$$

where $n_i$ is the occupation number of the $i$th natural spin−orbital, can also be easily derived from eq 20 just by replacing the exact expression for the exchange correlation density with the following approximate expression in terms of natural spin−orbitals:

$$\Gamma_{XC}(\vec{r}_1,\vec{r}_2) = -\sum_{i=1}^{N}\sum_{j=1}^{N} n_i^{1/2} n_j^{1/2}\phi_i^*(\vec{r}_1)\phi_i(\vec{r}_2)\phi_j(\vec{r}_1)\phi_j^*(\vec{r}_2) \quad (39)$$

This approximation to the exchange correlation density was suggested first by Müller in 1984,[126] and more recently, Buijse and Baerends have shown that it is quite accurate.[81] It is worth noting that, although eq 38 can be derived by substituting eq 39 into eq 20, no reference to the pair density was made by Fulton in his original work. Finally, it must be said that very recently Wang and Werstiuk[127] have proposed to use eq 38 as a means to compute correlated DIs. Preliminary results have been quite promising.[128]

Another similar expression has been proposed by Ángyán, Loos, and Mayer (ALM)[129] by performing an atomic partitioning of the exchange part of the pair density matrix within the framework of the AIM theory. For a closed-shell system, the Ángyán bond order reads as

$$B_{AB}^{A} = \sum_{i,j} n_i n_j S_{ij}(\Omega_A)S_{ij}(\Omega_B) \quad (40)$$

Considering only the diagonal terms, $i = j$, of the Ángyán bond order, one obtains the Cioslowski−Mixon covalent bond order, which is defined according to[130,131]

$$B_{AB}^{C} = \sum_{i} n_i^{2} S_{ii}(\Omega_A)S_{ii}(\Omega_B) \quad (41)$$

However, at variance with the Ángyán bond order, molecular orbitals $i$ and occupation numbers $n_i$ entering into eq 41 are not the usual natural orbitals and occupation numbers, but are obtained from them by applying the so-called isopycnic transformation.[132] As a consequence, the Cioslowski−Mixon bond orders are not invariant with respect to transformations of the orbital set. In general, as ALM pointed out,[129] on the basis of the population-localized orbitals Cioslowski−Mixon used, the neglected off-diagonal terms become small and the Ángyán and Cioslowski−Mixon bond orders are in fact quite similar.

We have already said that for unequally shared electron pairs the DI does not provide the expected value of bond order.[133] The difference between the formal bond multiplicity and the DI can be taken as a measure of bond polarity. (Another measure of bond polarity has been proposed by Raub and Jansen, combining the AIM and ELF partitions of the electron density.[134]) In fact, several authors using indices that are equivalent at the HF level to the DI defined in eq 22 have identified the DI with a *covalent* bond order.[130,135−137] However, in Bader's view[115,138] even the use of the DI as a *covalent* bond order can be criticized because, first, electrons are delocalized over every pair of atoms in a molecule and not just those linked by a bond path.[69,115,138,139] Second, atoms bonded to A or B may have an important effect on $\delta$(A,B) values, which are invariably somewhat less than the formal bond multiplicity because of the delocalization of density into the basins of the other atoms connected to A or B.[41] For instance, in acetylene, the delocalization of electrons from the C−C triple bond onto the H atoms decreases $\delta$(C,C′) from 3 to 2.86 electrons.[138] Moreover, we may also add that one can have significant DIs even for dissociative electronic states. For example, $H_2$ in the doubly excited singlet state $1\sigma_u^{*2}$ has a $\delta$(H,H′) of 1 at the HF level despite being in a dissociative state.[124,140,141] This is also a clear indication that the DI by itself gives no indication of the energy associated with the bonding.[122] We note in passing that the Wiberg−Mayer bond order does not distinguish between bonding and antibonding interactions, either.[142] Finally, it must be mentioned that for atoms sharing a unique electron pair in the Lewis model, it is possible to get DIs >1 (as in $F_2$, see Table 1), a result that must be usually attributed to the delocalization of lone pair electrons.[135] The contribution of lone pairs to bonding has been analyzed by Chesnut recently using Cioslowski bond orders.[143]

The same author[144−149] has recently reported that DIs reflect the expected formal bond orders provided one compares the ratio of molecular quantities rather than their absolute values. Despite the relevance of these results, the use of ratios for the definition of bond order is somewhat arbitrary because a particular bond of a given pair of atoms must be chosen as a reference to calculate bond orders. At this point, it is worth saying that some years ago, Bader, Slee, Cremer, and Kraka[150] proposed an empirical nonlinear relationship between the one-electron density at

the BCP and the bond order based upon a fitting to standard bond orders.

To end the discussion on bond orders and DIs, it must be said that the definition of the DI (and also of some other bond orders such as the Wiberg−Mayer ones) can be generalized to analyze the delocalization/bonding between three or more atoms. In particular, Bochicchio, Lain, Torre, and Ponec reported an AIM generalization of these multicenter bond indices, the three-center DI, which depends on the third-order electron density.[151,152] At the HF level, this three-center DI can be expressed for A ≠ B ≠ C as

$$\delta(\mathrm{A,B,C}) = 12\sum_{i,j,k} S_{ij}(\Omega_\mathrm{A})S_{jk}(\Omega_\mathrm{B})S_{ki}(\Omega_\mathrm{C}) \quad (42)$$

Ponec and others have used this DI to detect three-center bonding in several molecules. Positive $\delta$(A,B,C) values are characteristic of 3c−2e bonds, whereas negative values correspond to 3c−4e bonds. $\delta$(A,B,C) is close to 0 when no three-center bonding between the three atoms is present.[152−155] At this moment, it is worth remarking that the topological analysis of $\rho(\mathbf{r})$ defines only bonds between pairs of atoms, and the concept of three-center bonding is not considered in the context of the AIM theory.[64−66] However, $\delta$(A,B,C) can be used to justify the use of three-center bonding models in molecules difficult to describe with classical two-center bonds of the Lewis model.[152] Generalization of $\delta$(A,B,C) beyond the HF approximation, although possible in principle, is quite difficult, because it requires access to correlated high-order densities.[152]

In molecules having a plane of symmetry, the orbitals can be classified as $\sigma$ or $\pi$, depending on their symmetric or antisymmetric behavior with respect to reflection in the plane. In this case, the overlap integrals $S_{ij}(\Omega_\mathrm{A})$ vanish when $i$ and $j$ belong to different sets, and, consequently, the contributions of $\sigma$ or $\pi$ electrons to the LIs and DIs can be separated. Table 2 lists the $\sigma/\pi$ decomposition of the DIs performed by FAB for $N_2$, LiF, CO, $CN^-$, and $NO^+$.[21] These authors found that in $N_2$, exactly two $\pi$ electron pairs and somewhat more than one $\sigma$ pair contribute to $\delta$(N,N′). For LiF, the values of the $\sigma$ and $\pi$ components indicate that the $\pi$ electrons are essentially localized on F. Moreover, the principal contribution to $\delta$(Li,F) comes from the pair of electrons in the top $\sigma$ orbital with the remainder of the pair localized on F. The reduction in the DI of the CO, $CN^-$, and $NO^+$ polar molecules as compared to $N_2$ is due to a similar reduction in the $\sigma$ and $\pi$ contributions. This $\sigma/\pi$ separation, however, cannot be generalized to any set of orbitals belonging to different symmetry representations (for instance, $A_1$ and $B_2$ in $C_{2v}$ molecules) because a strict partition into orbital contributions requires that all of the overlap integrals between orbitals belonging to different sets be 0 within each atomic basin.[21]

**Table 2. HF/6-311++G(2d,2p) $\sigma$ and $\pi$ Orbital Contributions to Localization and Delocalization Indices (Electrons) of Some Diatomic Molecules[a]**

| molecule | atoms (A,B) | symmetry | $\lambda$(A) | $\lambda$(B) | $\delta$(A,B) |
|---|---|---|---|---|---|
| $N_2$ | N, N′ | $\sigma$ | 4.479 | 4.479 | 1.042 |
| | | $\pi$ | 0.500 | 0.500 | 1.000 |
| LiF | Li, F | $\sigma$ | 1.970 | 5.903 | 0.127 |
| | | $\pi$ | 0.000 | 1.974 | 0.026 |
| CO | C, O | $\sigma$ | 3.788 | 5.566 | 0.646 |
| | | $\pi$ | 0.036 | 1.500 | 0.464 |
| $CN^-$ | C, N | $\sigma$ | 3.883 | 5.383 | 0.734 |
| | | $\pi$ | 0.119 | 1.143 | 0.738 |
| $NO^+$ | N, O | $\sigma$ | 4.019 | 5.172 | 0.809 |
| | | $\pi$ | 0.152 | 1.050 | 0.798 |

[a] From ref 21.

At the HF level, LIs and DIs usually have a minor dependence on the basis set, converging smoothly to their appropriate limiting value with extension of the basis set.[21] For instance, $\delta$(N,N′) in $N_2$ is 3.042, 3.037, 3.040, and 3.042 and $\delta$(Li,F) in LiF is 0.208, 0.180, 0.183, and 0.178 with the 6-31G, 6-31G*, 6-311G(2d), and 6-311+G(2d) basis sets, respectively.[21,129] The basis set dependence of the DIs is small even if a Mulliken-like partition of space is used,[118,155,156] in contrast to the well-known basis set dependence of the Mulliken populations.[105,108] In general, LIs and DIs depend on the partition of electronic space because they are defined by integrations over basins. However, Chesnut and Bartolotti (CB)[157] have recently compared the DIs obtained from the AIM partition of space and ELF bond basin populations in some substituted cyclopentadienyl systems, reaching the conclusion that the two measures are essentially equal for the nonpolar C−C bond. As an example, the DI for the C−C double bond in the cyclopentadienyl cation is 1.65 and the ELF bond basin population equals 1.64 electrons. However, both measures become somewhat different for bonds that are polar and/or have lone pairs in close proximity, because lone pairs and core electrons occupy their own basins in ELF, whereas AIM atomic basins enclose lone pairs and core electrons.

Some authors have analyzed the effect of electron correlation on DIs and related bond order definitions.[21,127,128,158−160] Because the main source of correlation between the electrons of the same spin is the effect of antisymmetrization,[27] which is already included at the HF level, changes in LIs and DIs when going from an HF to a correlated wave function, that is, including Coulomb correlation, are predicted to be relatively small.[94] Table 3 collects the LIs and

**Table 3. Atomic Populations ($N$), Localization ($\lambda$), and Delocalization ($\delta$) Indices[a] for a Series of Diatomic Molecules at Configuration Interaction with Single and Double Excitations (CI) and B3LYP Levels of Theory Using the 6-311++G(2d,2p) Basis Set**

| | | $N$(A) | | $\lambda$(A) | | $\delta$(A,B) | |
|---|---|---|---|---|---|---|---|
| molecule | atom | DFT[b] | CI[c] | HF(DFT)[b] | CI[c] | HF(DFT)[b] | CI[c] |
| $H_2$ | H | 1.000 | 1.000 | 0.500 | 0.575 | 1.000 | 0.849 |
| $N_2$ | N | 7.000 | 7.000 | 5.477 | 5.891 | 3.046 | 2.219 |
| $F_2$ | F | 9.000 | 9.000 | 8.361 | 8.498 | 1.279 | 1.005 |
| LiF | Li | 2.079 | 2.067 | 1.969 | 1.973 | 0.221 | 0.193 |
| | F | 9.921 | 9.932 | 9.810 | 9.838 | | |
| CO | C | 4.853 | 4.794 | 3.946 | 4.072 | 1.814 | 1.443 |
| | O | 9.147 | 9.206 | 8.240 | 8.484 | | |
| $CN^-$ | C | 5.512 | 5.434 | 4.286 | 4.490 | 2.451 | 1.888 |
| | N | 8.488 | 8.566 | 7.262 | 7.621 | | |
| $NO^+$ | N | 5.857 | 5.803 | 4.529 | 4.837 | 2.656 | 1.934 |
| | O | 8.143 | 8.197 | 6.815 | 7.231 | | |

[a] Units are electrons. [b] From ref 158. [c] From ref 21.

DIs computed with the configuration interaction with single and double excitations (CISD) method of the same series of diatomic molecules analyzed in Table 1. From the CISD results one can conclude that in equally shared systems ($H_2$, $N_2$, and $F_2$), Coulomb correlation causes electron density to be removed from the vicinity of the interatomic surface and concentrated in each atomic basin, with a decrease in the number of electron pairs shared between the two atoms and an increase in the pairing within each atomic basin.[21] Therefore, the HF values of DIs represent upper bounds to the number of electron pairs shared between atoms.[21,115] On the other hand, in closed-shell or ionic systems (LiF), where the density is strongly localized within the basin of each atom, the net effect of Coulomb correlation on the pairing of electrons within each atomic basin is minimal. In shared polar interactions (CO, $CN^-$, and $NO^+$), the transfer of density from the interatomic region to the atomic basins is reduced with respect to homonuclear molecules. Taking the HF calculation as a reference, Coulomb correlation causes an increase of the population of the less electronegative atom, consistent with a reduction of the bond ionicity. However, the decrease of the DI is smaller than that observed in homonuclear species. It is important to mention that in some cases the introduction of Coulomb correlation is essential to get a correct picture of the chemical process. This is the case of the homolytic $H_2$ bond dissociation process that has been analyzed from the pair density by different authors.[61,85,140,141,161] As nuclei are moved apart, the HF wave function retains its DI of 1.[122,140,141] The requirement of MOs at the restricted HF level to be occupied simultaneously by a couple of electrons is responsible for localization to hold the same value [$\delta(H,H') = 1$] while dissociation is happening, thus reflecting through the DI the well-known deficiency of the HF method to deal with bond dissociation. When the CI method is used, the localizability of the electrons in the system turns into the intuitive scheme expected for homolytic dissociation: atomic electron localizability increases with interatomic distance until one electron localizes in each atom, whereas mutual shared electrons decrease to reach no sharing in the limit of non-interacting fragments.[122,129,137,141,161]

Calculations of LIs and DIs with the density functional theory (DFT) method are very common despite the fact that they cannot be performed exactly at this level of theory because the pair density is not available.[29,81,162] As an approximation, the KS orbitals obtained from DFT are usually employed to calculate HF-like LIs and DIs using eqs 25 and 26, respectively, in a scheme of calculation that we have denoted HF(DFT) (see Table 3).[158] Because the DFT one-electron density is clearly better than the HF one,[163] one may expect that HF(DFT) LIs and DIs are improved with respect to the HF results. The comparison between ab initio HF and KS orbitals for the calculation of LIs and DIs from eqs 25 and 26 shows that DIs derived from KS orbitals are very similar to (usually somewhat larger than) those obtained with the HF method.[135,139,158] This can be seen by comparing the HF(DFT) results computed with the B3LYP functional in Table 3 with the HF ones in Table 1. The usually larger HF(DFT) DIs indicate a slightly enhanced covalency as compared to HF.[135] As we have commented in the previous paragraph, the CISD DIs are in general smaller than the HF ones.[158] Therefore, LIs and DIs obtained with the KS orbitals are not improved as compared to the HF values. This is not totally unexpected given the fact that the DFT pair density calculated using the HF formalism is formally derived from an approximate monodeterminantal wave function constructed with KS orbitals that is, at least from an energetic point of view, worse than the HF wave function.

As shown in previous paragraphs, at the HF level, the definitions of bond order by ALM[129] (eq 41) and Fulton[122,123] (eq 38) are equivalent to one another and to the DI defined in eq 26. However, differences emerge when correlated wave functions are used.[137] Table 4 compares the CISD/6-311++G(2d,2p) indices

**Table 4. Delocalization Indices (Electrons) Obtained through Equations 24 and 38 for a Series of Diatomic Molecules with the Configuration Interaction with Single- and Double-Excitation Methods Using the 6-311++G(2d,2p) Basis Set**

| molecule | exact[a] | Fulton[b] |
|---|---|---|
| $H_2$ | 0.849 | 0.844 |
| $N_2$ | 2.219 | 2.419 |
| $F_2$ | 1.005 | 0.969 |
| LiF | 0.193 | 0.187 |
| CO | 1.443 | 1.474 |
| $CN^-$ | 1.888 | 1.975 |
| $NO^+$ | 1.934 | 2.084 |

[a] From ref 21. [b] From ref 86.

obtained from eq 24 using the exact correlated pair density and from eq 38.[86] Results in Table 4 show that in the two cases the DI decreases upon going from the HF to a CI wave function.[21,122,158] It is seen from results in this table and from the work by Wang and Werstiuk[127,128] that, in general, Fulton bond orders are good approximations to the exact DIs, with the advantage that calculation of Fulton bond orders does not require the use of second-order densities. Moreover, unlike ALM bond order definition,[129] the sum of Fulton's bond indices equals N at all levels of theory. Some comparisons between Fulton and Cioslowski−Mixon or Ángyán indices[129,147] as well as between the Wiberg−Mayer and the DI[118] have been reported.

The overlaps between MOs integrated within the basin of atom A, the $\{S_{ij}(\Omega_A)\}$ terms in eqs 21 and 22, needed to compute LIs and DIs, can be obtained using different programs. Historically, the first available software to compute these quantities was the AIMPAC suite of programs, developed by Bader's group.[164] The AIMPAC code provides the required $S_{ij}(\Omega_A)$ values, and then one has to program its own interface to read these values and calculate LIs and DIs. More recently, AIMPAC has evolved into an interactive and visualizing program called AIM2000,[165] which directly provides LIs and DIs computed from monodeterminantal wave functions. Other existing programs that perform AIM analysis

are the MORPHY98 code of Popelier,[166] the XAIM suite of programs by Ortíz and Bo,[167] and the TOPOND program developed by Gatti.[168] Finally, GAUSSIAN98,[169] the popular code for quantum mechanical calculations, also incorporates routines that grant access to AIM analysis (but not to LIs and DIs). However, it must be said that the latest version of this program, GAUSSIAN03,[170] does not allow AIM calculations. Until now, there is no available program that allows computation of exact LIs and DIs using correlated wave functions, although some authors have managed to compute CISD LIs and DIs[21,86] from eqs 23 and 24 by extracting the CISD pair density matrix expressed in terms of products of basis functions from the GAMESS program.[171]

### 2.2.2. Examples and Applications in Chemistry

The main results of the application of LIs and DIs to the analysis of molecular structure and reactivity, with the exception of aromaticity studies that will be treated in section 3.1, are briefly reviewed in this section. In particular, we will list applications devoted to the relationships between electron delocalization and the nuclear spin−spin coupling constant, the study of the molecular structure and bonding in main group elements, open-shell systems, transition metal (TM) complexes, the analysis of weak interactions, and the investigation of chemical reactivity.

Bader, Streitwiser, Neuhaus, Laidig, and Speers (BSNLS)[79] suggested for the first time in 1996 the existence of a relationship between the delocalization of the Fermi hole from one proton to another calculated at the HF level and the corresponding $^1$H NMR spin−spin coupling constants. This relation was verified by BSNLS in ethane by plotting the coupling constant ($J_{HH'}$) of vicinal protons obtained from the Karplus equation[172] and the corresponding DI [$\delta$(H,H′)] as a function of the torsion angle.[79] BSNLS found an excellent correlation between $\delta$(H,H′) and $J_{HH'}$. Some years later, Matta, Hernández-Trujillo, and Bader (MHB)[41,173] generalized the result obtained in ethane to a set of H atoms bonded to different carbons in several polycyclic aromatic hydrocarbons (PAH). MHB obtained a simple linear correlation with the HF-calculated DI and $J_{HH'}$ in the form $J_{HH'} = a + b \times \delta(H,H')$. In a subsequent paper, Matta showed that solvation has only a minor effect in the correlations found.[173] In the same year, Soncini and Lazzeretti[40] confirmed the role of Fermi correlation in the propagation of the nuclear-spin/electron-spin contact interaction by plotting Fermi hole density functions for a series of small molecules.

There are a number of applications of the DI and related bond order definitions to the study of the bonding and molecular structure of main group elements. Most efforts have been devoted to the analysis of multicenter bonding, hypervalency, and multiple bonding. As mentioned by Macchi and Sironi (MS),[174] in general, it is found that covalent bonds (C−C, C−H, etc.) between main group elements are characterized by a DI close to the formal bond order, intermediate interactions (polar bonds, donor−acceptor bonds, etc.) have DI lower than the formal bond order, and DIs close to 0 are typical of closed-shell interactions (ionic bonds, hydrogen bonds, and van der Waals interactions).

As far as the multicenter bonding is concerned, molecules with 3c−4e and 3c−2e bonding interactions have been extensively analyzed.[21,154,158,175] Apparently, a large DI between nonbonded atoms indicates the existence of 3c−4e bonding, whereas for 3c−2e a small DI between nonbonded terminal atoms is found. This is the case of the 3c−4e bond in $CO_2$ for which a large $\delta$(O,O′) between nonbonded oxygen atoms of 0.380 electron,[21,158] which mainly arises from the $\pi_g$ nonbonding orbital in $CO_2$, is found. Also, a large $\delta$(F,F′) is calculated between nonbonded fluorine atoms in 3c−4e molecules $FHF^-$ and $FFF^-$.[154,175] For $B_2H_6$, a paradigmatic example of a 3c−2e bond, there is a small $\delta$(B,B′) of 0.047 electron that has been attributed to the low electron density around each boron atom.[21,158] However, the best way to characterize 3c−2e and 3c−4e bonds is by means of the three-center bond index given by eq 42 as demonstrated by Ponec and co-workers. These authors found that this index allows for an easy differentiation between 3c−2e and 3c−4e bonding, the three-center bond index being positive for 3c−2e bonding and negative for 3c−4e bonding.[90,151,152,155,160,176]

As to hypervalency, Dobado, Martínez-García, Molina Molina, and Sundberg (DMMS)[177] analyzed the $Y_3X-CH_2$ (X = N, P, As; Y = H, F) and $H_2X-CH_2$ (X = O, S, Se) hypervalent molecules. DMMS found that the bonding depends on the electronegativity of the X atom. When X is a highly electronegative atom (N or O), the C−X bond is weaker than a single bond, with a $\delta$(X,C) <1, due to electrostatic repulsion. On the other hand, for X = P, As, S or Se, the values of $\delta$(X,C) are >1, and the bond is significantly stronger. Very recently, in a study by Sánchez-González, Martínez-García, Melchor, and Dobado (SMMD) on similar species,[178] the authors found that some increases in the bond multiplicity are not reflected in the DIs, and, consequently, SMMD cautioned against the use of DIs as a measure of bond multiplicity or bond order (vide supra). Mitrasinovic in a series of works[179,180] has studied the bonding in some simple ylides using the Fulton bond orders (eq 38) computed at the MP2 level of theory. Mitrasinovic showed that the DIs indicate that the P−C and N−C bonds in $PH_3CH_2$ and $NH_3CH_2$ are single bonds, whereas in $PHCH_2$ and $SH_2CH_2$ the DIs are between the values corresponding to prototypical single and double bonds. It is worth noting that Fulton in a recent comment[181] demands recognition for one of these works.[180] We can briefly mention here that an analysis of Fermi holes[19] and domain-averaged Fermi holes[89,90] has been also carried out for a set of hypervalent compounds.

With respect to multiple bonding in species formed by main group elements, the DI has been utilized to discuss the bonding in a series of molecules that have bonds with a not well-defined multiplicity. This is the case of the REER and $R_2EER_2$ systems (E = Si, Ge, Sn; R = H, $CH_3$)[182] and, in particular, $Si_2H_2$,[145] as well as the anions $Ga_2H_2^{2-}$,[138,146] $Ga_2H_4^{2-}$, and $Ga_2H_6^{2-}$.[146] We note in passing that an analysis of domain-averaged Fermi holes has been also carried out for

$Ga_2Ph_2^{2-}$.[92] DIs have been also used to evaluate bond multiplicity for the phosphoryl bond as compared to the conventional PO double bond,[147] for the SO sulforyl group in sulfoxides ($R_2SO$) and sulfones ($R_2SO_2$),[148] and to compare the multiplicity of the bonding in phosphine oxides with respect to amine sulfides[149] and amine oxides.[143]

In addition, the DI has been applied to examine the extent of homoconjugation in 6-tryciclo[3.2.1.$0^{2,4}$]-octyl cation,[183] the degree of delocalization of the CO electrons of the benzoyl group into the phenyl ring as well as into the urea moiety in two acylated glycolurils,[184] and the amount of localization in a series of $CR_2$ carbenes and $SiH_2$ in the quest for an understanding of the different stabilities of their lowest lying singlet and triplet states and their differing chemical reactivities.[185] Finally, the DIs have been used to get a measure of the weight of different resonance structures in pyrimidimic bases[139] and phenol derivatives.[186]

An interesting result obtained by Bader and Bayles (BB)[115] is that the degree of electron delocalization (measured using the corresponding DIs) for a given molecular group over the remaining groups in the molecule is transferable from one molecule to another. BB concluded that there is a conservation principle for the electronic delocalization of a given group of atoms as a result of the transferability of the pair density averaged over an atom or a group of atoms.

Open-shell systems of the main group elements are peculiar species from the point of view of electron delocalization. Fradera and Solà (FS)[140] showed that unpaired electrons have a significant effect on the interatomic DIs. Indeed, for many radicals, analysis of the spin components reveals that the interatomic delocalization is very different for α and $\beta$ spin electrons.[140] A paradigmatic working example is $H_2^-$ in its doublet ground state. Using eq 26, one can easily derive that the DI for $H_2^-$ at the ROHF level is $1.5-4[S_{ab}(A)]^2$, $S_{ab}$ being the overlap integral between the $\sigma_g$ and $\sigma_u^*$ orbitals over an atomic basin. Thus, the extra electron in $H_2^-$ has two different effects on $\delta$(H,H′). On the one hand, an electron in the $\sigma_u^*$ orbital, on its own, contributes 0.5 to $\delta$(H,H′). On the other hand, the extra electron correlates with one same-spin electron in the $\sigma_g$ orbital, leading to some localization and the consequent reduction by $-4[S_{ab}(A)]^2$ to $\delta$(H,H′). Depending on the degree of overlap between the $\sigma_g$ and $\sigma_u^*$ orbitals, the net effect will be an increase or decrease of the DI, with respect to $H_2$. At the ROHF/STO-3G level, $S_{ab}(A)$ is ±0.48, and $\delta$(H,H′) is 0.59 electron, sensibly lower than in $H_2$. On the contrary, at the ROHF/6-311++G(2d,2p) level, $S_{ab}(A)$ is ±0.14, and $\delta$(H,H′) is 1.42 electrons, larger than in $H_2$. The result in this case is clearly basis-set dependent. The ground state of $O_2$ has been analyzed by FS[140] and also by Chesnut.[143] They found that, at the HF level, each of the $\beta$ electrons in the $\pi_x$ and $\pi_y$ bonding orbitals does not interact directly with other electrons and is perfectly delocalized between the two O atoms. In contrast, the mutual repulsion between the α electrons in the bonding and antibonding $\pi_x$ and $\pi_y$ orbitals leads to a high localization of these α electrons.

The study of the molecular structure and bonding of TM complexes by means of DIs has been the subject of several works. The first work that we comment on here refers to the study performed by Poater, Solà, Rimola, Rodríguez-Santiago, and Sodupe (PSRRS)[187] of the ground and low-lying states of doublet $Cu(H_2O)^{2+}$ species, an open-shell TM complex. PSRRS found that at the CCSD(T) level $Cu^{2+}-H_2O$ presents $C_{2v}$ symmetry and the ground electronic state is a $^2A_1$. At this level of theory the relative order of the electronic states is $^2A_1 < {}^2B_1 < {}^2B_2 < {}^2A_2$. On the other hand, DFT results show that the relative stabilities of these states vary depending on the degree of mixing of exact HF and DFT exchange functional. For pure and hybrid functionals with low percentages of HF mixing (up to 20−25%), the $^2B_1$ state becomes more stable than the $^2A_1$ one. These changes are related to the electronic delocalization in the different electronic states that was measured using DIs. For $^2B_1$, pure functionals provide a delocalized picture of the electron hole, whereas in the $^2A_1$ state the hole is more localized at the metal atom. Because delocalized situations are overstabilized by DFT functionals, the $^2B_1$ state is wrongly predicted to be lower in energy than the $^2A_1$ by pure functionals. The admixture of exact exchange reduces the error by reducing the degree of delocalization.[188] It was found that 40−50% mixing provides results in very good agreement with CCSD(T).

The bonding to titanium has been studied in two works by means of DIs. For the hypovalent titanium alkoxide model complexes, Dobado, Molina Molina, Uggla, and Sundberg[189] found that the values of $\delta$(Ti,O) were consistent with a Ti−O multiple bond with significant covalent character. On the other hand, Bader and Matta (BM)[133] analyzed the nature of Ti−C contacts in a Ti bonded to cyclopentadienyl and a substituted dienyl complex to determine whether these interactions should be considered as short nonbonded contacts or agostic interactions. The low DIs found by BM were consistent with the former hypothesis.

Three recent works have examined the bonding in TM carbonyl complexes. In the first, Pilme, Silvi, and Alikhani (PSA) studied the M−CO complexes,[190] M being a first-row TM. These authors classify these TM−carbonyl complexes in three groups depending among other features on the $\delta$(M,C) values. Thus, according to PSA, low-spin complexes have large $\delta$(M,C) (∼1.6 e), high-spin complexes possess intermediate $\delta$(M,C) values (∼1.2 e), and small $\delta$(M,C) values correspond to conserved spin multiplicity complexes. In the second work,[174,191] MS analyzed the series of TM carbonyl complexes given in Table 5. MS found the expected decrease of the $\delta$(C,O) values in TM−carbonyl complexes as compared to free CO (see Table 5) due to a weakening of the C−O bonding when the carbonyl is coordinated to the TM following the $\sigma$-donation and $\pi$-back-donation scheme of Dewar−Chatt−Duncanson.[192] MS considered that the most reasonable sign of the back-donation mechanism comes from the $\delta$(M,O) values, which are relatively large. The reason is that $\sigma$-donation involves mainly

**Table 5. B3LYP Delocalization Indices δ(A,B) (Electrons) for Some Transition Metal Carbonyl Complexes[a]**

| molecule | δ(C,O) | δ(M,C) | δ(M,O) |
|---|---|---|---|
| CO | 1.80 | | |
| $H_3BCO$ | 1.65 | 0.50 | 0.04 |
| $(CO)_5Cr-CO$ | 1.62 | 0.83 | 0.14 |
| $(CO)_4Fe-CO_{eq}$ | 1.61 | 1.05 | 0.18 |
| $(CO)_4Fe-CO_{ax}$ | 1.61 | 0.98 | 0.17 |
| $[(CO)_3Co-CO]^-$ | 1.53 | 1.23 | 0.22 |
| $(CO)_3Ni-CO$ | 1.66 | 0.98 | 0.16 |
| $[(CO)Cu-CO]^+$ | 1.82 | 0.74 | 0.09 |

[a] From ref 174.

metal and carbon orbitals, whereas in π-back-donation the contribution coming from oxygen orbitals is significant. Finally, Chevreau, Martinsky, Sevin, Minot, and Silvi (CMSMS)[193] analyzed the nature of the chemical bonding in the $D_{3h}$ and $C_{2v}$ isomers of $Fe_3(CO)_{12}$. They found that the DIs are rather small for Fe−Fe interactions (∼0.4 e, closed shell interaction), of the order of 1 e for the Fe−C dative bond, and of the order of 1.6 e for C−O. In agreement with the results of MS, CMSMS found that back-donation decreases the δ(C,O) values in TM−carbonyl complexes by ∼0.2 e with respect to free CO.

The bonding in a series of 25 Fischer carbene complexes of the type $(CO)_5Cr{=}C(X)R$ (X = H, OH, $OCH_3$, $NH_2$, $NHCH_3$ and R = H, $CH_3$, $CH{=}CH_2$, Ph, C≡CH) have been also analyzed recently using DIs.[194] The electron delocalization between the Cr and C atoms and between the C atom and the X group have been found to be related to the π-donor strength of the X group and the degree of back-donation between the chromium pentacarbonyl and the carbene fragments. Three-center DIs (eq 42) between Cr, C, and X were found to be consistent with the hypothesis of a weak 3c−4e bonding interaction in the Cr=C−X group of atoms. Finally, it is worth noting that three recent works address the problem of the metal−metal bond in molybdenum complexes using DIs[195,196] and calculating domain-averaged Fermi holes.[91]

Weak interactions and, in particular, hydrogen bonds (H-bonds) have been also examined from the electronic delocalization point of view. Fulton and Perhacs (FP) using Fulton indices computed at the MP2/6-31++G** level found that the intermolecular DIs in FH−FH, FH−$OH_2$, and FH−$NH_3$ are 0.098, 0.169, and 0.249 e, thus increasing in the same order as H-bond dissociation energies. Daza, Dobado, Molina Molina, and Villaveces[197] studied the H-bond in $H_2O_2{\cdots}X$ (X = $NO^+$, $CN^-$, HCN, and CO) species at the B3LYP/6-311+G(3df,2p) level of theory, reaching also the conclusion that the strength of the H-bond and the DIs between the hydrogen-bonded atoms are well correlated. Later, Poater, Fradera, Solà, Duran, and Simon (PFSDS)[198] calculated B3LYP/6-311++G(d,p) DIs between hydrogen-bonded atoms in 20 molecular complexes formed between several H-donor and -acceptor molecules. According to PFSDS, there is not such a correlation between the DI of hydrogen-bonded atoms and the H-bond dissociation energy. In fact, the intermolecular DI between proton and proton-acceptor atoms, δ(X,H), was found to be strongly correlated only to the orbital interaction energy term (the covalent contribution) of the H-bond as obtained from a Morokuma-like energy decomposition scheme.[199] Because DIs can be calculated separately for each H-bond, this measure was used in a subsequent work[200] to quantify the electrostatic/covalent character of each of the three H-bonds present in the guanine−cytosine base pair and the effect on the nature of hydrogen bonds of metal cations (M = $Cu^+$, $Ca^{2+}$, $Cu^{2+}$) coordinated to the $N_7$ of guanine (see Figure 1). We must note that

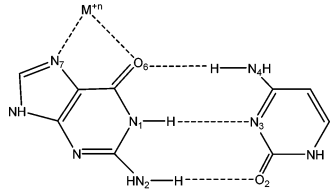


GC

**Figure 1.** Schematic representation of the cytosine−guanine base pair interacting with the metal cation. Reprinted with permission from ref 200. Copyright 2005 Taylor and Francis.

H-bonding in X−H···Y systems has been also analyzed using δ(X,H,Y) indices (eq 42) by Giambiagi, de Giambiagi, and de Oliveira Neto.[201] These authors found always negative values for δ(X,H,Y), which is consistent with a 3c−4e bond for H-bonds. This result is in line with the presence of a donor−acceptor interaction between the lone pair of the proton-acceptor Y atom pointing toward and the donating charge into the unoccupied $\sigma^*_{X-H}$ orbital. Finally, we must note that the delocalization between the two units of the tetracyanoethylene−quinone dimer, a charge resonance complex, has been found to be small according to the calculations by CB.[202]

DIs and bond order analysis have been applied to the study of electron reorganization in the course of several chemical reactions.[142,161,203−207] These studies are of high interest because they allow the evolution of bonding along the reaction coordinate to be followed. Among the different reactions that have been analyzed using DIs, we can mention the dissociation of molecular hydrogen,[61,85,140,141,161] the isomerization between HCN and HNC,[204,205] the $S_N2$ reaction between $CH_3Cl$ and $F^-$,[205] the addition of HF to ethylene,[205] the thermally allowed conrotatory ring opening of cyclobutene to *cis*-butadiene,[161,204] the Diels−Alder reaction between butadiene and ethylene to yield hexadiene,[161,204,205] which is often taken as the prototype of a pericyclic concerted reaction, the Menshutkin reaction between $CH_3Cl$ and $NH_3$ in the gas phase and in solution,[206] and the proton transfer in 1-amino-2-propenal that interconverts the keto and enol isomers.[207] To end this section, let us comment that FS have recently defined[208] new second-order atomic Fukui indices (AFIs) derived from the LIs and DIs, which complement those based on the one-electron density.[209] Calculations for a series of small molecules showed that, in general, the analysis based on second-order AFIs gives relevant information on the electronic structure of these molecules and helps to highlight the electronic reorganization pro-

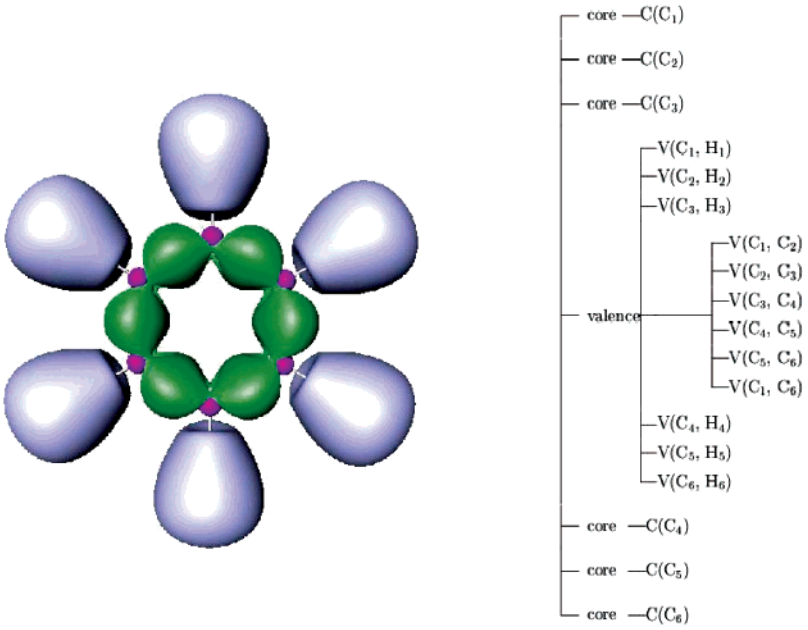


**Figure 2.** Localization domains and bifurcation diagram of the benzene molecule [color code: magenta, C(C); green, V(C,C); blue, V(C,H)].

cesses taking place in electrophilic, nucleophilic, or radicalary reactions.

## 2.3. Electron Delocalization from the Electron Localization Function

The electron delocalization is revealed by ELF in two different fashions. The homogeneous electron gas is considered as an "ideal" delocalized system; it is characterized by a constant value of the electron density and also of the ELF, which is equal to 0.5, and its ELF gradient vector field is uniformly 0. Therefore, any point is a nonhyperbolic critical point (i.e. with at least one 0 eigenvalue), which means that this vector field is structurally unstable. In real systems where this structural instability is removed, ELF values calculated at the attractors of two adjacent valence basins and at the (3,−1) critical point of their separatrix enable discussion of the electron delocalization: if these values are close, the electron density tends to behave like the homogeneous electron gas, whereas large differences indicate a rather low delocalization. This feature of the ELF gradient field is common to bulk metals[210] as well as to molecules. The hierarchy of the localization domains[211,212] is the convenient tool to achieve such an analysis: a localization domain is a volume bounded by a given isosurface defined by the value of the ELF function. A localization domain is said to be reducible if it contains more than one attractor. When the ELF value defining a reducible localization domain is increased, the latter is split for a given ELF value, giving rise to two new domains sharing a (3,−1) critical point. It is then possible to draw the so-called localization reduction diagram, the pattern of which indicates in which part of the molecule the delocalization occurs.

Figure 2 displays on the left side the localization domains of benzene bounded by the ELF($\mathbf{r}$) = 0.65 isosurface characterized by the aromatic domain in green and on the right side the bifurcation diagram. In the latter, the successive bifurcations occur for ELF($\mathbf{r}$) = 0.1 (core valence), 0.61 [V(C,H) from aromatic domain], and 0.65 (aromatic domain). Within the aromatic domain, the localization function does not undergo large variation, and therefore there exist closed paths along which the "local kinetic energy" is almost constant, which favors electron delocalization and makes possible the ring current. It is worth noting that the expression of $D(\mathbf{r})$ in eq 2 can be rewritten in terms of the ratio of the real time-independent electron transition current densities $\mathbf{j}_{ij} = (\psi_i\nabla\psi_j - \psi_j\nabla\psi_i)/2$ between the $i$th and $j$th orbitals and the one-electron density distribution $\rho(\mathbf{r})$.[213]

The study of the covariance matrix is another indicator of delocalization. On the one hand, its diagonal elements, the variance, are the square of the standard deviation of the basin population: a large variance betokens a large delocalization. On the other hand, the off-diagonal matrix elements indicate which basins are involved in the delocalization. The covariance analysis further enables one to build a classical phenomenological model in terms of weighted mesomeric structures. Within the ELF framework, where the basins are assumed to represent the space occupied by the cores, the lone pairs, and the bonds, each set of eigenvalues of the population operators is a distribution of the electrons among the different regions and, therefore, corresponds to a mesomeric structure (even a very exotic one). The weight of the dominant mesomeric structures is then estimated by a fit to the populations and to the covariance values. This technique has been successfully applied to the study of systems belonging to inorganic[190,195] as well as organic chemistries,[214,215] and the bonding cannot be explained without invoking delocalization.

These types of bonding are characterized by large covariance matrix elements between either monosynaptic basins or even between core basins. The three-electron bond (2c−3e) in radical anions has

been investigated in detail by Fourré, Silvi, Savin, and Chevreau.[113] The analyzed systems are of the $H_nXYH_m$ type with X, Y = Cl, S, P, Si, F, O, N, and C and $n, m = 0, 2$. The relaxed anions are characterized by the absence of a V(X,Y) disynaptic basin and by the transfer of the extra electron, initially in the V(X,Y) basin of the neutral molecule, into the V(X) and V(Y) monosynaptic basins. The spin density is localized within these basins, and at every intermolecular separation the covariance between them is $>0.25$, the lower bound at infinite separation.

Molina and Dobado[175] have reinvestigated the 3c−4e bond concept within the AIM and ELF frameworks. They did not find any trisynaptic basins, but showed a noticeable electron delocalization between ligands in linear structures such as $ClF_2^-$. This electron delocalization is weaker in T-shaped molecules and negligible in bipyramidal compounds. However, as the linear structures investigated in this paper are centrosymmetric anions, the origin of the delocalization should be due to the symmetry of the charge distribution rather than to a bonding effect. The $(Li)_2$TCNE−quinone complex provides an example in which an electron pair might be delocalized between two clearly separated chemical subunits.[202] In the singlet ground state, there is a net electron transfer of 0.5 $e^-$ from the quinone anion toward the TCNE moiety, which does not exist for the triplet state. The triplet state charge and spin density distribution is consistent with a picture in which both TCNE and quinone anions are in their doublet ground state. In the singlet state, each moiety behaves as the superposition of two weighted closed-shell mesomeric subsystems, namely, the neutral and the dianionic species.

The study of electron density in depleted homopolar chemical bonds[216] led to the introduction of the concept of a protocovalent bond. A protocovalent bond is characterized by two monosynaptic basins on the internuclear axis and by a value at (3,−1) critical point between them close to the attractor value, just like in the case of the formation or the dissociation of a covalent bond. $F_2$ and $H_2O_2$ are typical examples of protocovalent bonding. The populations of the monosynaptic basins on the internuclear axis are very low (0.14 for $F_2$ and 0.29 for $H_2O_2$), and there are large covariance matrix elements between the monosynaptic basins of the two atoms involved in the protocovalent bond. The charge-shift bond concept introduced by Shaik, Maitre, Sini, and Hiberty[217] in the context of the VB theory explains the stabilization of this kind of bond, which is a manifestation of lone pair bond weakening. Protocovalent bonds are encountered in most homopolar A−B bonds in which both the A and B atoms have lone pairs.[216,218]

An interesting example of bonding by delocalization is provided by bimetallic complexes. The nature of the chemical bond in complexes of the $M_2$(formamidinate)$_4$ (M = Nb, Mo, Tc, Ru, Rh, Pd) type, with different nominal bond orders ranging from 0 to 5, is a puzzling topical example that has been rationalized so far in terms of overlaps of the metal d orbitals giving rise to $\sigma$, $\pi$, and $\delta$ bonding and antibonding orbitals. In their ground state, the $M_2L_4$ complexes are diamagnetic and have an approximate $D_{4h}$ symmetry. A topological study of these systems has been recently published by Llusar, Beltrán, Andrés, Fuster, and Silvi.[195] ELF topological analysis shows a disynaptic V(M,M) basin for Ru and Rh, a group of four disynaptic V(M,M) basins for Nb and Mo, and nothing for Tc and Pd. The complexes of these two latter elements are those with the shortest (Tc) and the largest (Pd) intermetallic distances. The V(M,M) attractor multiplicity seems to be a consequence of the Pauli repulsion between the metallic cores, which mostly depends on the internuclear distance. Going from large to short distances there are four regimes with zero to four attractors. The covariance matrix elements between the two C(M) basin populations accounts for ~80% of C(M) variance. The value of this index can be rationalized by simple resonance concepts. The large electron fluctuation that occurs between the two metallic cores can be interpreted in terms of simple resonance arguments, exemplified here for the Mo complex. Because the metal dimer is in a closed-shell singlet state, there is no spin polarization, and each metallic core should be considered as a local closed-shell subsystem the orbitals of which fulfill the $D_{4h}$ point group symmetry requirements. The Mo core population is close to 40 $e^-$ with a covariance of 1.255 and, as a consequence, an average of four of the six electrons formally considered as valence according to the MO theory should now be incorporated into the core. Following the traditional Greek character nomenclature usually used to describe the quadruple metal−metal-bonding MOs ($\sigma^2\pi^4\delta^2$), the following core configurations are compatible with the molecular symmetry: [Kr]$\pi^4$, [Kr]$\sigma^2\delta^2$, and [Kr]$\pi^4\delta^2$ and [Kr]$\sigma^2$, [Kr]$\sigma^2\pi^4$, and [Kr]$\delta^2$. A resonance structure between the first two configurations, Mo([Kr]$\pi^4$)−Mo([Kr]$\sigma^2\delta^2$) ↔ Mo([Kr]$\sigma^2\delta^2$)−Mo([Kr]$\pi^4$), corresponds to an average core population of 40 $e^-$ with a variance of 0.

The bonding in trimetallic complexes has been studied in the case of the $[Mo_3S_4Cl_3(PH_3)_6]^+$ cluster.[196] In ELF topology, the [Mo] cluster unit behaves as a specific entity in which the bonding arises from the presence of a three-center bond associated with a group of basins involving three disynaptic V(Mo,Mo) and one trisynaptic V(Mo,Mo,Mo) basin. The total population of this [Mo] valence superbasin is 1.25 $e^-$, a large value as compared to the value of 0.68 $e^-$ calculated for the disynaptic intermetallic basin in the [$Mo_2$(formamidinate)$_4$] quadruply bonded dimer in which the metal−metal bond is considered to be due to the fluctuation of electrons within core areas. However, this is not the case for the [Mo] unit under consideration, where the MoMo core covariance is small, −0.14, despite the rather large value of the Mo core population covariance. The main contributors to this variance are the bridging sulfur lone pair V[S] basins, with −0.2 each, and the disynaptic V[Mo,S] basins, with −0.4 (ca. $2 \times -0.2$). The molybdenum core population of 39.22 $e^-$ corresponds approximately to $Mo^{3+}$ rather than to $Mo^{4+}$, which is the formal oxidation state assigned to Mo in this system. This situation is normal when the metal core

population in transition metal complexes is calculated.

In the case of period 4 transition metal−carbonyls, ELF basin population analysis led Pilmé, Silvi, and Alikhani[190] to deduce the following conclusion: except for Cr, Mn, and Cu, the $[Ar]d^{n+2}$ configuration must be considered to account for the metal core populations and variances by a weighted superposition of mesomeric structures; therefore, the spin multiplicity and the symmetry of the ground state are given by applying Hund's rule to the $[Ar]d^{n+2}$ configuration.

## 3. Applications to the Study of Aromaticity

This section presents an overview of the main applications to the analysis of electron delocalization in aromatic compounds that have been performed using the AIM (section 3.1) and ELF (section 3.2) approaches discussed in previous sections.

Before we proceed with this section further, let us introduce two aromaticity indices not based on electron delocalization, but often referred to in the present review. On the one hand, the most common structure-based index of aromaticity is the harmonic oscillator model of aromaticity (HOMA) index, defined by Kruszewski and Krygowski[219] as

$$\mathrm{HOMA} = 1 - \frac{\alpha}{n}\sum_{i=1}^{n}(R_{\mathrm{opt}} - R_i)^2 \qquad (43)$$

Here, $n$ is the number of bonds considered and $\alpha$ is an empirical constant fixed to give HOMA = 0 for a model nonaromatic system and HOMA = 1 for a system with all bonds equal to an optimal value $R_{\mathrm{opt}}$, assumed to be achieved for fully aromatic systems. $R_i$ stands for a running bond length. On the other hand, the most widely magnetic-based index of aromaticity is the nucleus-independent chemical shift (NICS), proposed by Schleyer and co-workers.[220] It is defined as the negative value of the absolute shielding computed at a ring center or at some other interesting point of the system. Rings with large negative NICS values have aromatic character. The more negative the NICS values, the more aromatic the rings.

### 3.1. View of Aromaticity from the Atoms in Molecules Theory

#### 3.1.1. Electron Delocalization in Aromatic Systems: Preliminary Studies

Bader and co-workers[16,79] proposed that the widely used chemical concept of electron delocalization could be quantified by means of the spatial distribution of the Fermi hole density. A significant delocalization of the Fermi hole density onto two centers implies a pairing of the electrons between them. In particular, to prove this proposal, the percentages of localization ($\Omega = \Omega'$) [$\lambda(\Omega)/N(\Omega) \times 100$] and delocalization ($\Omega \neq \Omega'$) ($^1/_2 \times \delta(\Omega,\Omega')/N(\Omega) \times 100$) of the density of the electrons on atom $\Omega$ within the basin of atom $\Omega'$ were calculated for a series of $\pi$-conjugated molecules (see Figure 3).[79] It was observed that the interatomic delocalization of the $\pi$-electrons on a given atom, in general, decreases with the distance of the second atom from the one in question (see Table 6). However,

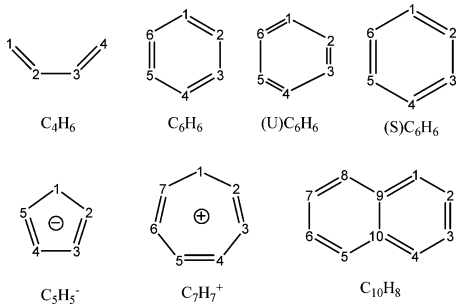


**Figure 3.** Schematic representation of the molecules taken into study with the corresponding numbering.

**Table 6. Percent Localization ($\Omega = \Omega'$) and Delocalization ($\Omega \neq \Omega'$) of the Density of the Electrons on Atom $\Omega$ (Reference Atom) within the Basin of Atom $\Omega'$ [a]**

| | | % localization/delocalization in the basin Ω of atoms | | | | | | | | | |
|---|---|---|---|---|---|---|---|---|---|---|---|
| molecule | ref atom | 1 | 2 | 3 | 4 | 5 | 6 | 7 | 8 | 9 | 10 |
| $C_4H_6$ | $C_1$ | 46.9 | 42.8 | 1.7 | 3.3 | | | | | | |
| | $C_2$ | 42.4 | 44.7 | 3.4 | 1.7 | | | | | | |
| $C_5H_5^-$ | $C_1$ | 50.6 | 18.7 | 3.6 | 3.6 | 18.7 | | | | | |
| $C_6H_6$ | $C_1$ | 44.4 | 21.8 | 2.0 | 4.7 | 2.0 | 21.8 | | | | |
| $(S)C_6H_6$ | $C_1$ | 45.1 | 22.0 | 1.8 | 4.8 | 1.8 | 22.0 | | | | |
| $(U)C_6H_6$ | $C_1$ | 44.7 | 31.8 | 1.9 | 3.9 | 1.8 | 12.6 | | | | |
| $C_7H_7^+$ | $C_1$ | 39.2 | 23.1 | 3.0 | 2.9 | 2.9 | 3.0 | 23.1 | | | |
| $C_{10}H_8$ | $C_1$ | 44.5 | 28.6 | 1.8 | 4.4 | 0.2 | 0.3 | 0.9 | 1.0 | 14.1 | 1.3 |
| | $C_2$ | 28.6 | 43.7 | 14.8 | 1.8 | 0.3 | 1.0 | 2.1 | 0.9 | 1.7 | 2.7 |
| | $C_9$ | 13.9 | 1.7 | 4.8 | 1.3 | 1.3 | 4.8 | 1.7 | 13.9 | 42.5 | 17.0 |

[a] From ref 79.

for benzene, there is significantly greater delocalization of the $\pi$ density into the basins of the para (4.7%) as compared to the meta carbons (2.0%), despite the distance being shorter in the latter. These data are in concordance with the energy ordering of the principal resonance structures, the Kekulé structures **a** and **b** in Figure 4 being of principal importance,

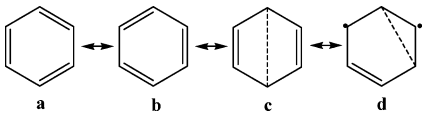


**Figure 4.** Most relevant Kekulé structures for benzene. Adapted with permission from ref 79. Copyright 1996 American Chemical Society.

followed by the structure connecting para-related carbon atoms (Figure 4c) that is, in turn, more relevant than those connecting meta-related ones (Figure 4d). To corroborate what happens in benzene, the effect of geometrical distortions on the delocalization of the $\pi$ electrons in benzene was studied by considering a symmetrical distortion (S), in which each equilibrium C−C bond length of 1.42 Å was increased by 0.06 Å in an $a_{1g}$ stretching mode, and a $b_{2u}$ unsymmetrical one (U) obtained by alternately increasing and decreasing the bond lengths to 1.54 and 1.34 Å (see Figure 3), respectively. The results in Table 6 for both systems show that there is no significant change in the delocalization of the $\pi$ electrons for S; however, for U it is seen how the delocalization between para carbons largely de-

creases. It must be noted that in this work by BSNLS[79] these quantitative data of electron delocalization were corroborated by means of contour maps of the Fermi hole density, which also indicated the larger delocalization of the reference electron in the basin in para than in meta. Naphthalene, another aromatic system, also presents the same tendency as benzene, as can be seen in Table 6.

Comparison of the localization of the Fermi hole density for the cyclic with those for the acyclic molecules demonstrated that the $\pi$ density is delocalized to a significantly greater extent in the former systems and that this delocalization is characteristic of so-called aromatic molecules.[79] This seminal work[79] was the first step toward the application of the AIM theory[64−66] to the analysis of such a complex concept as aromaticity, departing from its possibility of quantifying the electronic delocalization.[21] Integration of the Fermi hole density leads to the LI and DI. The values of the latter also confirm the larger delocalization in para than in meta. For the case of benzene, Bader and co-workers[21,79] obtained the following DIs at the HF/6-31G* level of theory: $\delta(C,C')_{para} = 0.101$ e and $\delta(C,C')_{meta} = 0.070$ e. At the same level of theory, it is important to recognize that Fulton and Mixon (FM)[123] reported some years before almost identical values for $\delta(C,C')_{para}$ and $\delta(C,C')_{meta}$. Interestingly, FM showed that the $\delta(C,C')_{para}$ has a large $\pi$ component (0.09 e), at variance with $\delta(C,C')_{meta}$.[123,186] The larger DI found between para-related carbon atoms than between meta-related carbons has been corroborated using larger basis sets and higher levels of calculation.[221] Therefore, this result is not an artifact of the method used and, consequently, it has a sound physical foundation that has been the basis for the definition of a new index of aromaticity (vide infra).

One year later after the landmark work of BSNLS,[79] Howard and Krygowski (HK)[222] proposed that indices based directly on the charge distribution could provide more sensitive measures of aromaticity than geometry-based ones (i.e., HOMA index).[47] In particular, they studied the aromaticity of a series of benzenoid hydrocarbons by means of a topological charge density analysis derived from the AIM theory.[65] Specifically, HK[222] determined the topological properties $\rho$, $\nabla^2\rho$, and the eigenvalues of the Hessian of $\rho$ at BCPs and ring critical points (RCPs). It was shown that the charge density descriptors at BCPs in benzenoid hydrocarbons are linearly related to the bond length, not providing any new valuable information beyond that present in the equilibrium structure; that is, they have little to add over and above already existing aromaticity indices based on structure.[47] On the other hand, a nice correlation is found between the HOMA or the NICS[220,223] and the same charge density descriptors evaluated at RCPs (see Figure 5). This correlation cannot be explained in any trivial way, opposite to what might be thought of the correlation between the HOMA and charge density descriptors evaluated at the BCPs. In particular, in this case, the curvature of $\rho$ at the RCP perpendicular to the ring plane ($\lambda_3$) gives the best results. Thus, it was proven that the characteristic distribution of

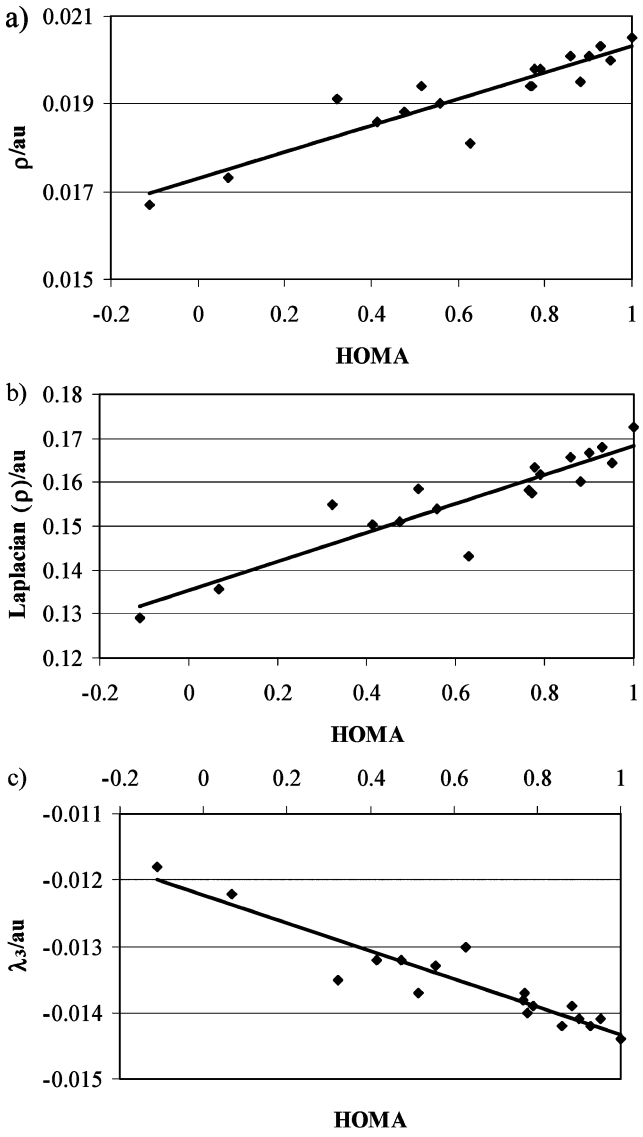


**Figure 5.** Relationship between HOMA and (a) $\rho_c$ ($r^2 = 0.842$), (b) $\nabla^2\rho_c$ ($r^2 = 0.829$), and (c) $\lambda_3$ ($r^2 = 0.876$) at 18 ring critical points of a series of PAHs. Adapted with permission from ref 222. Copyright 1997 NRC Research Press.

electrons in aromatic rings, conveniently summarized at the RCP, can be employed to examine aromaticity.

In line with the above commented work,[222] Molina Molina, El-Bergmi, Dobado, and Portal[224] analyzed the aromaticity of three-membered heterocycle $C_2H_2XOH$ (X = N, P, As) oxides by means of the one-electron density [$\rho(\mathbf{r})$] and its Laplacian [$\nabla^2\rho(\mathbf{r})$] at the different BCPs. The study of the electronic properties of these compounds was complemented by the representation of ELF[96,98,107] isosurface plots. It was concluded that an electronic delocalization, characteristic of aromatic structures, is present only for the unsaturated phosphorus and arsenic oxide derivatives. After that, the nonaromaticity of the amine oxide derivatives can be explained by negative hyperconjugative effects in the N−O bond formation and the similar electronegativity of the N compared to O.

Aromaticity has always been clearly related to the idea of electron delocalization. The above work by HK[222] has shown that an analysis based on only the

one-electron density ($\rho$) provides hardly any new information with respect to the aromatic character obtained from simpler structure-based aromaticity criteria.[47] Therefore, in principle, it seems that aromaticity should be better described by means of the pair density, more related to the concept of electronic delocalization, as already pointed out by BSNLS.[79]

### 3.1.2. New Electronic Aromaticity Criterion: Delocalization Index

CB[157] carried out the first aromaticity study based on the pair density, by applying the DI,[21] derived from the AIM theory,[64−66] to a series of substituted cyclopentadienyl species. This chosen series, from the fully aromatic cyclopentadienyl anion to the antiaromatic borol, was the same as that previously used by Schleyer and co-workers[220] to analyze the performance of the NICS index as a new magnetic-based aromaticity parameter. CB[157] proved that, for a given compound, there exists a good correlation between the DI of the formally single C−C bond (see the schematic representation in Figure 6) and the corresponding homomolecular−homodesmic resonance energy value. Three years later, Poater, Fradera, Duran, and Solà (PFDS)[225] analyzed the same series of compounds to perform a comparison of different aromaticity criteria. Table 7 lists the NICS, aromatic stabilization energies (ASEs), magnetic susceptibility exaltations ($\Lambda$), and DIs for the formally single C−C bond [$\delta$(C−C)] and the formally double C=C bonds [$\delta$(C=C)]. It can be seen that the more aromatic a compound is, the more negative its NICS and $\Lambda$ values and the more positive its ASE are. Also, as reported by CB,[157] the more aromatic the compound is, the smaller the $\delta$(C=C) value and the larger the $\delta$(C−C) value. This is equivalent to saying that the more aromatic the compound, the smaller the difference between the DIs of the formally single and double bonds, with a maximum of aromaticity for the cyclopentadienyl anion, which possesses five equivalent bonds and a totally delocalized five-membered ring (5-MR). To better describe this situation, the $\Delta$DI descriptor was defined as the difference between $\delta$(C=C) and $\delta$(C−C) DIs. It was found that this $\Delta$DI correlates better with other aromaticity criteria than $\delta$(C−C) alone, increasing with a reduction of aromaticity (see Figure 6). Table 7 also lists $\Delta r$, the difference between the single C−C and the double C=C bond lengths. It can be easily seen that larger bond length alternations are associated with lower aromaticities.

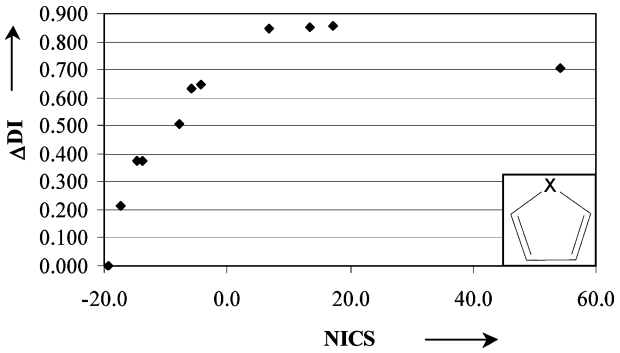


**Figure 6.** Plot of the difference of $\delta$(C=C) and $\delta$(C−C), $\Delta$DI, versus nucleus-independent chemical shifts (NICS) for the series of substituted cyclopentadienyl compounds. Reprinted with permission from ref 225. Copyright 2003 Wiley-VCH.

**Table 7. GIAO-SCF Calculated NICS (ppm), Magnetic Susceptibility Exaltations $\Lambda$ (ppm·cgs), Aromatic Stabilization Energies ASE (kcal·mol$^{-1}$), HF/6-31G* Delocalization Indices $\delta$ (Electrons), Differences between $\delta$(C=C) and $\delta$(C−C), $\Delta$DI (Electrons), and Differences between R(C=C) and R(C−C), $\Delta r$ (Å)[a]**

| $C_4H_4$−$X$ | NICS | ASE | $\Lambda$ | $\delta$(C=C) | $\delta$(C−C) | $\Delta$DI | $\Delta r$ |
|---|---|---|---|---|---|---|---|
| $CH^-$ | −19.4 | 28.8 | −17.2 | 1.388 | 1.388 | 0.000 | 0.000 |
| NH | −17.3 | 25.5 | −12.1 | 1.488 | 1.273 | 0.214 | 0.036 |
| S | −14.7 | 22.4 | −10.0 | 1.597 | 1.221 | 0.376 | 0.043 |
| O | −13.9 | 19.8 | −9.1 | 1.576 | 1.200 | 0.376 | 0.062 |
| $SiH^-$ | −8.0 | 13.8 | −7.7 | 1.684 | 1.179 | 0.505 | 0.054 |
| PH | −5.9 | 7.0 | −3.3 | 1.752 | 1.121 | 0.631 | 0.088 |
| $CH_2$ | −4.2 | 3.7 | −2.4 | 1.746 | 1.100 | 0.647 | 0.111 |
| AlH | 6.9 | −6.8 | 11.2 | 1.892 | 1.044 | 0.848 | 0.144 |
| $SiH^+$ | 13.4 | −24.1 | 13.2 | 1.860 | 1.009 | 0.851 | 0.161 |
| BH | 17.2 | −19.3 | 12.8 | 1.873 | 1.018 | 0.855 | 0.160 |
| $CH^+$ | 54.2 | −56.7 | 32.6 | 1.674 | 0.970 | 0.704 | 0.209 |

[a] All of these parameters have been obtained using the MP2/6-31G* geometries. From ref 225.

In the same work, PFDS[225] introduced a new electronic criterion of local aromaticity, the para-delocalization index (PDI). The proposal of this new index emerged from the observation, by BSNLS in 1996,[79] of a larger electronic delocalization between para-related carbons than between meta-related carbons in benzene, as already commented in section 3.1.1. PDI was defined as the mean of all DIs of para-related carbon atoms in a given six-membered ring (6-MR). PDI provides a local criterion of aromaticity for each of the rings in a polycyclic system, like HOMA and NICS. This fact makes it more useful than a global index of aromaticity for the whole molecule, especially when the aromaticity of large PAHs,[222] fullerenes,[38,226] or nanotubes[227] is being studied. The authors[225] carried out an aromaticity analysis of a series of PAHs to validate the above-introduced new PDI index.

Table 8 contains the magnetic criterion NICS and the geometric HOMA values to be compared to the new electronic PDI index for a series of 11 PAHs (see Figure 7). In general, it is shown that compounds with more negative NICS values also have larger HOMA and PDI measures. This can be better seen by means of panels a and b of Figure 8, which plot PDI versus HOMA and PDI versus NICS, respectively. A very good correlation is achieved between PDI and HOMA, both of which consider benzene to be the most aromatic species. On the other hand, there is some correlation between PDI and NICS, but with five clear exceptions: the aromaticity attributed to the 6B rings of anthracene and naphthacene systems, which have similar environments; the 6A rings of benzocyclobutadiene and biphenylene, which are in contact with a four-membered ring; and the 6A ring of pyracylene. These divergences have been attributed to the effect of the currents of adjacent rings, where NICS is calculated, causing, for instance, an overestimation of the aromaticity of the central rings of polyacenes[228] or an underestimation

**Table 8. HF/6-31+G* Calculated NICS (ppm) and Magnetic Susceptibility Exaltations Λ (ppm·cgs), Together with B3LPY/6-31G* HOMA and HF/6-31G* PDI Delocalization Indices (Electrons)[a]**

| molecule | ring | NICS | Λ | HOMA | PDI |
|---|---|---|---|---|---|
| benzene | 6A | −9.7 | −13.4 | 0.981 | 0.101 |
| naphthalene | 6A | −9.9 | −28.2 | 0.769 | 0.073 |
| phenanthrene | 6A | −10.2 | −47.9 | 0.854 | 0.082 |
| | 6B | −6.5 | | 0.433 | 0.044 |
| triphenylene | 6A | −9.3 | −57.6 | 0.889 | 0.086 |
| | 6B | −2.2 | | 0.047 | 0.025 |
| anthracene | 6A | −8.2 | −49.8 | 0.616 | 0.061 |
| | 6B | −13.3 | | 0.692 | 0.067 |
| chrysene | 6A | −10.1 | | 0.804 | 0.079 |
| | 6B | −7.6 | | 0.541 | 0.052 |
| naphthacene | 6A | −6.8 | | 0.456 | 0.055 |
| | 6B | −13.1 | | 0.602 | 0.062 |
| benzocyclobutadiene | 6A | −2.5 | 9.0 | 0.664 | 0.083 |
| | 4B | 22.5 | | −1.570 | |
| biphenylene | 6A | −5.1 | −7.9 | 0.835 | 0.089 |
| | 4B | 19.0 | | −1.044 | |
| acenaphthylene | 6A | −8.6 | −32.5 | 0.834 | 0.070 |
| | 5B | 2.9 | | 0.142 | |
| pyracylene | 6A | −0.1 | −8.4 | 0.755 | 0.067 |
| | 5B | 12.8 | | −0.164 | |

[a] All of these parameters have been obtained at the B3LYP/6-31G* geometry. From ref 225.

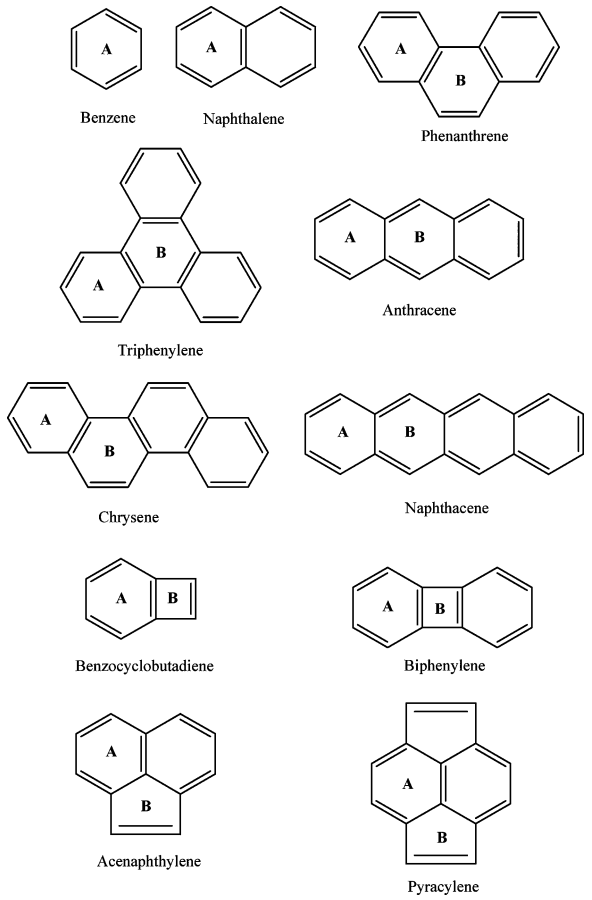


**Figure 7.** Labels for the molecules and rings listed in Table 8, corresponding to the planar polycyclic aromatic hydrocarbons studied. Reprinted with permission from ref 225. Copyright 2003 Wiley-VCH.

for the rings in contact with nonaromatic and paratropic 4- and 5-MRs. This point will be analyzed in more detail later in the present review for pyracylene.[229] It is worth mentioning here that paratropic effects can be exaggerated by single Slater determinant methods. In this sense, Kutzelnigg and coworkers[230] have proven that electron correlation effects (MC-IGLO method) are needed to describe the magnetic properties of antiaromatic systems.

In general, all three aromaticity criteria yield similar results, despite being based on different physical manifestations of aromaticity, which at the same time is the reason for the divergences.[231] This fact is in line with the multidimensional character of aromaticity.[47,231,232] It is considered that only when different aromaticity criteria provide the same ordering can one be quite sure about the relative aromaticity of a series of rings.

At this point a work carried out by Luaña, Martín Pendás, Costales, Carriedo, and García-Alonso[233] should be noted, in which they analyze the topology of cyclophosphazenes, $(NPCl_2)_n$. Similarly to the C−C bond in benzene, the P−N bond in the phosphazene ring also presents a character intermediate between those of single and double bonds. However, opposite to benzene, the phosphazene ring shows neither evidence of the existence of ring currents nor any other sign of aromaticity. The aromaticity of the $(NPCl_2)_3$ system was studied by means of the DIs.[21,65] Whereas for benzene an electronic sharing distributed across the whole $C_6$ ring [$\delta(C,C)_{ortho} = 1.39$ e, $\delta(C,C)_{meta} = 0.07$ e, $\delta(C,C)_{para} = 0.10$ e], for the $[PN]_3$ ring exists, the PN bond presents a large ionic component [$\delta(P,N)_{ortho} = 0.63$ e] and, accordingly, a much reduced pair sharing, with a large electron transfer from P to N. Sharing across the ring is negligible except for the $N_3$ group formed by the N atoms in meta [$\delta(N,N)_{meta} = 0.20$ e, $\delta(P,P)_{meta} < 0.01$ e].

Slightly after the introduction of the PDI as a new electronic aromaticity criterion,[225] Matta and Hernández-Trujillo (MH)[173,234] proposed another local aromaticity index, $\theta$, similar to the geometric HOMA,[47] but using the DI as a measure of electron-sharing alternation within a ring. The HOMA was reformulated in terms of DIs,[21,65] thus $\theta$ was defined as

$$\theta = 1 - \frac{c}{n}\sqrt{\sum_{i=1}^{n}(\delta_0 - \delta_i)^2} \qquad (44)$$

where $c$ (= 0.1641) is a constant such that $\theta = 0$ for cyclohexane, $n$ is the number of members in the ring, $\delta_0$ (= 3.0170) is a reference value, the total electron delocalization of a carbon atom of benzene with all other C atoms in that molecule, and $\delta_i$ is the total electron delocalization of a carbon atom with the other carbon atoms forming a ring in a given PAH.

MH[234] calculated $\theta$ for a series of PAHs (see Figures 7 and 9 and Table 9). As for PDI, the highest value of $\theta$ corresponds to benzene ($\theta = 1$), obtaining aromatic dilution in all other cases. When compared to other already existing local aromaticity criteria, $\theta$ perfectly correlated with HOMA, and a relatively good correlation with NICS was also found (values of HOMA and NICS were not included in their paper). Also, $\theta$ values appear over a wider range than HOMA values, indicating that $\theta$ is a sensitive and appropriate measure of aromaticity. Therefore, it is seen how the values of $\theta$ parallel those of the HOMA

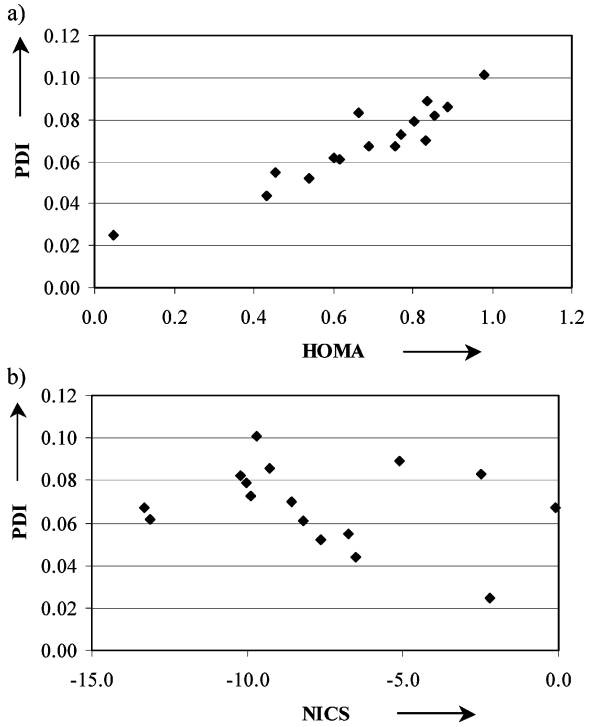


**Figure 8.** (a) Plot of PDI versus HOMA for the series of planar polycyclic aromatic hydrocarbons ($r^2 = 0.871$); (b) plot of PDI versus NICS for the series of planar polycyclic aromatic hydrocarbons ($r^2 = 0.070$). Reprinted with permission from ref 225. Copyright 2003 Wiley-VCH.

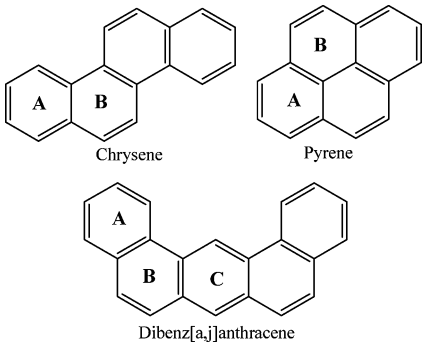


**Figure 9.** Ring labels for some of the polycyclic aromatic hydrocarbons listed in Table 9. Adapted from ref 234. Copyright 2003 American Chemical Society.

index, a bond length alternation model the foundation of which lies in the strong correlation between bond length and bond order. By comparison of these $\theta$ values with previously obtained PDI values (see Table 8) for common molecules (benzene, naphthalene, phenanthrene, and anthracene), it can be seen how both measures follow the same behavior. This is in line with the above-commented good correlation between PDI and HOMA for a similar series of PAHs. At variance with PDI, the index $\theta$ comprises all atoms connected to each other in any ring.

Noticeably, in the same work, MH[234] also established a link between the two-electron indices and both the geometric as well as the one-electron properties. For a series of PAHs, strong correlations were found between different bonding descriptors: carbon−carbon bond length, electron density at the BCP, the Laplacian of the electron density at the BCP, the bond ellipticity, and the carbon−carbon DI. Thus, in some cases, it may be enough just to focus on properties derived from the one-electron density because of the lower computational cost. However, more accurate results make it necessary to refer to the pair density to quantify the electron delocalization of a system.

**Table 9. Electron-Delocalization-Based Local Aromaticity Index $\theta$ for Rings in Some Polycyclic Hydrocarbons and Related Systems[a]**

| | $\theta$ | | |
|---|---|---|---|
| molecule | A | B | C |
| benzene | 1.000 | | |
| biphenyl | 0.963 | | |
| 9,10-dihydroanthracene | 0.960 | 0.278 | |
| tetralin | 0.960 | 0.133 | |
| biphenyl (TS) | 0.959 | | |
| 9,10-dihydrophenanthrene | 0.942 | 0.274 | |
| phenanthrene | 0.863 | 0.650 | |
| chrysene | 0.844 | 0.707 | |
| pyrene | 0.816 | 0.619 | |
| naphthalene | 0.807 | | |
| anthracene | 0.722 | 0.764 | |
| dibenz[*a*,*j*]anthracene | 0.604 | 0.809 | 0.877 |
| 1,3-cyclohexadiene | 0.456 | | |
| cyclohexene | 0.206 | | |
| cyclohexane | 0.000 | | |

[a] From ref 234.

### 3.1.3. Homoaromaticity, a Particular Case

A particular case of aromaticity, homoaromaticity,[235] has also been taken into study by means of the AIM theory.[236,237] The concept of homoaromaticity was introduced into chemistry by Winstein,[238] triggering numerous experimental investigations.[239] However, a theoretical formulation of homoaromaticity is still an unresolved problem. In general, one essential feature of homoaromaticity is the union of a cyclopropane moiety with an unsaturated linear segment (see Figure 10a).[240] In 1983, Cremer, Kraka,

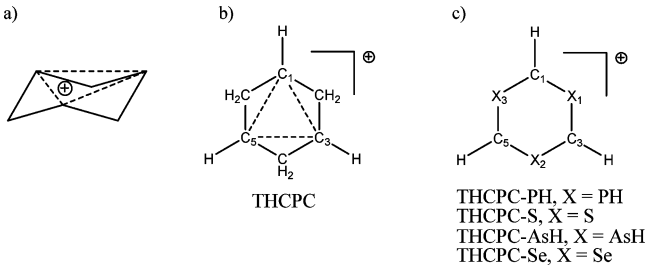


**Figure 10.** Schematic representation of THCPC and derived systems taken under study. Adapted from ref 237. Copyright 2003 American Chemical Society.

Slee, Bader, Lau, Nguyendang, and MacDougall (CKSBLNM)[236] carried out a study illustrating how the AIM theory can be used to provide an answer to whether homoaromatic conjugation is present in a given system. The proximity of the RCPs and BCPs induces cyclopropane to possess significant ellipticities, a key characteristic of these homoaromatic species. Thus, a lengthening of the inserted CC bond (dashed line in Figure 10a) of cyclopropane will cause the RCP to move closer to the CC BCP, thereby enhancing its ellipticity and reducing its bond order. A conceivable result of such an interaction is a ring

of CC bonds, all with equal ellipticities and all with their major axes parallel to the ring axis, thus, an aromatic system. In particular, the requirements for the formation of a homoaromatic system were established by CKSBLNM as (a) a C1−C3 bond path (see Figure 10b), which closes a potentially aromatic ring of CC bonds; (b) the C1−C3 bond path being longer that that in an isolated cyclopropane, thus lowering the C1−C3 bond order to a value less than unity; and (c) the angle between the plane of the three-membered ring and the unsaturated framework being ~90° to obtain the proper alignment of major axes.[236]

More recently, Werstiuk and Wang (WW)[237] have tried to elucidate the aromaticity of trishomocyclopropenyl cation (THCPC) and related species, predicted to possess three pentacoordinated carbons in 6-MRs (see Figure 10c). In this case, at difference with the above work,[236] the pair density has been used and DIs[21] have been calculated, in addition to criteria derived from the one-electron density. Figure 11 displays the molecular graphs for some

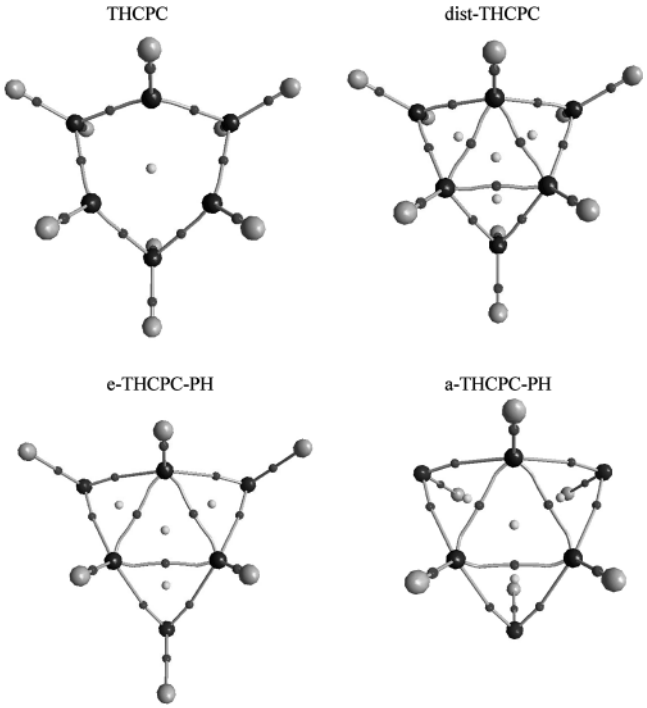


**Figure 11.** Displays of molecular graphs of THCPC and some derived systems, including bond and ring critical points. Adapted from ref 237. Copyright 2003 American Chemical Society.

of the systems studied: THCPC, dist-THCPC, e-THCPC-PH, and a-THCPC-PH (the prefix dist- refers to longer C−C distances, and e- and a- refer to the isomers in which the hydrogens are equatorial and axial, respectively), including the BCPs and RCPs found. For THCPC, no bond paths between C1, C3, and C5 are found at any level of theory, so there are no pentacoordinated carbons in this carbocation. Only when the C1−C3, C3−C5, and C1−C5 are fixed at 1.576 Å (dist-THCPC) does it become a $\sigma,\sigma$-bond homoconjugated species, although it is topologically unstable given the proximity of the BCPs to the RCP. On the other hand, when $CH_2$ groups of THCPC are replaced with PH (see Figure 11), S, AsH, or Se, bond paths are found, giving the presence of three pentacoordinated carbons in the 6-MRs. Table 10 contains the main DIs corresponding to the systems studied. It is seen how THCPC possesses the lowest $\delta$(C1,C3), in concordance with the no existence of bond path between two carbon atoms, compared to the rest of the systems. In addition, the AIM DIs show that more than three electrons are delocalized in each system (see Table 10). Delocalization of the two electrons from the remote C1−C3 bond is the driving force for the formation of the $C_{3v}$ structure, and this results in the involvement of more bonds/electrons in the delocalization. This includes the C−X and C−H bonds and the lone pairs on X.[237]

**Table 10. Delocalization Indices $\delta$(A,B) (Electrons) at the B3PW91/6-311G(d,p) Level for THCPC and Related Species[a]**

| cation[b] | $\delta$(C1,C3) | $\delta$(C,X) | $\delta$(C,H) | $\Sigma\delta$(A,B)[c] |
|---|---|---|---|---|
| THCPC | 0.477 | 0.987 | 0.917 | 3.845 |
| e-THCPC-PH | 0.677 | 0.781 | 0.926 | 3.842 |
| a-THCPC-PH | 0.648 | 0.788 | 0.929 | 3.801 |
| THCPC-S | 0.523 | 1.077 | 0.884 | 4.084 |
| e-THCPC-AsH | 0.650 | 0.845 | 0.923 | 3.913 |
| a-THCPC-AsH | 0.621 | 0.857 | 0.927 | 3.883 |
| THCPC-Se | 0.573 | 1.023 | 0.892 | 4.084 |

[a] From ref 237. [b] The prefixes e- and a- refer to the isomers in which the hydrogens are equatorial and axial, respectively. [c] $\Sigma\delta(A,B) = 2\delta(C1,C3) + 2\delta(C,X) + \delta(C,H)$.

Therefore, it was shown that THCPC does not have homoaromaticity, being necessary a high-energy distortion to convert it into a species that presents three pentacoordinate carbons. However, by replacing the methylenes of THCPC by PH, S, AsH, and Se, homoaromatic species are achieved. Thus, WW[237] concluded that, for these species to be homoaromatic, the presence of long polarizable C−X bonds with ionic character is required. In the formation of these pentacoordinated compounds, the DIs between C1−C3, C3−C5, and C1−C5 increase, whereas the DIs to the X atoms decrease to maintain the sum of the DIs at the optimal value. It must be mentioned that this work was complemented by ELF analysis.[96]

In 2000, El-Bergmi, Dobado, Portal, and Molina Molina[241] also studied the stabilization of neutral bicyclic sulfoxide compounds, which were supposed to be due to homoaromaticity, by means of the AIM theory.[21,65] By comparison to previously analyzed similar compounds such as 7-norbornadienyl chloride [stabilized by a (0.2.2) longicyclic interaction] or 7-norbornenyl chloride (stabilized by a homoaromatic 3c−2e interation),[242] they concluded that 5-thiabicyclo-[2.1.1]hex-2-ene *S*-oxide derivatives were stabilized in the same way as the former compound because of the presence of a C2−C3 double bond and the S−O bond in an *exo* configuration (see Figure 12).[241] Thus, once again, the efficiency of the AIM theory as a tool to analyze homoaromaticity was proven.

### *3.1.4. Aromaticity of Planar and Bowl-Shaped Polycyclic Aromatic Hydrocarbons and Fullerenes*

Fullerenes[243] present an ambiguous aromatic character,[38,244,245] with some properties that support the aromatic view of these systems and others that do

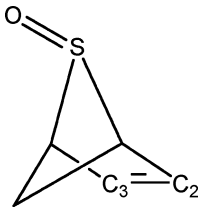


**Figure 12.** Schematic representation of 5-thiabicyclo-[2.1.1]hex-2-ene *S*-oxide.

not. For instance, magnetic properties show extensive cyclic $\pi$-electron delocalization and substantial ring currents; however, against their aromaticity, these systems are very reactive. On the other hand, buckybowls (curved PAHs) display fullerene-like physicochemical properties, thus, in principle, having aromaticity similar to that of fullerenes. To clarify such an important property of fullerenes, especially relevant to an understanding of its reactivity, a study based on the electronic aromaticity criterion PDI[225] was carried out by PFDS.[226,246] PDI, HOMA, and NICS measures were calculated to analyze the local aromaticity of a series of planar and bowl-shaped PAHs and fullerenes. The work focused on the change of local aromaticity of 6-MRs when going from benzene to buckminsterfullerene ($C_{60}$).

Table 11 contains the HF/6-31G*//AM1 values of the NICS, HOMA, and PDI indices and the average

**Table 11. HF/6-31G*//AM1 Calculated Values of NICS (ppm), HOMA, Para-delocalization (PDI) (Electrons) Indices, and Average Pyramidalization Angles for the Carbon Atoms Present in a Given Ring (Pyr) (Degrees) for a Series of Aromatic Compounds[a]**

| molecule | ring | NICS | HOMA | PDI | Pyr |
|---|---|---|---|---|---|
| $C_6H_6$ | 6A | −11.7 | 0.987 | 0.101 | 0.0 |
| $C_{10}H_8$ | 6A | −11.3 | 0.807 | 0.074 | 0.0 |
| $C_{14}H_8$ | 6A | −2.7 | 0.603 | 0.067 | 0.0 |
| | 5B | 13.1 | −0.205 | | 0.0 |
| $C_{20}H_{10}$ | 6A | −8.6 | 0.652 | 0.058 | 4.6 |
| | 5B | 7.6 | 0.357 | | 9.1 |
| $C_{26}H_{12}$ | 6A | −5.6 | 0.474 | 0.037 | 6.9 |
| | 5B | 3.9 | −0.142 | | 6.3 |
| | 6C | −10.0 | 0.746 | 0.078 | 2.8 |
| $C_{30}H_{12}$ | 6A | −6.5 | 0.390 | 0.043 | 9.2 |
| | 5B | 6.8 | 0.113 | | 10.1 |
| | 6C | −9.4 | 0.652 | 0.061 | 5.1 |
| | 6D | −8.1 | 0.614 | 0.057 | 4.6 |
| $C_{60}$ | 6A | −6.8 | 0.256 | 0.046 | 11.6 |
| | 5B | 6.3 | −0.485 | | 11.6 |

[a] From ref 246.

of the pyramidalization angles for several rings of the studied planar ($C_6H_6$, $C_{10}H_8$, $C_{14}H_8$) and curved ($C_{20}H_{20}$, $C_{26}H_{12}$, $C_{30}H_{12}$) molecules and for $C_{60}$ (see Figures 7 and 13). It is seen that the three local indices of aromaticity almost give the same order for the different rings of the PAHs studied. A clear aromatic character is assigned to the hexagonal rings of benzene, naphthalene, and $C_{20}H_{10}$ and to the outer 6-MRs of $C_{26}H_{12}$ (C) and $C_{30}H_{12}$ (C and D), whereas the inner 6-MRs of $C_{26}H_{12}$ (A), $C_{30}H_{12}$ (A), and $C_{60}$ are found to be moderately aromatic. Although the 6-MRs of PAHs and fullerenes display significant local aromaticities, the 5-MRs have antiaromatic character. Noticeably, all aromaticity criteria coincide to indicate that benzene presents the largest aromaticity of this series. The results also show that there is a certain convergence in the local aromaticity of the inner 6-MRs when going from the most aromatic benzene to the partially aromatic $C_{60}$. Finally, for the bowl-shaped PAHs, unexpectedly, the most pyramidalized outer rings possess the largest local aromaticities. It is worth mentioning a previous work by Melchor Ferrer and Molina Molina[247] in which the electronic structure and aromaticity of $C_{30}H_{12}$ in four different conformations were studied by means of a one-electron density AIM analysis and by NICS, respectively. The aromaticity given by NICS values coincides with that for the equivalent structure reported above.

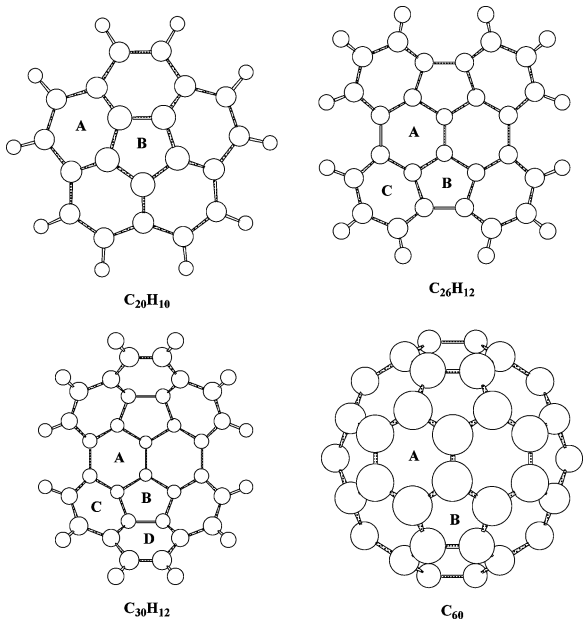


**Figure 13.** Some of the molecules listed in Table 11 with the labels for the different rings studied. Reprinted with permission from ref 246. Copyright 2003 Wiley-VCH.

The aromaticity of $C_{70}$ fullerene is also worth analyzing,[246] as the structure arises from the insertion of an equatorial belt of five 6-MRs to $C_{60}$, thus increasing the number of different bonds (from two to eight) and rings (from two to five) with respect to $C_{60}$ (see Figure 14).[248] This makes $C_{70}$ display different reactivities and local aromaticities.[249,250] The larger reactivity of the pole suggests that this region

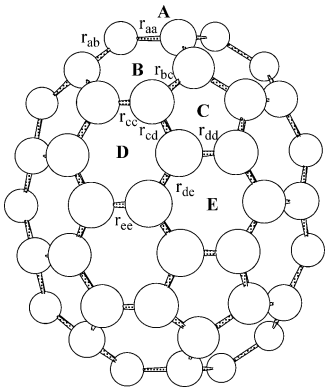


**Figure 14.** Structure of the $C_{70}$ fullerene, together with the labels given to each ring and to each bond studied. Reprinted with permission from ref 246. Copyright 2003 Wiley-VCH.

must be less aromatic than the equatorial belt. To confirm this hypothesis, PFDS[246] calculated the PDI, HOMA, and NICS[37] indices for the different rings, the values of which are listed in Table 12. All three

**Table 12. HF/6-31G*//AM1 Calculated Values of NICS (ppm), HOMA, Para-delocalization (PDI) (Electrons) Indices, and Average Pyramidalization Angles for the Carbon Atoms Present in a Given Ring (Pyr) (Degrees) for the $C_{70}$ Fullerene[a]**

| molecule | ring | NICS | HOMA | PDI | Pyr |
|---|---|---|---|---|---|
| $C_{70}$ | 5A | 2.8 | −0.481 | | 11.9 |
| | 6B | −11.5 | 0.294 | 0.046 | 11.8 |
| | 5C | −1.3 | −0.301 | | 11.0 |
| | 6D | −8.8 | 0.141 | 0.028 | 10.1 |
| | 6E | −17.3 | 0.697 | 0.059 | 9.6 |

[a] From ref 246.

aromaticity criteria coincide in showing that ring E, as expected, presents the largest aromaticity, followed by ring B, which is located in the pole, and, unexpectedly, by ring D, even though this is located in the equatorial belt. By comparison to the $C_{60}$ results in Table 11, rings B and E are more aromatic than the 6-MRs of $C_{60}$. This agrees with the generally accepted greater aromaticity of $C_{70}$ than of $C_{60}$,[38,244] despite the former being more reactive.[249,251] On the other hand, somewhat surprising are the NICS values of $C_{70}$, with the value for ring E (−17.3) being considerably larger than that of benzene (−11.7), or the aromaticity of ring B (−11.5) being much larger than that of $C_{60}$ (−6.8), even though they present similar geometric environments and pyramidalization angles. PDI and HOMA values give more reasonable results, indicating that ring E of $C_{70}$ has a lower aromaticity than benzene and that ring B of $C_{70}$ has a similar aromaticity as compared to the 6-MR of $C_{60}$.

In line with the above-discussed aromaticity of buckminsterfullerene ($C_{60}$), recently, Poater, Duran, and Solà[252] have measured the electron delocalization in $C_{60}$, with the aim of discussing whether the electron charge of each carbon is more or less localized into the corresponding atomic basin as compared to the values found for prototypical aromatic molecules such as benzene or naphthalene. It has been seen that the electron charge of an atom in $C_{60}$ is mostly delocalized into the 13 closest atoms (first layer), enclosing two 6-MRs and two 5-MRs. As one moves away from the first layer, the DIs rapidly tend to 0. In addition, the global electron delocalization of $C_{60}$ per carbon atom cannot be considered poor, being very similar to that of clearly aromatic systems, even though it does not behave in the same way. This is attributed to the fact that the electron charge of each carbon atom in $C_{60}$ can be delocalized into many more atoms than in smaller aromatic systems such as benzene or naphthalene, thus giving an unexpectedly large value for the global DI per carbon atom. However, when the electron delocalization is analyzed from a local point of view, it is seen that $C_{60}$ has a lower delocalization and aromaticity than typical aromatic molecules, because of its partial $\pi$-bond localization that disfavors particularly the delocalization between carbon atoms in para positions.

Noticeably, Giambiagi, de Giambiagi, dos Santos Silva, and de Figueiredo (GGSF)[253] also carried out an aromaticity study on linear and angular hydrocarbons with benzenoid rings by means of a MO multicenter bond index involving the $\sigma + \pi$ electron population of all atoms constituting the ring. The multicenter bond index ($I_{ring}$)[253] introduced by GGSF is an extension of the two- (eq 26) and three-center (eq 42) bond indices.[254] It must be emphasized that the $I_{ring}$ index does not make use of the AIM partition of the molecular space in atomic basins. Instead, it replaces the integrations over atomic basins by a Mulliken-like partitioning. Then, with respect to the results,[253] for PAHs with linearly fused rings, $I_{ring}$ increases, going from the external ring toward the internal ones, whereas for phenanthrene the opposite tendency is observed. These results are in agreement with those obtained by means of the PDI index.[255]

### 3.1.5. Substituent Effect and Aromaticity

The benzene molecule is considered to be the archetype of aromaticity, fulfilling all criteria attributed to this property.[46] This molecule has been used as the reference for the proposal of quantitative descriptors of the substituent effects, that is, the Hammett substituent constants.[256] Recently, Krygowski, Ejsmont, Stepién, Cyrañski, Poater, and Solà (KESCPS)[257] have tried to establish a relationship between the substituent effect and the changes suffered by the $\pi$-electron delocalization structure, which is responsible for its aromaticity.

KESCPS[257] have taken a series of monosubstituted derivatives of benzene in order to study this relationship between aromaticity and the substituent effect. Aromaticity has been measured by means of the magnetic-based NICS, the geometry-based HOMA, and the electronic-based PDI indices, with the corresponding values listed in Table 13. Meanwhile, the substituent effect has been taken into account through different substituent constants, which are also listed in Table 13. From the results it is seen that, even

**Table 13. GIAO/HF/6-31+G* NICS, B3LYP/6-311+G** HOMA, and B3LYP/6-311G** PDI Aromaticity Indices, Calculated at the B3LYP/6-311+G** Geometry for the Different Substituted Benzene Structures[a]**

| X | NICS | HOMA | PDI | $\sigma^+/\sigma^-$ | $\sigma_m$ | $\sigma_p$ | $R^+/R^-$ |
|---|---|---|---|---|---|---|---|
| $NN^+$ | −10.6 | 0.96 | 0.080 | 3.43 | 1.76 | 1.91 | 1.85 |
| NO | −9.8 | 0.98 | 0.091 | 1.63 | 0.62 | 0.91 | 1.14 |
| $NO_2$ | −10.9 | 0.99 | 0.096 | 1.27 | 0.71 | 0.78 | 0.62 |
| CN | −10.3 | 0.98 | 0.096 | 1 | 0.56 | 0.66 | 0.49 |
| COCl | −9.9 | 0.98 | 0.095 | 1.24 | 0.51 | 0.61 | 0.78 |
| $COCH_3$ | −9.7 | 0.98 | 0.097 | 0.84 | 0.38 | 0.5 | 0.51 |
| $COOCH_3$ | −9.8 | 0.98 | 0.097 | 0.75 | 0.37 | 0.45 | 0.14 |
| COOH | −9.7 | 0.98 | 0.097 | 0.77 | 0.37 | 0.45 | 0.43 |
| CHO | −9.6 | 0.97 | 0.095 | 1.03 | 0.35 | 0.42 | 0.70 |
| $CONH_2$ | −9.9 | 0.98 | 0.098 | 0.61 | 0.28 | 0.36 | 0.35 |
| CCH | −10.1 | 0.97 | 0.096 | 0.53 | 0.21 | 0.23 | 0.31 |
| Cl | −10.7 | 0.99 | 0.099 | 0.19 | 0.37 | 0.23 | −0.31 |
| F | −11.7 | 0.99 | 0.098 | −0.03 | 0.34 | 0.06 | −0.52 |
| H | −9.7 | 0.99 | 0.103 | 0 | 0 | 0 | 0 |
| Ph | −9.3 | 0.98 | 0.098 | −0.18 | 0.06 | −0.01 | −0.30 |
| $CH_3$ | −9.7 | 0.98 | 0.100 | −0.31 | −0.07 | −0.17 | −0.32 |
| $OCH_3$ | −10.8 | 0.98 | 0.094 | −0.78 | 0.12 | −0.27 | −1.07 |
| $NH_2$ | −9.8 | 0.98 | 0.093 | −1.3 | −0.16 | −0.66 | −1.38 |
| OH | −10.8 | 0.99 | 0.095 | −0.92 | 0.12 | −0.37 | −1.25 |

[a] Substituent constants: $\sigma^+$, $\sigma^-$, $\sigma_m$, $\sigma_p$, $R^+$, and $R^-$. From ref 257.

though the natures of the substituents vary in a considerable extent along the series ($\sigma_p$ varying from −0.66 for a strongly electron-donating $NH_2$ substituent to 0.91 for a strongly electron-accepting $NN^+$ one), no apparent aromaticity changes are observed. This is perfectly seen through the low variation of the aromaticity indices considered, proving the high resistance of the $\pi$-electron structure of benzene. This also agrees with the preference of benzene for substitution reactions, allowing it to keep its initial $\pi$-electron structure, instead of undergoing addition reactions. When KESCPS[257] looked for a direct relationship between the aromaticity indices and the substituent constants, only the PDI index presented a significant correlation. Therefore, PDI proves to be a good descriptor of the changes of $\pi$-electron delocalization in substituted benzenes. It must be also said that ASEs derived from homodesmic reaction schemes were also calculated for the present series (values not included). However, it was shown that ASE values, like HOMA and NICS, do not reflect the effect of substituents to the $\pi$-electron structure of monosubstituted benzene, achieving values probably contaminated by some additional effects (i.e., strain, conjugation, etc).

Also recently, Poater, García-Cruz, Illas, and Solà (PGIS)[258] have analyzed the substituent effect in a series of carbazole derivatives (see Figure 15) by

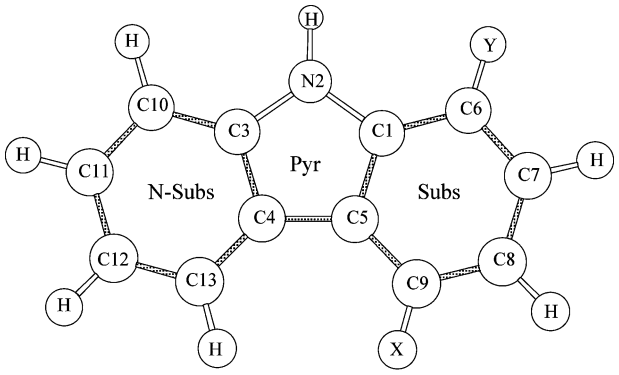


X = H, $CH_3$, OH, Br, CN, $COCH_3$, COOH
Y = H, $COCH_3$

**Figure 15.** Schematic representation of carbazole and the different substituted compounds analyzed. Reprinted with permission from ref 258. Copyright 2004 Royal Society of Chemistry.

measuring different local aromaticity criteria. The work was carried out with the aim of finding quantitative predictions about the reactivity of these systems as a function of the substituent. As for the previous work, NICS, HOMA, and PDI indices have been used to evaluate the aromaticity of the three different rings. The corresponding values are given in Table 14. The results from the three aromaticity criteria are scattered over a narrow range of values, especially those of NICS and PDI. In addition, a clear divergence in the ordering of the different systems by local aromaticity values given by the three methods is observed. Figure 16 clearly shows the diverse

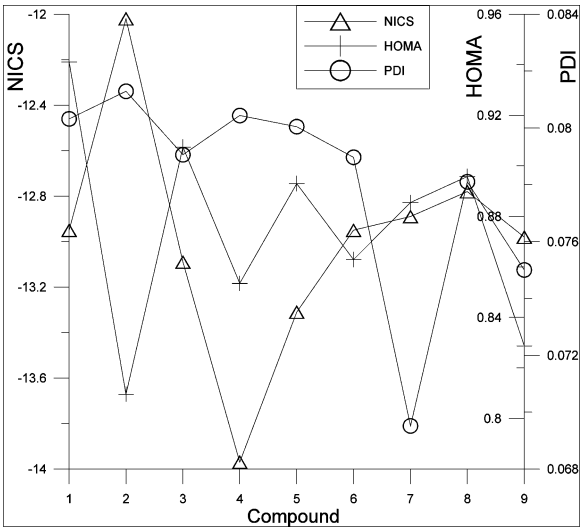


**Figure 16.** Comparative plot of HOMA, NICS, and PDI for the substituted ring (Subs in Table 14) for the series of carbazole derivatives studied. The *x*-plot numeration can be found in Table 14. Reprinted with permission from ref 258. Copyright 2004 Royal Society of Chemistry.

ordering afforded by the different methods by means of an overall comparison of the values for the substituted 6-MR. Therefore, at variance with previous aromaticity analyses that presented a relatively good agreement among the different aromaticity criteria, in this case one must be very cautious with the results. It is also seen in this case that substituents slightly affect the $\pi$-electron structure of the aromatic ring, as reflected by the small variations in the values of the aromaticity indices used. Moreover, all of these indices change in different ways when going from one substituent to another, which is not completely unexpected considering that the aromaticity descrip-

**Table 14. B3LYP/6-31++G** NICS (ppm), PDI (Electrons), and HOMA Calculated Values for the Substituted (Subs), Pyrrolic (Pyr), and Nonsubstituted (N-Subs) Rings of the Series of Carbazole Derivatives Studied[a]**

| | | | | NICS | | | PDI | | HOMA | | |
|---|---|---|---|---|---|---|---|---|---|---|---|
| molecule | | X | Y | Subs | Pyr | N-Subs | Subs | N-Subs | Subs | Pyr | N-Subs |
| CZ | 1 | H | H | −12.95 | −10.24 | −12.95 | 0.082 | 0.082 | 0.919 | 0.679 | 0.919 |
| N− | 2 | - | H | −12.02 | −12.02 | −12.02 | 0.071 | 0.071 | 0.929 | 0.690 | 0.929 |
| CZ−$CH_3$ | 3 | $CH_3$ | H | −13.09 | −10.33 | −12.81 | 0.079 | 0.082 | 0.904 | 0.648 | 0.912 |
| CZ−OH | 4 | OH | H | −13.97 | −10.83 | −13.35 | 0.075 | 0.082 | 0.920 | 0.653 | 0.912 |
| CZ−Br | 5 | Br | H | −13.31 | −10.92 | −13.85 | 0.078 | 0.082 | 0.915 | 0.654 | 0.919 |
| CZ−CN | 6 | CN | H | −12.95 | −10.67 | −13.32 | 0.075 | 0.082 | 0.903 | 0.694 | 0.916 |
| CZ−$COCH_3$ | 7 | $COCH_3$ | H | −12.89 | −10.61 | −12.92 | 0.077 | 0.081 | 0.797 | 0.400 | 0.891 |
| CZ−COOH | 8 | COOH | H | −12.78 | −10.66 | −13.10 | 0.078 | 0.082 | 0.894 | 0.599 | 0.908 |
| $CH_3$−CZ−$COCH_3$ | 9 | $CH_3$ | $COCH_3$ | −12.98 | −9.67 | −12.07 | 0.072 | 0.083 | 0.859 | 0.636 | 0.928 |

[a] From ref 258.

tors employed are all based on different physical properties. Because the different indices provide different orderings of the rings according to their aromaticity, it is important to remark that it is not possible to have a definitive answer about the relative aromaticity of the aromatic rings in these carbazole derivatives.

At this point, it is also worth analyzing how metal cations or ionization affects the aromaticity of the Watson−Crick guanine−cytosine base pair (GC). This subject has been treated by Poater, Sodupe, Bertran, and Solà,[200] in particular, the interaction of $Cu^+$, $Ca^{2+}$, and $Cu^{2+}$ with GC. Table 15 contains the

**Table 15. NICS (ppm), PDI (Electrons), and HOMA Aromaticity Measures of the Five- and Six-Membered Rings of Guanine (G) and the Six-Membered Ring of Cytosine (C) Computed with the B3LYP Method[a]**

| | NICS | | | PDI | | HOMA | | |
|---|---|---|---|---|---|---|---|---|
| system | G-5 | G-6 | C-6 | G-6 | C-6 | G-5 | G-6 | C-6 |
| GC | −11.94 | −4.10 | −1.86 | 0.036 | 0.040 | 0.848 | 0.795 | 0.703 |
| $[GC]^{\bullet+}$ | −5.41 | −0.31 | −2.49 | 0.023 | 0.042 | 0.829 | 0.550 | 0.773 |
| $Ca^{2+}$−GC | −10.67 | −4.76 | −2.53 | 0.044 | 0.045 | 0.843 | 0.886 | 0.797 |
| $Cu^{+}$−GC | −10.64 | −4.59 | −2.25 | 0.040 | 0.043 | 0.869 | 0.898 | 0.761 |
| $Cu^{2+}$−GC | −7.37 | −2.00 | −3.07 | 0.022 | 0.040 | 0.915 | 0.760 | 0.822 |

[a] From ref 200. Details about the basis set used can be found in ref 200.

aromaticity results (HOMA, PDI, and NICS) for the 6- and 5-MRs of the systems taken into study (see Figure 1). The H-bond formation in GC implies a certain loss of $\pi$ charge on $N_1$ and a gain on $O_6$, respectively, thus increasing the relevance of the resonance structure **2** (see Figure 17), which favors

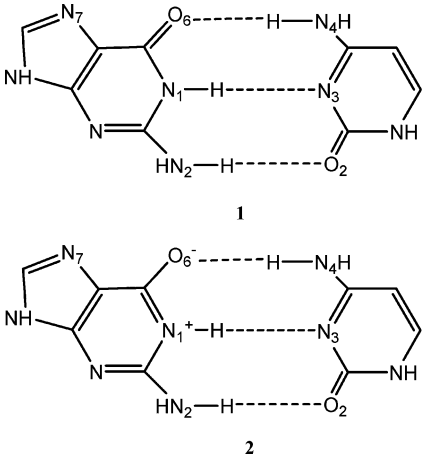


**Figure 17.** Schematic representation of the charge transfer in GC base pair. Reprinted with permission from ref 200. Copyright 2005 Taylor and Francis.

the intensification of the aromatic character of the guanine 6-MR. The increase of the aromaticity of the guanine and cytosine 6-MRs because of the interactions with $Cu^+$ and $Ca^{2+}$ was also attributed to the strengthening of H-bonding in the GC pair, which stabilizes the charge separation resonance structure **2**.[259] This effect is stronger for the divalent $Ca^{2+}$ metal cation than for the monovalent $Cu^+$. Meanwhile, the observed reduction of aromaticity in the 5-MRs and 6-MRs of guanine due to ionization or interaction with $Cu^{2+}$ is caused by the oxidation process that removes a $\pi$ electron, disrupting the $\pi$ electron distribution.

Connected to the above work, more recently, Krygowski, Zachara, and Szatylowicz[260] have presented a study on how H-bonding affects the aromaticity of the ring in the case of phenol and *p*-nitrophenol complexes interacting with fluoride. They have concluded that aromaticity depends monotonically on the strength of the H-bond. The overall effect of changes is substantial: HOMA ranges in ∼0.45 unit and $NICS(1)_{zz}$ in ∼14 ppm, and both variations strongly depend on the substituent effect.

### *3.1.6. Aromaticity Divergences in Pyracylene*

In the work[225] in which the PDI index was introduced as a new electronic aromaticity criterion, the authors found that the 6-MR of pyracylene was one of the rings showing a bad correlation between NICS and PDI values with respect to its local aromaticity (see point 2 of the present section). NICS found the 6-MRs of pyracylene to be nonaromatic, whereas HOMA and PDI attributed a medium aromaticity to them. In a very recent work, Poater, Solà, Viglione, and Zanasi (PSVZ)[229] have analyzed the origin of these differences in pyracylene. There are at least two reasons for considering that this difference is due to an underestimation of aromaticity by NICS. First, at difference with HOMA and PDI, which show a regular reduction of aromaticity when going from naphthalene to acenaphthylene and to pyracylene, NICS shows a surprising drop of aromaticity from acenaphthylene to pyracylene (see Figure 7 and Table 16).[225] This drop is unexpected considering previous

**Table 16. HF/6-31+G* Calculated NICS (ppm), B3LYP/6-31G* HOMA, and HF/6-31G* PDI Delocalization Indices (Electrons)[a]**

| compound | NICS | HOMA | PDI |
|---|---|---|---|
| naphthalene | −9.9 | 0.769 | 0.073 |
| acenaphthylene | −8.6 | 0.834 | 0.070 |
| pyracylene | −0.1 | 0.755 | 0.067 |

[a] All of these parameters refer to the six-membered ring of each species and have been obtained at the B3LYP/6-31G* geometry. From ref 229.

works that have shown that cyclopentafusion causes only a small reduction of local aromaticity of the pyrene system.[261] Second, the NICS of $C_{60}$ is −6.8 ppm, being much more aromatic than pyracylene, although the latter is the structural unit of the former.[37,38,246] To prove the hypothesis of a possible underestimation by NICS of the aromaticity of the 6-MR in pyracylene, PSVZ[229] have analyzed the effect of pyracylene pyramidalization by imposing angles of $\theta$°[262] between the planes defined by the rings (see Figure 18),

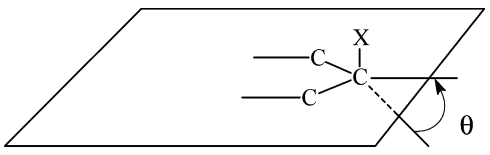


**Figure 18.** Schematic representation of how pyracylene has been pyramidalized. Reprinted with permission from ref 229. Copyright 2004 American Chemical Society.

**Table 17. $\theta$ Angle (Degrees), PDI (Electrons), and HOMA Indices at Hexagons, HOMO−LUMO Energy Difference (eV), NICS Values at Hexagons (ppm), and Average Magnetizabilities (ppm au) for the Different Distorted Pyracylene Molecules Optimized at the B3LYP/6-31G** Level of Theory[a]**

| $\theta$ | PDI | HOMA | $\Delta E_{HOMO-LUMO}$ | NICS(0) | $NICS(1)_{in}$ | $NICS(1)_{out}$ | $\chi$ |
|---|---|---|---|---|---|---|---|
| 0 | 0.0675 | 0.755 | 2.84 | −0.1 | −2.8 | −2.8 | −875 |
| 10 | 0.0672 | 0.761 | 2.83 | −0.1 | −3.8 | −2.1 | −917 |
| 20 | 0.0666 | 0.771 | 2.82 | −0.6 | −5.5 | −1.6 | −989 |
| 30 | 0.0656 | 0.744 | 2.80 | −1.7 | −7.6 | −1.2 | −1076 |
| 40 | 0.0646 | 0.572 | 2.79 | −3.7 | −9.9 | −0.8 | −1057 |

[a] From ref 229.

on NICS, HOMA, and PDI indices, and ring currents.

Table 17 lists the values obtained from the global (HOMO−LUMO difference and average magnetizability) and local [HOMA, NICS(0) and PDI] aromaticity criteria for the different pyramidalized pyracylenes. With respect to PDI, there is a small reduction of local aromaticity with an increase of the angle of distortion, in agreement with previous experimental[42,263] and theoretical results[264,265] on distorted aromatic rings. HOMA yields a similar trend with a slight deviation for $\theta = 10$ and 20°, as well as the HOMO−LUMO gap, which slightly decreases when the pyramidalization increases. On the other hand, unexpectedly, the local NICS(0) and the global average magnetizability magnetic-based measures show an increase of aromaticity with the distortion of the pyracylene plane. To get a deeper insight into the origin of the apparent failure of magnetic-based indices of aromaticity for this system, the ring current density maps (at 0.9 au above the ring plane studied) of pyracylene were analyzed.[266] For the planar pyracylene, dominant paratropic ring currents circulating on pentagons can be observed, more intense than the diatropic ring current flowing on the naphthalene perimeter (see Figure 19). However, when the pyramidalization increases, the diatropic ring current remains quite constant (see Figure 20a), but the paratropic ring current in the pentagonal rings decreases to a breaking point for $\theta = 40°$ (see Figure 20b). Moreover, it is also possible to get quantitative information from the ring currents by calculating the magnetic shielding tensors. In particular, the out-of-plane component, $\sigma_{out}$, is the negative of the $NICS(0)_{zz}$ value, recently defined as a better aromaticity measure than NICS(0) itself.[267,268] $\sigma_{out}$ is −6.2 for the 6-MR of the plane pyracylene, compared with 8.2 for benzene. The unexpected negative value of pyracylene for a diatropic ring can only be attributed to the intense paratropic ring currents on pentagons ($\sigma_{out} = -61.5$), thus largely influencing the value for the 6-MRs. When bending, $\sigma_{out}$ for pentagons becomes less negative; thus, $\sigma_{out}$ for hexagons also increases up to 7.9 for $\theta = 40°$, a value very close to that of benzene. Therefore, these values perfectly corroborate that information already obtained from the ring current density maps.

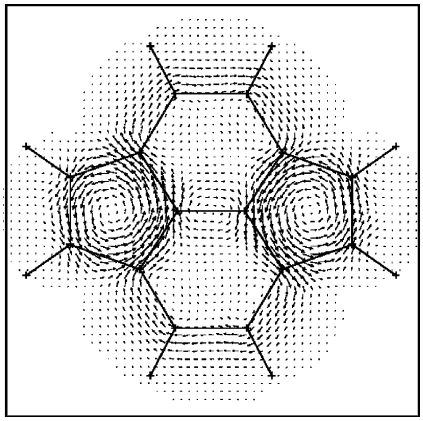

**Figure 19.** First-order $\pi$-electron current density map in planar pyracylene calculated with the 6-31G** basis set using the CTOCD-DZ2 approach at the B3LYP/6-31G** optimized geometry. The plot plane lies at 0.9 au above the molecular plane. The unitary-inducing magnetic field is perpendicular and pointing outward so that diatropic/paratropic circulations are clockwise/counterclockwise. Reprinted with permission from ref 229. Copyright 2004 American Chemical Society.

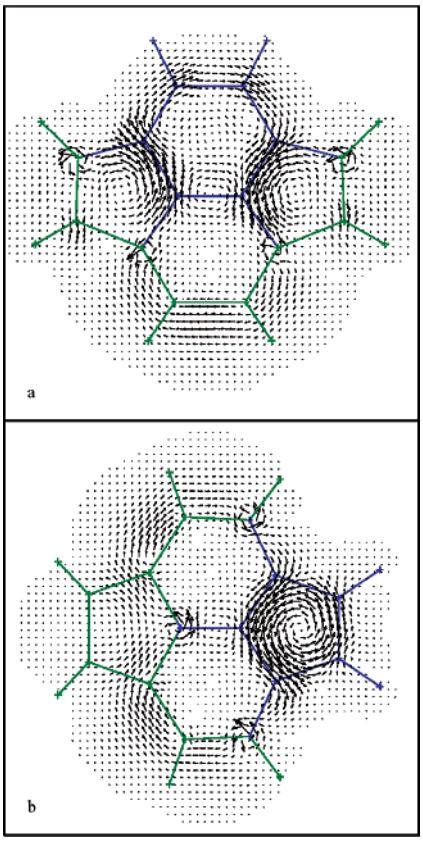


**Figure 20.** Same as Figure 19 for the distorted $\theta = 40°$ pyracylene. The plot plane is parallel to (a) a 6-MR ring (in blue) or (b) a 5-MR (in blue). The green portion of the molecular frame lies above the plot plane. Reprinted with permission from ref 229. Copyright 2004 American Chemical Society.

In addition, the NICS at 1 Å above and below the center of the ring [$NICS(1)_{out}$ and $NICS(1)_{in}$, respectively], considered to better reflect the $\pi$-electron effects,[267,269] have also been calculated for these systems. The values in Table 17 show that NICS(0) and $NICS(1)_{in}$ follow the same trend, thus increasing the aromaticity with bending; however, $NICS(1)_{out}$ follows the expected opposite behavior, like HOMA and PDI. Therefore, it is seen that pyracylene is a problematic case for the NICS indicator of aromaticity, which yields different results depending on where it is calculated. Ring current density maps have proven that there is not a real increase of aromaticity when bending. The observed NICS(0) reduction in the 6-MRs of pyracylene upon bending is due to, first, a strong reduction of the paratropic ring current in the adjacent pentagonal rings and, second, the fact that the paratropic currents point in other directions their effects.

### 3.1.7. Fluctuation of Electronic Charge as Aromaticity Descriptor

The most recent work about the application of the AIM theory[65] to analyze aromaticity has been carried out by Matito, Duran, and Solà (MDS).[270] A new electronic aromaticity measure, the aromatic fluctuation index (FLU), which describes the fluctuation of electronic charge between adjacent atoms in a given ring, has been introduced. The FLU index is based on the fact that aromaticity is related to the cyclic delocalized circulation of $\pi$ electrons, and it is defined by considering not only the amount of electron sharing between contiguous atoms, which should be substantial in aromatic molecules, but also the similarity of electron sharing between adjacent atoms. It is defined as

$$\mathrm{FLU} = \frac{1}{n}\sum_{\mathrm{A-B}}^{\mathrm{RING}}\left[\left(\frac{\mathrm{Flu(A\rightarrow B)}}{\mathrm{Flu(B\rightarrow A)}}\right)^{\delta}\left(\frac{\delta(\mathrm{A,B}) - \delta_{\mathrm{ref}}(\mathrm{A,B})}{\delta_{\mathrm{ref}}(\mathrm{A,B})}\right)\right]^2 \quad (45)$$

with $n$ equal to the number of members in the ring, $\delta_{ref}(C,C) = 1.4$, which was taken from benzene as in ref 21, and fluctuation from atom A to atom B reads as

$$\mathrm{Flu(A\rightarrow B)} = \frac{\delta(\mathrm{A,B})}{\sum_{\mathrm{B}\neq\mathrm{A}}\delta(\mathrm{A,B})} = \frac{\delta(\mathrm{A,B})}{2[N(\mathrm{A}) - \lambda(\mathrm{A})]} \quad (46)$$

where $\delta(A,B)$ is the DI between basins A and B, $N(A)$ is the population of basin A, and $\lambda(A)$ is the number of electrons localized in basin A.

To validate their index, MDS[270] have applied the FLU index to a series of planar PAHs, and the results have been compared to those given by other aromaticity criteria, such as NICS, HOMA, and PDI. The series of molecules taken into study is represented in Figures 7 and 21, whereas Table 18 lists the corresponding aromaticity criteria values. In general, a good relationship is found among the different indices; thus, systems with more negative NICS values have also larger HOMA and PDI measures and lower FLU indices. This good correspondence can be better seen through Figure 22, panels a−c, which plot FLU in front of HOMA, NICS, and PDI, respectively. From the plots, in general, significant correlations are achieved among these aromaticity indices, although based on different physical properties. Noticeably, the PDI index, which is the most related to the newly defined FLU index, as both are based on the electronic delocalization, presents a lower correlation than HOMA or NICS. With respect to NICS measures, although only NICS(0) values have been included in Table 18, MDS[270] have also calculated NICS(1) and the corresponding out-of-plane

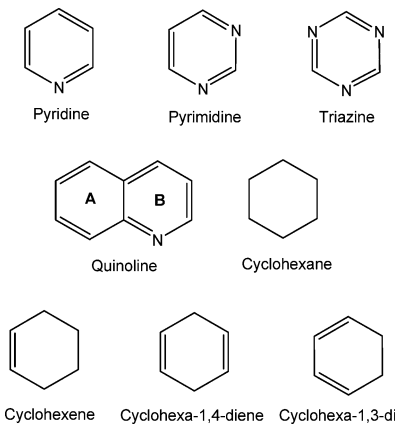


**Figure 21.** Labels for the molecules and rings studied in Table 18. Reprinted with permission from ref 270. Copyright 2004 American Institute of Physics.

**Table 18. HF/6-31G(d) Calculated HOMA, NICS (ppm), PDI (Electrons), and FLU Values for the Studied Systems[a]**

| molecule | ring | HOMA | NICS(0) | PDI | FLU | $FLU_\pi$ |
|---|---|---|---|---|---|---|
| benzene | | 1.001 | −11.5 | 0.105 | 0.000 | 0.000 |
| naphthalene | | 0.779 | −10.9 | 0.073 | 0.012 | 0.114 |
| anthracene | A | 0.517 | −8.7 | 0.059 | 0.024 | 0.251 |
| | B | 0.884 | −14.2 | 0.070 | 0.007 | 0.024 |
| naphthacene | A | 0.325 | −6.7 | 0.051 | 0.031 | 0.350 |
| | B | 0.774 | −13.8 | 0.063 | 0.011 | 0.071 |
| chrysene | A | 0.859 | −11.1 | 0.079 | 0.008 | 0.067 |
| | B | 0.553 | −8.2 | 0.052 | 0.019 | 0.182 |
| triphenylene | A | 0.930 | −10.6 | 0.086 | 0.003 | 0.026 |
| | B | 0.067 | −2.6 | 0.025 | 0.027 | 0.181 |
| pyracylene | A | 0.671 | −4.9 | 0.067 | 0.014 | 0.128 |
| | B | −0.328 | 10.1 | *b* | 0.050 | 0.676 |
| phenanthrene | A | 0.902 | −11.4 | 0.082 | 0.005 | 0.045 |
| | B | 0.402 | −6.8 | 0.053 | 0.025 | 0.255 |
| acenaphthylene | A | 0.797 | −9.6 | 0.070 | 0.013 | 0.114 |
| | B | −0.039 | 2.2 | *b* | 0.045 | 0.578 |
| biphenylene | A | 0.807 | −6.7 | 0.088 | 0.008 | 0.066 |
| | B | −0.930 | 17.4 | *b* | 0.048 | 0.297 |
| benzocyclobutadiene | A | 0.497 | −4.0 | 0.080 | 0.022 | 0.191 |
| | B | −1.437 | 20.2 | *b* | 0.071 | 1.047 |
| pyridine | | 1.005 | −9.5 | 0.097 | 0.001 | 0.001 |
| pyrimidine | | 0.985 | −7.5 | 0.089 | 0.005 | 0.003 |
| triazine | | 0.977 | −5.3 | 0.075 | 0.013 | 0.000 |
| quinoline | A | 0.792 | −11.0 | 0.072 | 0.015 | 0.125 |
| | B | 0.830 | −9.1 | 0.071 | 0.017 | 0.121 |
| cyclohexane | | −4.340 | −2.1 | 0.007 | 0.091 | *c* |
| cyclohexene | | −3.601 | −1.6 | 0.019 | 0.089 | *c* |
| cyclohexa-1,4-diene | | −1.763 | 1.5 | 0.014 | 0.084 | *c* |
| cyclohexa-1,3-diene | | −2.138 | 3.2 | 0.031 | 0.078 | *c* |

[a] From ref 270. [b] PDI cannot be computed for non-6-MRs. [c] Nonplanar molecules that prevent easy and exact $\sigma-\pi$ separation.

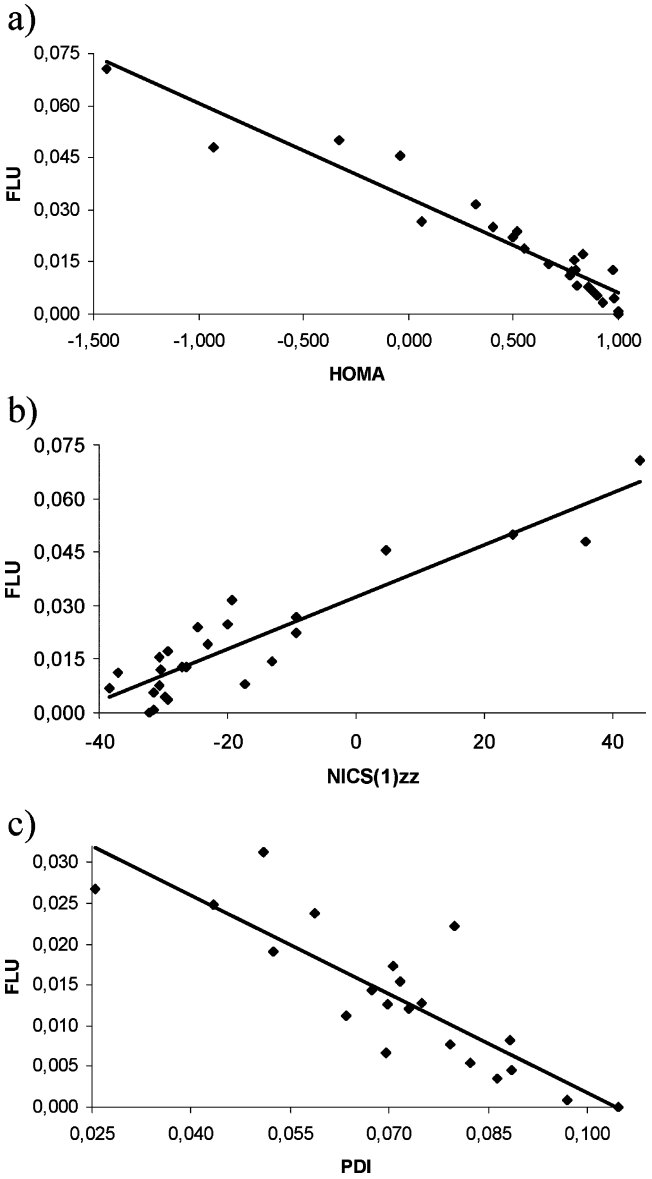


**Figure 22.** Plots of (a) FLU versus HOMA ($r^2 = 0.916$), (b) FLU versus NICS ($r^2 = 0.843$), and (c) FLU versus PDI ($r^2 = 0.706$). Reprinted with permission from ref 270. Copyright 2004 American Institute of Physics.

components [$NICS(0)_{zz}$ and $NICS(1)_{zz}$]. In general, a good correlation is achieved between the four different NICS values and the FLU index.

It is also worth mentioning that, in the same work, MDS[270] have calculated the $FLU_\pi$ index (see Table 18), which takes into account only the $\pi$-component of the DIs and for which, at difference with FLU, no reference parameters are required. The correlation between FLU and $FLU_\pi$ is very good; thus, the use of $FLU_\pi$ for planar systems is encouraged. At variance with the PDI index, which can evaluate only the local aromaticity of 6-MRs, FLU can be applied to any ring or group of rings, thus allowing the measure of both local and global aromaticities.

#### *3.1.8. Summary of the Application of AIM to Aromaticity*

As a whole, in the above section we have shown the efficiency of the AIM theory[65] to analyze aromaticity.[79] Properties derived from the one-electron density ($\rho$, $\nabla^2\rho$, or $\lambda_3$), especially those evaluated at the RCPs, have proven to be useful to study aromatic systems.[222] However, some deficiencies emerge from them, which cause, in some cases, no further valuable information to be obtained from that reached from a structural analysis.[222] This makes it necessary to focus our attention on the pair density, which, in fact, should better describe the electron delocalization, the basis of aromaticity. Based on the pair density, the PDI[225] and FLU[270] indices have proven to be very useful tools to analyze the local aromaticity in different series of compounds. Good correlations have been obtained between PDI and FLU and other widely used existing aromaticity criteria such as HOMA or NICS.[225,246]

The introduction of new aromaticity indices is very important because of the multidimensional character of aromaticity. Katritzky, Krygowski, and co-workers[47,231,232,271] found that mutual relationships between different aromaticity parameters depend strongly on the selection of molecules in the sample. That is why the use of more than one aromaticity parameter for comparisons restricted to some regions or groups of relatively similar compounds is recommended.[231] Accordingly, Krygowski and co-workers pointed out that fully aromatic systems are those cyclic $\pi$-electron species that follow all of the main aromatic criteria, whereas those that do not follow all of them should be considered as partly aromatic.[47,231] So far, the most widely used indices of aromaticity have been based on structural, magnetic, and energetic measures. In this sense, it is very relevant to introduce new aromaticity indices based on other manifestations of aromaticity. The recently introduced PDI[225] and FLU[270] are electronically based indices that exploit the key idea of electron delocalization so often found in textbook definitions of aromaticity.

### 3.2. Electron Localization Function Contributions to Aromaticity

The studies of the properties of aromatic molecules from the ELF topological approach can be classified in three groups. The first group is concerned with the reactivity of aromatic molecules and more specifically the substituent effects in the electrophilic substitution (the Holleman rules).[213,272,273] The second one looks for correlations between ELF indicators and other aromaticity-related properties,[157,274,275] and the third one explicitly discusses the delocalization.[112,211,214,215,276]

#### *3.2.1. Electrophilic Substitution Indicators*

The reactivity of aromatic molecules and more especially the so-called electrophilic substitution has been widely studied and empirically classified according to Holleman's rules[277] and has given rise to fundamental contributions in the MO approach.[278] Topological contributions to this subject are due to Bader[68,279] within the AIM framework and to Gadre and Suresh[280] and to Cubero, Orozco, and Luque[281] within the electrostatic potential topography. The

ELF gradient field enables one to introduce electrophilic substitution positional indices[272] defined as

$$\mathrm{RI}_c(S) = \eta(\mathrm{X}_i,\mathrm{S}) - \eta(\mathrm{X}_i,\mathrm{H}) \quad (47)$$

in which the subscript c denotes the position of the carbon labeled by $i$, that is, ortho, meta, or para. The electrophilic substitution positional index is just the difference of the ELF values at equivalent topological invariants in the S-derivative and in benzene. They are local measures of the perturbation of the ELF by the substituent. These invariants are the index 1 or (3,−1) critical points between two V(C,C) basins sharing the same carbon. These points correspond to the turning points of the bifurcation diagram,[211,212] and the ELF value at these points has been interpreted as a measure of the interaction between different basins and chemically as a measure of electron delocalization.[98,211] As a general rule, for a given species the ortho and para indices have the same sign and the meta index has the opposite sign. A positive index betokens a favored electrophilic substitution position. The ortho, meta, and para positional indices of a series of monosubstituted benzenes calculated at the 6-31G** level are reported in Table 19.

**Table 19. Calculated Electrophilic Positional Indices of Monosubstituted Benzenes ($C_6H_5$-S)[a]**

| S | ortho | meta | para |
|---|---|---|---|
| $NH_2$ | 0.039 | −0.017 | 0.024 |
| OH | 0.030 | −0.012 | 0.018 |
| F | 0.019 | −0.006 | 0.009 |
| $CH_3$ | 0.016 | −0.004 | 0.006 |
| $C_6H_5$ | 0.009 | −0.002 | 0.004 |
| Cl | 0.08 | −0.001 | 0.002 |
| H | 0.0 | 0.0 | 0.0 |
| $CCl_3$ | −0.003 | 0.0 | −0.004 |
| $CF_3$ | −0.008 | 0.001 | −0.006 |
| CN | −0.010 | 0.002 | −0.009 |
| CHO | −0.020 | 0.004 | −0.011 |
| $NO_2$ | −0.030 | 0.006 | −0.015 |

[a] From ref 272.

The electrophilic substitution positional indices are nicely correlated with the Hammett constants,[256] enabling the proposal of the relationships

$$\sigma_{\mathrm{para}} = \sigma' - 40.2\mathrm{RI}_{\mathrm{para}}$$
$$\sigma_{\mathrm{meta}} = \sigma' - 17.8\mathrm{RI}_{\mathrm{meta}} \quad (48)$$

where $\sigma'$ is the so-called polar substituent constant. Moreover, the values of the positional indices of polysubstituted benzenes can be estimated thanks to an additivity rule

$$\mathrm{RI}_{c1c2}(S_1,S_2) = \mathrm{RI}_{c1}(S_1) + \mathrm{RI}_{c2}(S_2) \quad (49)$$

illustrated by the difluorobenzene case in Table 20.

This approach has been generalized to polyaromatic molecules and to aromatic heterocycles[273] for which the ELF function at the (3,−1) critical points between disynaptic basins related to a given center provides a criterion to determine substitutional sites.

**Table 20. Calculated and Estimated Positional Indices of Difluorobenzenes[a]**

| molecule | $c_1$[b] | $c_2$[b] | calcd | estd |
|---|---|---|---|---|
| *o*-$C_6H_4F_2$ | meta | ortho | 0.012 | 0.013 |
| | meta | para | 0.003 | 0.003 |
| | para | meta | 0.003 | 0.003 |
| | ortho | meta | 0.012 | 0.013 |
| *m*-$C_6H_4F_2$ | ortho | ortho | 0.039 | 0.038 |
| | para | ortho | 0.028 | 0.028 |
| | meta | meta | −0.012 | −0.012 |
| | ortho | para | 0.028 | 0.028 |
| *p*-$C_6H_4F_2$ | ortho | meta | 0.013 | 0.013 |

[a] From ref 272. [b] $c_1$ and $c_2$ indicate the position with respect to the substituted carbons.

### 3.2.2. Correlation with Other Indicators

To build an ELF-based aromaticity scale, CB have investigated the correlations between the V(C,C) populations and pair populations with the resonance energies calculated in the homomolecular homodesmic approach.[274] Their study reports excellent correlations for the $C_4H_4X$ (X = BH, $CH^+$, $CH_2$, $CH^-$, N, O, AlH, $SiH_3$, PH, $P^-$, S, $Ge_2$, AsH, Se) series, which can be rationalized by Guggenheim-type curves,[282] that is

$$\rho_r = 1 + \frac{3}{4}(1 - T_r) \pm \frac{7}{4}(1 - T_r)^{1/3} \quad (50)$$

where $\rho_r$ and $T_r$ stand for scaled expressions of the basin populations and of the resonance energies $E(H)$, respectively. Figure 23 displays the C−C bond populations versus $E(H)$ for the $C_4H_4X$ series.

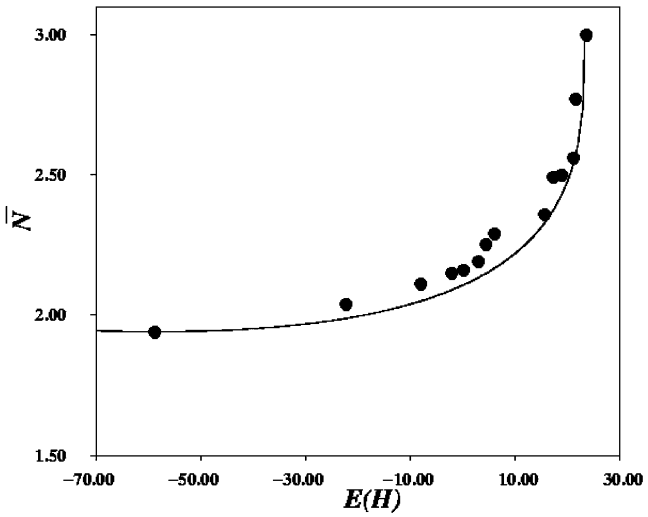


**Figure 23.** ELF V(C,C) basin populations versus resonance energies (kcal/mol). The full line corresponds to Guggenheim's curve.

In a second article[157] the same authors completed their analysis on the same series of molecules considering the interbasins pair numbers $\bar{N}(\Omega_i,\Omega_j) - \bar{N}(\Omega_i)\bar{N}(\Omega_j)$ for both AIM and ELF partitions. The ELF results for the C−C bonds could be rather well fit by the Guggenheim equation,[282] whereas the AIM

values are more sensitive to the bond polarity or the presence of nearby lone pairs.

The AIM and ELF descriptors of the electronic structure of 88 aromatic compounds have been considered to build a database further analyzed within the counter-propagation Kohonen-type neural network framework.[283] It was shown that the constructed descriptor space containing AIM, ELF, and non-quantum-chemical descriptors was successfully able to recognize molecular similarities in a set of 88 compounds and, in particular, to reproduce the dipole moment, the refractive index, and the *n*-octanol/water partition coefficient as target values.

### 3.2.3. $ELF_\pi$ Scale

In two recent papers, Santos et al.[275,284] have proposed new aromaticity scales based on the value of $ELF_\sigma$ and $ELF_\pi$ functions at the (3,−1) critical points of the ELF gradient field between two V(C,C) basins sharing the same carbon already used to define the electrophilic substitution positional indices. The $ELF_\sigma$ and $ELF_\pi$ functions are evaluated by restricting the ELF formula to the $\sigma$ and $\pi$ orbitals, respectively. Table 21 reports the ELF, $ELF_\sigma$, and $ELF_\pi$ values at the bifurcation points.

**Table 21. Bifurcation Values of Total, $\sigma$, and $\pi$ ELF Functions for a Selection of Cyclic and Polycyclic Molecules[a]**

| molecule | total | $\sigma$ | $\pi$ | average |
|---|---|---|---|---|
| $C_6H_6$ ($D_{6h}$) | 0.68 | 0.76 | 0.91 | 0.84 |
| naphthalene | 0.65 | 0.76 | 0.78 | 0.77 |
| anthracene | 0.69 | 0.77 | 0.70 | 0.74 |
| phenanthrene | 0.68 | 0.75 | 0.64 | 0.70 |
| corolene | 0.67 | 0.76 | 0.75 | 0.76 |
| $C_5H_5^-$ ($D_{5h}$) | 0.75 | 0.75 | 0.82 | 0.79 |
| $B_6(CO)_6$ ($D_{6h}$) | 0.60 | 0.68 | 0.85 | 0.77 |
| $Al_4^{2-}$ ($D_{4h}$) | 0.82 | 0.88 | 0.99 | 0.94 |
| $N_5^-$ ($D_{5h}$) | 0.73 | 0.81 | 0.78 | 0.80 |
| $C_4H_4$ ($D_{2h}$) | 0.69 | 0.79 | 0.11 | 0.45 |
| $C_6H_4$ ($D_{2h}$) | 0.69 | 0.78 | 0.15 | 0.47 |
| $C_8H_8$ ($D_{4h}$) | 0.65 | 0.73 | 0.35 | 0.54 |
| $C_6H_6$ ($D_{3h}$) | 0.68 | 0.77 | 0.57 | 0.67 |

[a] From refs 275 and 284.

The analysis, carried out over 13 molecular species, enables one to clearly discriminate aromatic systems from antiaroamatic ones. The values of $ELF_\pi$ are in the 0.11−0.35 range for antiaromatic compounds, whereas they are >0.70 for aromatic compounds. The aromaticity of PAHs is well predicted, and this new indicator also enables one to discuss $\sigma$ and $\pi$ aromaticities. The average value of $ELF_\sigma$ and $ELF_\pi$ of organic molecules is >0.70, whereas the antiaromatic compounds have values of <0.55. The latter scale predicts an overall antiaromatic character for the controversial $Al_4^{2-}$-containing clusters.

### 3.2.4. ELF Covariance Analysis

The ELF covariance analysis of benzene[111] yields unexpected puzzling results. In the case of this molecule, chemical intuition expects the two Kekulé structures to be the dominant mesomeric structures, which is consistent with the traditional VB analysis of Pauling and Wheland,[11] where they account for ~80% of the resonance energy, the remaining being brought by the three Dewar structures (see Figure 4). Approximate V(C,C) basin populations and covariance matrix elements can be estimated in a straightforward way by neglecting the two latter structures:

$$\begin{bmatrix} \bar{N}[V(C1,C2)] = 3.0 \\ \bar{N}[V(C2,C3)] = 3.0 \\ \bar{N}[V(C3,C4)] = 3.0 \\ \bar{N}[V(C4,C5)] = 3.0 \\ \bar{N}[V(C5,C6)] = 3.0 \\ \bar{N}[V(C6,C1)] = 3.0 \end{bmatrix}$$

$$\langle \mathrm{cov} \rangle = \begin{pmatrix} 1 & -1 & 1 & -1 & 1 & -1 \\ -1 & 1 & -1 & 1 & -1 & 1 \\ 1 & -1 & 1 & -1 & 1 & -1 \\ -1 & 1 & -1 & 1 & -1 & 1 \\ 1 & -1 & 1 & -1 & 1 & -1 \\ -1 & 1 & -1 & 1 & -1 & 1 \end{pmatrix} \quad (51)$$

In fact, the results provided by the actual ELF calculation are different: on the one hand, the populations of the *V*(C,C) basin are lower, that is, 2.775, because there is an excess electron population in both carbon cores (2.09) and in the *V*(C,H) basins (2.13). On the other hand, the covariance matrix elements are noticeably smaller than in the ideal Kekulé case; for example, the sum of the other *V*(C,C) contributions to the variance of a given *V*(C,C) basin is only 0.62 and the dominating contributions are those of the two adjacent *V*(C,C) basins. Moreover, there are no positive covariance matrix elements. In the case of planar molecules such as benzene it is possible to partition the populations as well as the covariances in contributions arising from the $\sigma$ and $\pi$ molecular orbitals because the molecular plane is a symmetry element for the whole system as well as to each individual basin. For populations, the $\sigma$ and $\pi$ contributions amount, respectively, to 2.02 and 0.755, whereas for covariance one gets for the first line of the covariance matrix

| | | | | | | |
|---|---|---|---|---|---|---|
| $\sigma$ | 0.30 | −0.14 | −0.01 | 0.0 | −0.01 | −0.14 |
| $\pi$ | 0.32 | −0.13 | −0.02 | −0.02 | −0.02 | −0.13 |
| total | 0.62 | −0.27 | −0.03 | −0.02 | −0.03 | −0.27 |

A possible explanation of the discrepancy with the picture proposed by Pauling and Wheland[11] is that their resonance scheme involves only the Kekulé and Dewar structures and it surprisingly neglects the *ionic structures*, which have been found to noticeably contribute at both SCF and CI levels.[285] In the mesomeric model the resonance structures are necessary to account for the population excess of the *V*(C,H) basins and the noticeable covariance matrix elements between the *V*(C,C) and *V*(C,H) basins, which amounts to −0.22.

The covariance analysis has also been used to discuss the out-of-plane aromaticity and in-plane homoaromaticity in the ring carbomers of [N]annulenes.[214] Figure 24 displays the atomic orbitals that contribute to the conjugation and homoconjugation. The carbomer structure of any given molecule is obtained by inserting a dicarbon $C_2$ unit into each

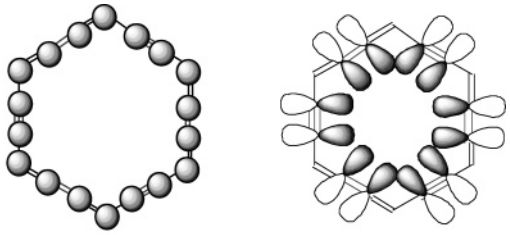


**Figure 24.** Out-of-plane $\pi_z$ conjugation (left) and in-plane $\pi_{xy}$ homoconjugation (right) in the carbobenzene molecule. Reprinted with permission from ref 214. Copyright 2003 American Chemical Society.

bond of its Lewis structure. For example, the carbomer of $H_2$ is HC≡CH, and the ring carbomer of benzene is $C_{18}H_6$:

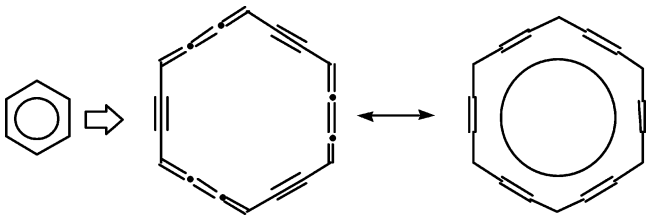

The ELF population and covariance analysis has been carried out on the ring carbomers of benzene ($C_{18}H_6$), cyclopentadienyl cation ($C_{15}H_5^+$), cyclobutadiene ($C_{12}H_4$) in the singlet and triplet spin states, and cyclopropylium anion ($C_9H_3^-$), enabling one to discriminate out-of-plane and in-plane (homo)aromaticities on the basis of the weights of mesomeric structures reported in Table 22.

**Table 22. Relative Weights of Mesomeric Structures of the Carbo[*N*]annulenes from ELF Analysis[a]**

| molecule | point group | no. of $\pi_z$ electrons | no. of $\pi_{xy}$ electrons | out-of-plane contribution | in-plane contribution |
|---|---|---|---|---|---|
| $C_{18}H_6$ | $D_{6h}$ | 18 | 12 | 0.96 | 0.04 |
| $C_{15}H_5^+$ | $D_{5h}$ | 10 | 10 | 0.87 | 0.13 |
| $C_{12}H_4$ | $D_{2h}$ | 12 | 8 | 1.0[b] | 0.0 |
| $C_9H_3^-$ | $D_{3h}$ | 10 | 6 | 0.84 | 0.16 |

[a] From ref 214. [b] For $C_{12}H_4$ the structures considered preserve $D_{2h}$ symmetry and therefore do not really contribute to the in-plane aromaticity.

The carbo[N]annulenes follow Hückel's $4n+2$ rule for both in-plane and out-of-plane (homo)aromaticities: on the one hand the ring carbomer of cyclobutadiene with 8 $\pi_{xy}$ electrons is found to be anti-(homo)aromatic in the singlet spin state, whereas in-plane electron homodelocalization is noticeable only for $C_{15}H_5^+$ and $C_9H_3^-$ involving 10 and 6 $\pi_{xy}$ electrons, respectively. In the [N]pericyclines (the ring carbomers of cycloalkanes) the in-plane homoaromaticity is always weak and the ELF analysis is in good agreement with the NICS values. Indeed, the largest in-plane electron homodelocalization is found for $C_9H_6^-$, which is the only one of the series to exhibit a small negative NICS. The ELF analysis was also used to investigate the ring carbomers of aromatic heterocycles.[215] In contrast to six-membered heterocycles, the ring carbomer of five-membered heterocycles is found to be antiaromatic from both ELF and NICS criteria, whereas both parent molecules are aromatic.

The $V$(C,C) basin populations and their variances provide pieces of information enabling one to discuss the delocalization in aromatic rings. Savin, Silvi, and Colonna[211] pointed out that the $V$(C,C) basin populations in benzene are intermediate between a single bond and a double bond and that the variance is >1, which is consistent with the Kékulé picture. Recently, Hernández-Trujillo, García-Cruz, and Martínez-Madagán[276] have investigated the topological properties of the charge distribution of pyrene of three derived monoradicals and of didehydrogenated pyrene. In pyrene as well as in monoradicals, the populations of all $V$(C,C) basins range between 2.33 and 2.84 except for the two external CC bonds of the rings labeled B in Figure 9, which are clearly double bonds. This representation agrees with results using other indices[286] and with Clar's sextet rule,[287] in which the two rings A are two aromatic sextets and where each ring B has a fixed double bond.

## 4. Concluding Remarks

It has been said that electron delocalization is at the heart of aromaticity. Indeed, delocalization of $\pi$-electrons is invoked in most textbook definitions as the driving force of aromaticity. In this review we have described several criteria of aromaticity that are based on the analysis of electron delocalization. Electron localization/delocalization is not observable and, as a consequence, there are available several theoretical methods to quantify it. In this review, we have concentrated our efforts in the description of those works that analyze electron delocalization and aromaticity employing the most common methods to measure delocalization: the atoms in molecules theory and the electron localization function. We have shown that theoretical studies of electron delocalization have significantly improved our understanding of aromaticity, providing useful information concerning the analysis of some interesting features of this phenomenon such as the aromaticity in fullerenes, substituent effects, electrophilic substitution, and homoaromaticity.

It should be clear from this review that with the state-of-the-art quantum mechanical calculations of electron delocalization one can extract information extremely helpful for the analysis of aromaticity. There is, however, a particular aspect that should be improved in the future. From the examples analyzed in this review, it emerges clearly that, as yet, there is not a single measure of aromaticity that can be universally applied. Indeed, all defined criteria of aromaticity have their own limitations. For instance, NICS overestimates the local aromaticity of the central rings in polyacenes[46,265] and it also fails when predicting an increase of aromaticity with bending in pyracylene.[229] On the other hand, PDI wrongly describes the local aromaticity of largely positively charged fullerenes such as $C_{60}^{10+}$,[221] and both HOMA and FLU fail to describe the changes of aromaticity along the reaction coordinate of the Diels−Alder reaction.[288] Therefore, before studying the aromatic-

ity in a given set of molecules, one has to perform a careful analysis to decide which indices are the most suitable for each situation. The lack of universal nature of all indices available until now reinforces the stated belief of multidimensional character of aromaticity[47,231,232] and the need to look for several aromaticity criteria before a definite conclusion on the aromaticity of a given ring can be reached. Without doubt, the quest for a universal index of aromaticity is likely to be among the main priorities during the coming years in the field of aromaticity.

## 5. Acknowledgments

Financial help has been furnished by the Spanish MCyT Projects BQU2002-0412-C02-02 and BQU2002-03334 and by the DURSI Project 2001SGR-00290. M.S. is indebted to the DURSI of the Generalitat de Catalunya for financial support through the Distinguished University Research Promotion, 2001. J.P., M.D., and M.S. thank Dr. Xavier Fradera and Eduard Matito for stimulating discussions and collaborations. J.P. acknowledges a postdoctoral fellowship (2004BE00028) from the DURSI of the Generalitat de Catalunya.

## 6. Abbreviations

| | |
|---|---|
| 3c-2e | three-center two-electron bond |
| 3c-4e | three-center four-electron bond |
| 5-MR | five-membered ring |
| 6-MR | six-membered ring |
| AFI | atomic Fukui index |
| AIM | atoms in molecules[64−66] |
| AM1 | Austin model 1[289] |
| AO | atomic orbital |
| ASE | aromatic stabilization energies[44] |
| B3LYP | Becke's three-parameter nonlocal exchange and Lee−Yang−Parr 1988 nonlocal correlation functional[290,291] |
| B3PW91 | Becke's three-parameter nonlocal exchange and Perdew−Wang 1991 nonlocal correlation functional[290,292] |
| BCP | bond critical point[64−66] |
| CA | contribution analysis |
| CCSD(T) | coupled-cluster theory with singles and doubles and noniterative estimation of triple excitations method |
| CI | configuration interaction method |
| CISD | configuration interaction with single and double substitutions |
| DFT | density functional theory |
| DI | delocalization index[21] |
| ELF | electron localization function[96] |
| FLU | aromatic fluctuation index[270] |
| GIAO | gauge-independent atomic orbital[293] |
| H-bond | hydrogen bond |
| HF | Hartree−Fock method |
| HOMA | harmonic oscillator model of aromaticity[219] |
| KS | Kohn−Sham |
| LCAO | linear combination of atomic orbitals |
| LI | localization index[21] |
| method 1// method 2 | single-point energy calculation by method 1 at the optimized geometry obtained with method 2 |
| MO | molecular orbital |
| MP2 | second-order Møller−Plesset perturbation theory and quadruple excitations |
| NBO | natural bond orbital[53] |
| NICS | nucleus-independent chemical shift[220] |
| NMR | nuclear magnetic resonance |
| PDI | para-delocalization index[225] |
| PAH | polycyclic aromatic hydrocarbon |
| RCP | ring critical point[64−66] |
| ROHF | restricted open Hartree−Fock |
| SCF | self-consistent field |
| THCPC | trishomocyclopropenyl cation |
| TM | transition metal |
| TS | transition state |
| VB | valence bond |
| VSEPR | valence shell electron pair repulsion[22] |

## 7. References

(1) Brush, S. G. *Stud. Hist. Philos. Sci.* **1999**, *30*, 21.
(2) Brush, S. G. *Stud. Hist. Philos. Sci.* **1999**, *30*, 263.
(3) Kekulé, A. *Justus Liebigs Ann. Chem.* **1865**, *137*, 129. Kekulé, A. *Bull. Acad. R. Belg.* **1865**, *19*, 551. Kekulé, A. *Bull. Soc. Chim. Fr. (Paris)* **1865**, *3*, 98.
(4) Claus, A. *Ber. Ver. Nat. Freiburg i. B* **1867**, *4*, 116.
(5) Armstrong, H. E. *Philos. Mag.* **1887**, *23*, 73. v. Baeyer, A. *Justus Liebigs Ann. Chem.* **1888**, *245*, 103.
(6) Dewar, J. *Proc. R. Soc. Edinburgh* **1867**, *6*, 82.
(7) Thiele, J. *Justus Liebigs Ann. Chem.* **1899**, *306*, 87.
(8) Ingold, C. K. *J. Chem. Soc.* **1922**, *121*, 1133. Ingold, C. K. *J. Chem. Soc.* **1933**, *143*, 1120.
(9) Ingold, C. K. *Chem. Rev.* **1934**, *15*, 225. Ingold, C. K. *Nature* **1934**, *133*, 946. Ingold, C. K. *Proc. R. Soc.* **1938**, *A169*, 149.
(10) Hückel, E. *Z. Physik* **1931**, *70*, 104. Hückel, E. *Z. Physik* **1931**, *72*, 310. Hückel, E. *Z. Physik* **1932**, *76*, 628. Hückel, E. *Z. Elektrochemie* **1937**, *43*, 752.
(11) Pauling, L.; Wheland, G. W. *J. Chem. Phys.* **1933**, *1*, 362.
(12) Ingold, C. K. *Nature* **1938**, *141*, 314.
(13) Shaik, S. S.; Hiberty, P. C.; Le Four, J.-M.; Ohanessian, G. *J. Am. Chem. Soc.* **1987**, *109*, 363. Shaik, S. S.; Shurki, A.; Danovich, D.; Hiberty, P. C. *J. Mol. Struct. (THEOCHEM)* **1997**, *389−399*, 155. Hiberty, P. C.; Shaik, S. S. *Phys. Chem. Chem. Phys.* **2004**, *6*, 224.
(14) Schleyer, P. v. R. *Chem. Rev.* **2001**, *101*, 1115.
(15) Daudel, R.; Bader, R. F. W.; Stephens, M. E.; Borrett, D. S. *Can. J. Chem.* **1974**, *52*, 1310.
(16) Bader, R. F. W.; Stephens, M. E. *J. Am. Chem. Soc.* **1975**, *97*, 7391.
(17) Daudel, R.; Brion, H.; Odiot, S. *J. Chem. Phys.* **1955**, *23*, 2080.
(18) Ponec, R. *J. Math. Chem.* **1997**, *21*, 323.
(19) Ponec, R.; Duben, A. J. *J. Comput. Chem.* **1999**, *20*, 760.
(20) Lewis, G. N. *J. Am. Chem. Soc.* **1916**, *38*, 762.
(21) Fradera, X.; Austen, M. A.; Bader, R. F. W. *J. Phys. Chem. A* **1999**, *103*, 304.
(22) Gillespie, R. J.; Hargittai, I. *The VSEPR Model of Molecular Geometry*; Allyn and Bacon: Boston, MA, 1991. Gillespie, R. J.; Robinson, E. A. *Angew. Chem., Int. Ed. Engl.* **1996**, *35*, 495.
(23) Gillespie, R. J.; Popelier, P. L. A. *Chemical Bonding and Molecular Geometries: From Lewis to Electron Densities*; Oxford University Press: New York, 2001.
(24) Bader, R. F. W.; Stephens, M. E. *Chem. Phys. Lett.* **1974**, *26*, 445.
(25) Bader, R. F. W. In *Localization and Delocalitzation in Quantum Chemistry*; Chalvet, O., Daudel, R., Diner, S., Malrieu, J. P., Eds.; Reidel: Dordrecht, The Netherlands, 1975; Vol. I. Claverie, P.; Diner, S. In *Localization and Delocalization in Quantum Chemistry*; Chalvet, O., Daudel, R., Diner, S., Malrieu, J. P., Eds.; Reidel: Dordrecht, The Netherlands, 1976; Vol. II.
(26) Ziesche, P. *J. Mol. Struct. (THEOCHEM)* **2000**, *527*, 35.
(27) Buijse, M. A.; Baerends, E. J. In *Density Functional Theory of Molecules, Clusters and Solids*; Ellis, D. E., Ed.; Kluwer: Dordrecht, The Netherlands, 1995.
(28) Dobson, J. F. *J. Chem. Phys.* **1991**, *94*, 4328. March, N. H. *Top. Curr. Chem.* **1999**, *203*, 201. Ziesche, P. In *Electron Correlations and Material Properties*; Gonis, A., Kioussis, N., Ciftan, M., Eds.; Kluwer/Plenum: New York, 1999. Baerends, E. J. *Phys. Rev. Lett.* **2001**, *87*, 133004.
(29) Ernzerhof, M.; Burke, K.; Perdew, J. P. In *Recent Developments and Applications of Modern Density Functional Theory*; Seminario, J. M., Ed.; Elsevier: Amsterdam, The Netherlands, 1996.
(30) Baerends, E. J.; Gritsenko, O. V. *J. Phys. Chem. A* **1997**, *101*, 5383.
(31) Web of Knowledge−Institute for Science Information; retrieved in October 2004, Philadelphia, PA.
(32) Hentschel, M.; Kienberger, R.; Spielmann, C.; Reider, G. A.; Milosevic, N.; Brabec, T.; Corkuin, P.; Heinzmann, U.; Drescher, M.; Krausz, F. *Nature (London)* **2001**, *414*, 509. Drescher, M.; Hentschel, M.; Kienberger, R.; Uiberacker, M.; Yakovlev, V.; Scrinzi, A.; Westerwalbeslch, T.; Kleineberg, U.; Heinzmann, U.;

Krausz, F. *Nature (London)* **2002**, *419*, 803. Kienberger, R.; Hentschel, M.; Uiberacker, M.; Spielmann, C.; Kitzler, M.; Scrinzi, A.; Wieland, M.; Westerwalbeslch, T.; Kleineberg, U.; Heinzmann, U.; Drescher, M.; Krausz, F. *Science* **2002**, *297*, 1144. Bandrauk, A. D.; Chelkowski, S.; Nguyen, H. S. *Int. J. Quantum Chem.* **2004**, *100*, 834. Itatani, J.; Levesque, J.; Zeidler, D.; Niikura, H.; Pépin, H.; Kieffer, J. C.; Corkum, P. B.; Villeneuve, D. M. *Nature* **2004**, *432*, 867.
(33) Wiberg, K. B. In *Theoretical and Computational Chemistry*; Maksic, Z. B., Orville-Thomas, W. J., Eds.; Elsevier: Amsterdam, The Netherlands, 1999; Vol. 6.
(34) Gomes, J. A. N. F.; Mallion, R. B. *Chem. Rev.* **2001**, *101*, 1349.
(35) Mitchell, R. H. *Chem. Rev.* **2001**, *101*, 1301.
(36) Saunders: M.; Jiménez-Vázquez, H. A.; Cross, R. J.; Mroczkowski, S.; Freedberg, D. I.; Anet, F. A. *Nature* **1994**, *367*, 256. Saunders, M.; Cross, R. J.; Jiménez-Vázquez, H. A.; Shimshi, R.; Khong, A. *Science* **1996**, *271*, 1693.
(37) Bühl, M. *Chem. Eur. J.* **1998**, *4*, 734.
(38) Bühl, M.; Hirsch, A. *Chem. Rev.* **2001**, *101*, 1153.
(39) McGrady, J. E.; Lovell, T.; Stranger, R. *Inorg. Chem.* **1997**, *36*, 3242. Chevreau, H.; Moreira, I. d. P. R.; Silvi, B.; Illas, F. *J. Phys. Chem. A* **2001**, *105*, 3570. Cabrero, J.; Calzado, C. J.; Maynau, D.; Caballol, R.; Malrieu, J. P. *J. Phys. Chem. A* **2002**, *106*, 8146. Suaud, N.; Gaita-Ariño, A.; Clemente-Juan, J. M.; Coronado, E. *Chem. Eur. J.* **2004**, *10*, 4041.
(40) Soncini, A.; Lazzeretti, P. *J. Chem. Phys.* **2003**, *119*, 1343.
(41) Matta, C. F.; Hernández-Trujillo, J.; Bader, R. F. W. *J. Phys. Chem. A* **2002**, *106*, 7369.
(42) Gready, J. E.; Hambley, T. W.; Kakiuchi, K.; Kobiro, K.; Sternhell, S.; Tansey, C. W.; Tobe, Y. *J. Am. Chem. Soc.* **1990**, *112*, 7537.
(43) Dabestani, R.; Ivanov, I. N. *Photochem. Photobiol.* **1999**, *70*, 10. Hupp, J. T.; Williams, R. D. *Acc. Chem. Res.* **2001**, *34*, 808. Szeghalmi, A. V.; Erdmann, M.; Engel, V.; Schmitt, M.; Amthor, S.; Kriegisch, V.; Nöll, G.; Stahl, R.; Lambert, C.; Leusser, D.; Stalke, D.; Zabel, M.; Popp, J. *J. Am. Chem. Soc.* **2004**, *126*, 7834.
(44) Slayden, S. W.; Liebman, J. F. *Chem. Rev.* **2001**, *101*, 1541.
(45) Glukhovtsev, M. N. *J. Chem. Educ.* **1997**, *74*, 132.
(46) Krygowski, T. M.; Cyrañski, M. K.; Czarnocki, Z.; Häfelinger, G.; Katritzky, A. R. *Tetrahedron* **2000**, *56*, 1783.
(47) Krygowski, T. M.; Cyrañski, M. K. *Chem. Rev.* **2001**, *101*, 1385.
(48) Grabowski, S. J. *J. Mol. Struct.* **2001**, *562*, 137.
(49) Gerratt, J.; Cooper, D. L.; Karadakov, P. B.; Raimondi, M. *Chem. Soc. Rev.* **1997**, 87. Mo, Y.; Song, L.; Wu, W.; Cao, Z.; Zhang, Q. *J. Theor. Comput. Chem.* **2002**, *1*, 137. Solà, M.; Lledós, A.; Duran, M.; Bertran, J. *Int. J. Quantum Chem.* **1991**, *40*, 511. Karafiloglou, P.; Sánchez-Marcos, E. *Int. J. Quantum Chem.* **1992**, *44*, 337. Parrondo, R. M.; Karafiloglou, P.; Pappalardo, R.; Sánchez-Marcos, E. *J. Phys. Chem.* **1995**, *99*, 6461. Karafiloglou, P.; Surpateanu, G. *Int. J. Quantum Chem.* **2004**, *98*, 456. Parrondo, R. M.; Karafiloglou, P.; Sánchez-Marcos, E. *Int. J. Quantum Chem.* **1993**, *47*, 191.
(50) Edmiston, C.; Ruedenberg, K. *Rev. Mod. Phys.* **1963**, *35*, 457.
(51) Boys, S. F. *Rev. Mod. Phys.* **1960**, *32*, 296. Foster, J. M.; Boys, S. F. *Rev. Mod. Phys.* **1960**, *32*, 300.
(52) Daudel, R.; Stephens, M. E.; Kapuy, E.; Kozmutza, C. *Chem. Phys. Lett.* **1976**, *40*, 194.
(53) Foster, J. P.; Weinhold, F. *J. Am. Chem. Soc.* **1980**, *102*, 7211. Reed, A. E.; Curtiss, L. A.; Weinhold, F. *Chem. Rev.* **1988**, *88*, 899.
(54) Giuffreda, M. G.; Bruschi, M.; Lüthi, H. P. *Chem. Eur. J.* **2004**, *10*, 5671. Bharatan, P. V.; Iqbal, P.; Malde, A.; Tiwari, R. *J. Phys. Chem. A* **2004**, *108*, 1059.
(55) Bean, G. P. *J. Org. Chem.* **1998**, *63*, 2497. Sadlej-Sosnowska, N. *J. Org. Chem.* **2001**, *66*, 8737.
(56) Bickelhaupt, F. M.; Baerends, E. J. *Angew. Chem., Int. Ed.* **2003**, *42*, 4183.
(57) Daudel, R. In *The Fundamentals of Theoretical Chemistry*; Pergamon Press: Oxford, U.K., 1965. Aslangul, C.; Constanciel, R.; Daudel, R.; Kottis, P. *Adv. Quantum Chem.* **1972**, *6*, 93.
(58) Chamorro, E.; Fuentealba, P.; Savin, A. *J. Comput. Chem.* **2003**, *24*, 496. Cancès, E.; Keriven, R.; Lodier, F.; Savin, A. *Theor. Chem. Acc.* **2004**, *111*, 373. Gallegos, A.; Carbó-Dorca, R.; Lodier, F.; Cances, E.; Savin, A. *J. Comput. Chem.* **2005**, *26*, 455.
(59) Ziesche, P.; Tao, J.; Seidl, M.; Perdew, J. P. *Int. J. Quantum Chem.* **2000**, *77*, 819.
(60) Fulde, P. *Correlations in Molecules and Solids*; Springer: Berlin, Germany, 1995.
(61) Mödl, M.; Dolg, M.; Fulde, P.; Stoll, H. *J. Chem. Phys.* **1996**, *105*, 2353.
(62) Yu, M.; Dolg, M. *Chem. Phys. Lett.* **1997**, *273*, 329. Yu, M.; Dolg, M.; Fulde, P.; Stoll, H. *Int. J. Quantum Chem.* **1998**, *67*, 157.
(63) Bader, R. F. W.; MacDougall, P. J.; Lau, C. D. H. *J. Am. Chem. Soc.* **1984**, *106*, 1594.
(64) Bader, R. F. W. *Acc. Chem. Res.* **1985**, *18*, 9.
(65) Bader, R. F. W. *Atoms in Molecules: A Quantum Theory*; Clarendon: Oxford, U.K., 1990.
(66) Bader, R. F. W. *Chem. Rev.* **1991**, *91*, 893.
(67) Bader, R. F. W. *Can. J. Chem.* **1998**, *76*, 973.
(68) Bader, R. F. W.; Chang, C. *J. Phys. Chem.* **1989**, *93*, 2946.
(69) Bader, R. F. W. *J. Phys. Chem. A* **1998**, *102*, 7314.
(70) Bader, R. F. W. *Coord. Chem. Rev.* **2000**, *197*, 71.
(71) Scherer, W.; Sirsch, P.; Grosche, M.; Spiegler, M.; Mason, S. A.; Gardiner, M. G. *Chem. Commun.* **2001**, 2072.
(72) Scherer, W.; Sirsch, P.; Shorokhov, D.; Tafipolsky, M.; McGrady, G. S.; Gullo, E. *Chem. Eur. J.* **2003**, *9*, 6057.
(73) Bader, R. F. W.; Johnson, S.; Tang, T. H.; Popelier, P. L. A. *J. Phys. Chem.* **1996**, *100*, 15398.
(74) Davidson, E. R. *Reduced Density Matrices in Quantum Chemistry*; Academic: New York, 1976.
(75) McWeeny, R. In *Methods of Molecular Quantum Mechanics*, 2nd ed.; Academic Press: London, U.K., 1992.
(76) Coleman, A. J. *Int. J. Quantum Chem.* **2001**, *85*, 196. Cioslowski, J. *Many-Electron Densities and Reduced Density Matrices*; Kluwer Academic/Plenum Publishers: New York, 2000. Coleman, A. J. In *The Fundamentals of Electron Density, Density Matrix and Density Functional Theory*; Gidopoulos, N. I., Wilson, S., Eds.; Kluwer Academic Publishers: Dordrecht, The Netherlands, 2003.
(77) Wigner, E.; Seitz, F. *Phys. Rev.* **1933**, *43*, 804.
(78) Maslen, V. W. *Proc. Phys. Soc. A* **1956**, *69*, 734. Cooper, I. L.; Pounder, C. N. M. *Theor. Chim. Acta* **1978**, *47*, 51. Cooper, D. L.; Pounder, C. N. M. *Int. J. Quantum Chem.* **1980**, *17*, 759. Luken, W. L.; Beratan, D. N. *Theor. Chim. Acta* **1982**, *61*, 265. Luken, W. L. *Int. J. Quantum Chem.* **1982**, *22*, 889. Tschinke, V.; Ziegler, T. *J. Chem. Phys.* **1990**, *93*, 8051. Kutzelnigg, W. In *Explicitly Correlated Wave Functions in Chemistry and Physics*; Rychlewski, J., Ed.; Kluwer Academic Publishers: Dordrecht, The Netherlands, 2003; Vol. 13. Ludeña, E. V.; Ugalde, J. M.; Fernández-Rico, J.; Ramírez, G. *J. Chem. Phys.* **2004**, *120*, 540.
(79) Bader, R. F. W.; Streitwieser, A.; Neuhaus, A.; Laidig, K. E.; Speers, P. *J. Am. Chem. Soc.* **1996**, *118*, 4959.
(80) Bader, R. F. W.; Heard, G. L. *J. Chem. Phys.* **1999**, *111*, 8789.
(81) Buijse, M. A.; Baerends, E. J. *Mol. Phys.* **2002**, *100*, 401.
(82) Bo, C.; Sarasa, J. P.; Poblet, J. M. *J. Phys. Chem.* **1993**, *97*, 6362. Laidig, K. E.; Cameron, L. M. *J. Am. Chem. Soc.* **1996**, *118*, 1737.
(83) Julg, A.; Julg, P. *Int. J. Quantum Chem.* **1978**, *13*, 483.
(84) Ponec, R. *Int. J. Quantum Chem.* **1998**, *69*, 193.
(85) Ponec, R.; Carbó-Dorca, R. *Int. J. Quantum Chem.* **1999**, *72*, 85.
(86) Fradera, X.; Poater, J.; Simon, S.; Duran, M.; Solà, M. *Theor. Chem. Acc.* **2002**, *108*, 214.
(87) Bader, R. F. W. In *Encyclopedia of Computational Chemistry*; Schleyer, P. v. R., Ed.; Wiley: Chichester, U.K., 1998; pp 64−86. Popelier, P. L. A. *Atoms in Molecules: An Introduction*; Prentice Hall: Harlow, U.K., 2000.
(88) Fradera, X.; Duran, M.; Mestres, J. *J. Comput. Chem.* **2000**, *21*, 1361.
(89) Ponec, R.; Roithová, J. *Theor. Chem. Acc.* **2001**, *105*, 383. Ponec, R.; Roithová, J.; Gironés, X.; Lain, L.; Torre, A.; Bochicchio, R. *J. Phys. Chem. A* **2002**, *106*, 1019. Ponec, R.; Yuzhakov, G.; Cooper, D. L. *Theor. Chem. Acc.* **2004**, *112*, 419.
(90) Ponec, R.; Roithová, J.; Gironés, X.; Jug, K. *J. Mol. Struct. (THEOCHEM)* **2001**, *545*, 255.
(91) Ponec, R.; Yuzhakov, G.; Carbó-Dorca, R. *J. Comput. Chem.* **2003**, *24*, 1829.
(92) Ponec, R.; Yuzhakov, G.; Gironés, X.; Frenking, G. *Organometallics* **2004**, *23*, 1790.
(93) Bochicchio, R. C.; Torre, A.; Lain, L. *J. Chem. Phys.* **2005**, *122*, 084117.
(94) Gillespie, R. J.; Bayles, D.; Platts, J.; Heard, G. L.; Bader, R. F. W. *J. Phys. Chem. A* **1998**, *102*, 3407.
(95) Lennard-Jones, J. *Proc. R. Soc.* **1949**, *A198*, 1. Lennard-Jones, J. *J. Chem. Phys.* **1952**, *20*, 1024.
(96) Becke, A. D.; Edgecombe, K. E. *J. Chem. Phys.* **1990**, *92*, 5397.
(97) Savin, A.; Becke, A. D.; Flad, J.; Nesper, R.; Preuss, H.; Vonschnering, H. G. *Angew. Chem., Int. Ed. Engl.* **1991**, *30*, 409.
(98) Savin, A.; Nesper, R.; Wengert, S.; Fassler, T. F. *Angew. Chem., Int. Ed. Engl.* **1997**, *36*, 1809.
(99) Silvi, B. *J. Phys. Chem. A* **2003**, *107*, 3081.
(100) Kohout, M. *Int. J. Quantum Chem.* **2004**, *97*, 651. Kohout, M.; Pernal, K.; Wagner, F. R.; Grin, Y. *Theor. Chem. Acc.* **2004**, *112*, 453.
(101) Scemama, A.; Chaquin, P.; Caffarel, M. *J. Chem. Phys.* **2004**, *121*, 1725.
(102) Wigner, E.; Seitz, F. *Phys. Rev.* **1934**, *46*, 509.
(103) Andersen, O. K. *Phys. Rev. B* **1975**, *12*, 3060.
(104) Voronoi, G. F.; Reine, Z. *Angew. Math.* **1908**, *134*, 198.
(105) Fonseca-Guerra, C.; Handgraaf, J.-W.; Baerends, E. J.; Bickelhaupt, F. M. *J. Comput. Chem.* **2003**, *25*, 189.
(106) Gadre, S. R.; Kulkarni, S. A.; Shrivastava, I. H. *J. Chem. Phys.* **1992**, *96*, 5253. Gadre, S. R.; Shirsat, R. N. *Electrostatic of Atoms and Molecules*; University Press: Hyderabad, India, 2000.
(107) Silvi, B.; Savin, A. *Nature* **1994**, *371*, 683.
(108) Mulliken, R. S. *J. Chem. Phys.* **1955**, *23*, 1833.
(109) Noury, S.; Colonna, A.; Savin, A. *J. Mol. Struct. (THEOCHEM)* **1998**, *450*, 59.
(110) Silvi, B. *J. Mol. Struct.* **2002**, *614*, 3.

(111) Diner, S.; Claverie, P. In *Localization and Delocalization in Quantum Chemistry*; Chalvet, O., Daudel, R., Diner, S., Malrieu, J. P., Eds.; Reidel: Dordrecht, The Netherlands, 1976; Vol. II.
(112) Silvi, B. *Phys. Chem. Chem. Phys.* **2004**, *6*, 256.
(113) Fourré, I.; Silvi, B.; Sevin, A.; Chevreau, H. *J. Phys. Chem. A* **2002**, *106*, 2561.
(114) Bader, R. F. W.; Matta, C. F. *Int. J. Quantum Chem.* **2001**, *85*, 592.
(115) Bader, R. F. W.; Bayles, D. *J. Phys. Chem. A* **2000**, *104*, 5579.
(116) Wiberg, K. B. *Tetrahedron* **1968**, *24*, 1083.
(117) Mayer, I. *Chem. Phys. Lett.* **1983**, *97*, 270.
(118) Bochicchio, R.; Ponec, R.; Lain, L.; Torre, A. *J. Phys. Chem. A* **2000**, *104*, 9130. Matito, E.; Poater, J.; Solà, M.; Duran, M.; Salvador, P. *J. Chem. Phys.*, submitted for publication.
(119) Mayer, I. *Int. J. Quantum Chem.* **1986**, *29*, 477. Mayer, I. *Int. J. Quantum Chem.* **1986**, *29*, 73.
(120) Mayer, I.; Knapp-Mohammady, M. *Chem. Phys. Lett.* **2004**, *389*, 34.
(121) Mayer, I.; Salvador, P. *Chem. Phys. Lett.* **2004**, *383*, 368.
(122) Fulton, R. L. *J. Phys. Chem.* **1993**, *97*, 7516.
(123) Fulton, R. L.; Mixon, S. T. *J. Phys. Chem.* **1993**, *97*, 7530.
(124) Fulton, R. L.; Perhacs, P. *J. Phys. Chem. A* **1998**, *102*, 9001.
(125) Fulton, R. L.; Perhacs, P. *J. Phys. Chem. A* **1998**, *102*, 8988. Fulton, R. L. *J. Phys. Chem. A* **2004**, *108*, 11691.
(126) Müller, A. M. K. *Phys. Lett. A* **1984**, *105*, 446.
(127) Wang, Y.-G.; Werstiuk, N. H. *J. Comput. Chem.* **2003**, *24*, 379.
(128) Wang, Y.-G.; Matta, C. F.; Werstiuk, N. H. *J. Comput. Chem.* **2003**, *24*, 1720. Wang, Y.-G.; Matta, C. F.; Werstiuk, N. H. *J. Comput. Chem.* **2004**, *25*, 309 (erratum).
(129) Ángyán, J. G.; Loos, M.; Mayer, I. *J. Phys. Chem.* **1994**, *98*, 5244.
(130) Cioslowski, J.; Mixon, S. T. *J. Am. Chem. Soc.* **1991**, *113*, 4142.
(131) Cioslowski, J.; Mixon, S. T. *Inorg. Chem.* **1993**, *32*, 3209.
(132) Cioslowski, J. *Int. J. Quantum Chem.* **1990**, *S24*, 15. Cioslowski, J. *J. Math. Chem.* **1991**, *8*, 169.
(133) Bader, R. F. W.; Matta, C. F. *Inorg. Chem.* **2001**, *40*, 5603.
(134) Raub, S.; Jansen, G. *Theor. Chem. Acc.* **2001**, *106*, 223.
(135) Kar, T.; Ángyán, J. G.; Sannigrahi, A. B. *J. Phys. Chem. A* **2000**, *104*, 9953.
(136) Kar, T.; Ángyán, J. G.; Sannigrahi, A. B. *J. Phys. Chem. A* **2001**, *105*, 660 (erratum).
(137) Ángyán, J. G.; Rosta, E.; Surján, P. R. *Chem. Phys. Lett.* **1999**, *299*, 1.
(138) Molina Molina, J.; Dobado, J. A.; Heard, G. L.; Bader, R. F. W.; Sundberg, M. R. *Theor. Chem. Acc.* **2001**, *105*, 365.
(139) González Moa, M. J.; Mosquera, R. A. *J. Phys. Chem. A* **2003**, *107*, 5361.
(140) Fradera, X.; Solà, M. *J. Comput. Chem.* **2002**, *23*, 1347.
(141) Matito, E.; Duran, M.; Solà, M. *J. Chem. Educ.* **2005**, in press.
(142) Clark, A. E.; Davidson, E. R. *J. Phys. Chem. A* **2002**, *106*, 6890.
(143) Chesnut, D. B. *Chem. Phys.* **2003**, *291*, 141.
(144) Chesnut, D. B. *Chem. Phys.* **2001**, *271*, 9. Chesnut, D. B. *J. Comput. Chem.* **2001**, *22*, 1702.
(145) Chesnut, D. B. *Heteroat. Chem.* **2002**, *13*, 53.
(146) Chesnut, D. B. *Heteroat. Chem.* **2003**, *14*, 175.
(147) Chesnut, D. B. *J. Phys. Chem. A* **2003**, *107*, 4307.
(148) Chesnut, D. B.; Quin, L. D. *J. Comput. Chem.* **2004**, *25*, 734.
(149) Chesnut, D. B.; Quin, L. D. *Heteroat. Chem.* **2004**, *15*, 216.
(150) Bader, R. F. W.; Slee, T. S.; Cremer, D.; Kraka, E. *J. Am. Chem. Soc.* **1983**, *105*, 5061.
(151) Bochicchio, R.; Lain, L.; Torre, A.; Ponec, R. *J. Math. Chem.* **2000**, *28*, 83.
(152) Bochicchio, R.; Ponec, R.; Torre, A.; Lain, L. *Theor. Chem. Acc.* **2001**, *105*, 292.
(153) Sannigrahi, A. B.; Kar, T. *Chem. Phys. Lett.* **1990**, *173*, 569. Giambiagi, M.; de Giambiagi, M. S.; Mundim, K. C. *Struct. Chem.* **1990**, *1*, 423. Mundim, K. C.; Giambiagi, M.; de Giambiagi, M. S. *J. Phys. Chem.* **1994**, *98*, 6118.
(154) Kar, T.; Sánchez-Marcos, E. *Chem. Phys. Lett.* **1992**, *192*, 14.
(155) Ponec, R.; Mayer, I. *J. Phys. Chem. A* **1997**, *101*, 1738.
(156) Bochicchio, R. C.; Ponec, R.; Uhlík, F. *Inorg. Chem.* **1997**, *36*, 5363. Ponec, R.; Bochicchio, R. C. *Int. J. Quantum Chem.* **1999**, *72*, 127.
(157) Chesnut, D. B.; Bartolotti, L. J. *Chem. Phys.* **2000**, *257*, 175.
(158) Poater, J.; Solà, M.; Duran, M.; Fradera, X. *Theor. Chem. Acc.* **2002**, *107*, 362.
(159) Torre, A.; Lain, L.; Bochicchio, R.; Ponec, R. *J. Math. Chem.* **2002**, *32*, 241. Bochicchio, R. C.; Lain, L.; Torre, A. *Chem. Phys. Lett.* **2003**, *374*, 567. Bochicchio, R.; Lain, L.; Torre, A. *J. Comput. Chem.* **2003**, *24*, 1902. Mitrasinovic, P. M. *Chem. Phys. Lett.* **2004**, *392*, 419.
(160) Lain, L.; Torre, A.; Bochicchio, R. *J. Phys. Chem. A* **2004**, *108*, 4132.
(161) Ponec, R.; Yuzhakov, G.; Cooper, D. L. *J. Phys. Chem. A* **2003**, *107*, 2100.
(162) Valderrama, E.; Ugalde, J. M. *Int. J. Quantum Chem.* **2002**, *86*, 40.
(163) Solà, M.; Mestres, J.; Carbó, R.; Duran, M. *J. Chem. Phys.* **1996**, *104*, 636. Wang, J.; Eriksson, L. A.; Boyd, R. J.; Shi, Z.; Johnson, B. G. *J. Phys. Chem.* **1994**, *98*, 1844. Wang, J.; Shi, Z.; Boyd, R. J.; Gonzalez, C. *J. Phys. Chem.* **1994**, *98*, 6988.
(164) Biegler-König, F. W.; Bader, R. F. W.; Tang, T.-H. *J. Comput. Chem.* **1982**, *3*, 317 (http://www.chemistry.mcmaster.ca/aimpac/).
(165) Biegler-König, F. W. *J. Comput. Chem.* **2000**, *21*, 1040. Biegler-König, F. W.; Schönbohm, J.; Bayles, D. *J. Comput. Chem.* **2001**, *22*, 545. Biegler-König, F. W.; Schönbohm, J. *J. Comput. Chem.* **2002**, *23*, 1489.
(166) Popelier, P. L. A. *Comput. Phys. Commun.* **1996**, *93*, 212. Popelier, P. L. A.; *MORPHY98*; UMIST, Manchester, U.K., 1998; http://morphy.ch.umist.ac.uk/. Malcolm, N. O. J.; Popelier, P. L. A. *J. Comput. Chem.* **2003**, *24*, 1276.
(167) Ortíz, J. C.; Bo, C.; *Xaim*; Universitat Rovira i Virgili, Tarragona, Spain; http://www.quimica.urv.es/XAIM (accessed 2005).
(168) Gatti, C.; Saunders, V. R.; Roetti, C. *J. Chem. Phys.* **1994**, *101*, 10686.
(169) Frisch, M. J.; Trucks, G. W.; Schlegel, H. B.; Scuseria, G. E.; Robb, M. A.; Cheeseman, J. R.; Zakrzewski, V. G.; Montgomery, J. A.; Stratmann, R. E.; Burant, J. C.; Dapprich, S.; Millam, J. M.; Daniels, A. D.; Kudin, K. N.; Strain, M. C.; Farkas, O.; Tomasi, J.; Barone, V.; Cossi, M.; Cammi, R.; Mennucci, B.; Pomelli, C.; Adamo, C.; Clifford, S.; Ochterski, J.; Petersson, G. A.; Ayala, P. Y.; Cui, Q.; Morokuma, K.; Salvador, P.; Dannenberg, J. J.; Malick, D. K.; Rabuck, A. D.; Raghavachari, K.; Foresman, J. B.; Cioslowski, J.; Ortiz, J. V.; Baboul, A. G.; Stefanov, B. B.; Liu, G.; Liashenko, A.; Piskorz, P.; Komaromi, I.; Gomperts, R.; Martin, R. L.; Fox, D. J.; Keith, T.; Al-Laham, M.; Peng, C.; Nanayakkara, A.; Challacombe, M.; Gill, P. M. W.; Johnson, B. G.; Chen, W.; Wong, M. W.; Andres, J. L.; Gonzalez, R.; Head-Gordon, M.; Replogle, E. S.; Pople, J. A. *Gaussian 98*, rev. A11; Pittsburgh, PA, 1998.
(170) Frisch, M. J.; Trucks, G. W.; Schlegel, H. B.; Scuseria, G. E.; Robb, M. A.; Cheeseman, J. R.; Montgomery, J. A., Jr.; Vreven, T.; Kudin, K. N.; Burant, J. C.; Millam, J. M.; Iyengar, S. S.; Tomasi, J.; Barone, V.; Mennucci, B.; Cossi, M.; Scalmani, G.; Rega, N.; Petersson, G. A.; Nakatsuji, H.; Hada, M.; Ehara, M.; Toyota, K.; Fukuda, R.; Hasegawa, J.; Ishida, M.; Nakajima, T.; Honda, Y.; Kitao, O.; Nakai, H.; Klene, M.; Li, X.; Knox, J. E.; Hratchian, H. P.; Cross, J. B.; Bakken, V.; Adamo, C.; Jaramillo, J.; Gomperts, R.; Stratmann, R. E.; Yazyev, O.; Austin, A. J.; Cammi, R.; Pomelli, C.; Ochterski, J. W.; Ayala, P. Y.; Morokuma, K.; Voth, G. A.; Salvador, P.; Dannenberg, J. J.; Zakrzewski, G.; Dapprich, S.; Daniels, A. D.; Strain, M. C.; Farkas, O.; Malick, D. K.; Rabuck, A. D.; Raghavachari, K.; Foresman, J. B.; Ortiz, J. V.; Cui, Q.; Baboul, A. G.; Clifford, S.; Cioslowski, J.; Stefanov, B. B.; Liu, G.; Liashenko, A.; Piskorz, P.; Komaromi, I.; Martin, R. L.; Fox, D. J.; Keith, T.; Al-Laham, M. A.; Peng, C. Y.; Nanayakkara, A.; Challacombe, M.; Gill, P. M. W.; Johnson, B.; Chen, W.; Wong, M. W.; Gonzalez, C.; Pople, J. A. *Gaussian 03*, revison C.01 ed.; Gaussian, Inc.: Pittsburgh, PA, 2003.
(171) Schmidt, M. W.; Baldridge, K. K.; Boate, J. A.; Elbert, S. T.; Gordon, M. S.; Jensen, J. H.; Koseki, S.; Matsunaga, N.; Nguyen, K. A.; Su, S. S.; Windus, T. L.; Dupuis, M.; Montgomery, J. A. *J. Comput. Chem.* **1993**, *14*, 1347.
(172) Karplus, M. *J. Chem. Phys.* **1959**, *30*, 11.
(173) Matta, C. F. *J. Comput. Chem.* **2003**, *24*, 453.
(174) Macchi, P.; Sironi, A. *Coord. Chem. Rev.* **2003**, *238*−*239*, 383.
(175) Molina Molina, J.; Dobado, J. A. *Theor. Chem. Acc.* **2001**, *105*, 328.
(176) Ponec, R.; Cooper, D. L. *Int. J. Quantum Chem.* **2004**, *97*, 1002. Ponec, R.; Yuzhakov, G.; Tantillo, D. J. *J. Org. Chem.* **2004**, *69*, 2992.
(177) Dobado, J. A.; García, H. M.; Molina Molina, J.; Sundberg, M. R. *J. Am. Chem. Soc.* **2000**, *122*, 1144.
(178) Sánchez-González, A.; Martínez-García, H.; Melchor, S.; Dobado, J. A. *J. Phys. Chem. A* **2004**, *108*, 9188.
(179) Mitrasinovic, P. M. *J. Comput. Chem.* **2001**, *22*, 1387. Mitrasinovic, P. M. *J. Comput. Chem.* **2002**, *106*, 7026. Mitrasinovic, P. M. *Chem. Phys.* **2003**, *286*, 1.
(180) Mitrasinovic, P. M. *J. Phys. Chem. A* **2002**, *106*, 7026.
(181) Fulton, R. L. *J. Phys. Chem. A* **2004**, *108*, 11855.
(182) Malcolm, N. O. J.; Gillespie, R. J.; Popelier, P. L. A. *J. Chem. Soc., Dalton Trans.* **2002**, 3333.
(183) Werstiuk, N. H.; Wang, Y.-G. *J. Phys. Chem. A* **2001**, *105*, 11515.
(184) Matta, C. F.; Cow, C. N.; Harrison, P. H. M. *J. Mol. Struct.* **2003**, *660*, 81.
(185) MacDougall, P. J.; Bader, R. F. W. *Can. J. Chem.* **1986**, *64*, 1496.
(186) Mandado, M.; Mosquera, R. A.; Graña, A. *Chem. Phys. Lett.* **2004**, *386*, 454.
(187) Poater, J.; Solà, M.; Rimola, A.; Rodríguez-Santiago, L.; Sodupe, M. *J. Phys. Chem. A* **2004**, *108*, 6072.
(188) Poater, J.; Duran, M.; Solà, M. *J. Comput. Chem.* **2001**, *22*, 1666.
(189) Dobado, J. A.; Molina Molina, J.; Uggla, R.; Sundberg, M. R. *Inorg. Chem.* **2000**, *39*, 2831.
(190) Pilme, J.; Silvi, B.; Alikhani, M. E. *J. Phys. Chem. A* **2003**, *107*, 4506.

(191) Macchi, P.; Garlaschelli, L.; Sironi, A. *J. Am. Chem. Soc.* **2002**, *124*, 14173.
(192) Dewar, M. J. S. *Bull. Soc. Chim. Fr. (Paris)* **1951**, *18*, C79. Chatt, J.; Duncanson, J. S. *J. Chem. Soc.* **1953**, 2929.
(193) Chevreau, H.; Martinsky, C.; Sevin, A.; Minot, C.; Silvi, B. *New J. Chem.* **2003**, *27*, 1049.
(194) Poater, J.; Cases, M.; Fradera, X.; Duran, M.; Solà, M. *Chem. Phys.* **2003**, *294*, 129.
(195) Llusar, R.; Beltrán, A.; Andrés, J. L.; Fuster, F.; Silvi, B. *J. Phys. Chem. A* **2001**, *105*, 9460.
(196) Feliz, M.; Llusar, R.; Andrés, J.; Berski, S.; Silvi, B. *New J. Chem.* **2002**, *26*, 844.
(197) Daza, M. C.; Dobado, J. A.; Molina Molina, J.; Villaveces, J. L. *Phys. Chem. Chem. Phys.* **2002**, *2*, 4089.
(198) Poater, J.; Fradera, X.; Solà, M.; Duran, M.; Simon, S. *Chem. Phys. Lett.* **2003**, *369*, 248.
(199) Morokuma, K. *Acc. Chem. Res.* **1977**, *10*, 294.
(200) Poater, J.; Sodupe, M.; Bertran, J.; Solà, M. *Mol. Phys.* **2005**, *103*, 163.
(201) de Oliveira Neto, M.; de Giambiagi, M. S.; Giambiagi, M. *Chem. Phys. Lett.* **1998**, *290*, 205. Giambiagi, M.; de Giambiagi, M. S.; de Oliveira Neto, M. *Phys. Chem. Chem. Phys.* **2001**, *3*, 5059.
(202) Chesnut, D. B.; Bartolotti, L. J. *Chem. Phys.* **2002**, *278*, 101.
(203) Lendvay, G. *J. Phys. Chem.* **1994**, *98*, 6098. Rao, S. V. *J. Comput. Chem.* **2000**, *21*, 1283. Ponec, R. *Int. J. Quantum Chem.* **1997**, *62*, 171.
(204) Ponec, R. *Collect. Czech. Chem. Commun.* **1997**, *62*, 1821.
(205) Poater, J.; Solà, M.; Duran, M.; Fradera, X. *J. Phys. Chem. A* **2001**, *105*, 2052. Poater, J.; Solà, M.; Duran, M.; Fradera, X. *J. Phys. Chem. A* **2002**, *106*, 4794 (erratum).
(206) Poater, J.; Solà, M.; Duran, M.; Fradera, X. *J. Phys. Chem. A* **2001**, *105*, 6249.
(207) Poater, J.; Solà, M.; Duran, M.; Robles, J.; Fradera, X. In *Reviews of Modern Quantum Chemistry. A Celebration of the Contributions of Robert G. Parr*; Sen, K. D., Ed.; World Scientific: Singapore, 2002.
(208) Fradera, X.; Solà, M. *J. Comput. Chem.* **2004**, *25*, 439.
(209) Parr, R. G.; Yang, W. *Density-Functional Theory of Atoms and Molecules*; Oxford Univesity Press: New York, 1989.
(210) Silvi, B.; Gatti, C. *J. Phys. Chem. A* **2000**, *104*, 947.
(211) Savin, A.; Silvi, B.; Colonna, F. *Can. J. Chem.* **1996**, *74*, 1088.
(212) Calatayud, M.; Andrés, J. L.; Beltrán, A.; Silvi, B. *Theor. Chem. Acc.* **2001**, *105*, 299.
(213) Silvi, B.; Kryachko, E. S.; Tishchenko, O.; Fuster, F.; Nguyen, M. T. *Mol. Phys.* **2002**, *100*, 1659.
(214) Lepetit, C.; Silvi, B.; Chauvin, R. *J. Phys. Chem. A* **2003**, *107*, 464.
(215) Lepetit, C.; Peyrou, V.; Chauvin, R. *Phys. Chem. Chem. Phys.* **2004**, *6*, 303.
(216) Llusar, R.; Beltrán, A.; Noury, S.; Silvi, B. *J. Comput. Chem.* **1999**, *20*, 1517.
(217) Shaik, S. S.; Maitre, P.; Sini, G.; Hiberty, P. C. *J. Am. Chem. Soc.* **1992**, *114*, 7861.
(218) Beltrán, A.; Andrés, J.; Noury, S.; Silvi, B. *J. Phys. Chem. A* **1999**, *103*, 3078.
(219) Kruszewski, J.; Krygowski, T. M. *Tetrahedron Lett.* **1972**, *13*, 3839. Krygowski, T. M. *J. Chem. Inf. Comput. Sci.* **1993**, *33*, 70.
(220) Schleyer, P. v. R.; Maerker, C.; Dransfeld, A.; Jiao, H.; van Eikema Hommes, N. J. R. *J. Am. Chem. Soc.* **1996**, *118*, 6317.
(221) Fradera, X.; Poater, J.; Duran, M.; Solà, M. Unpublished results, 2001.
(222) Howard, S. T.; Krygowski, T. M. *Can. J. Chem.* **1997**, *75*, 1174.
(223) Schleyer, P. v. R.; Jiao, H. *Pure Appl. Chem.* **1996**, *68*, 209.
(224) Molina Molina, J.; El-Bergmi, R.; Dobado, J. A.; Portal, D. *J. Org. Chem.* **2000**, *65*, 8574.
(225) Poater, J.; Fradera, X.; Duran, M.; Solà, M. *Chem. Eur. J.* **2003**, *9*, 400.
(226) Poater, J.; Fradera, X.; Duran, M.; Solà, M. In *Fullerenes: The Exciting World of Nanocages and Nanotubes*; Kamat, P. V., Kadish, K. M., Guldi, D., Eds.; The Electrochemical Society: Pennington, NJ, 2002; Vol. 12.
(227) Van Lier, G.; Fowler, P.; De Proft, F.; Geerlings, P. *J. Phys. Chem. A* **2002**, *106*, 5128.
(228) Steiner, E.; Fowler, P. W. *Int. J. Quantum Chem.* **1996**, *60*, 609. Steiner, E.; Fowler, P. W.; Havenith, R. W. A. *J. Phys. Chem. A* **2002**, *106*, 7048.
(229) Poater, J.; Solà, M.; Viglione, R. G.; Zanasi, R. *J. Org. Chem.* **2004**, *69*, 7537.
(230) van Wüllen, C.; Kutzelnigg, W. *Chem. Phys. Lett.* **1993**, *205*, 563. Kutzelnigg, W.; Van Wüllen, C.; Fleischer, U.; Franke, R.; Von Mourik, T. In *Nuclear Magnetic Shieldings and Molecular Structure*; Tossell, J. A., Ed.; Kluwer Academic Publisher: Dordrecht, The Netherlands, 1993; Vol. 386.
(231) Cyrañski, M. K.; Krygowski, T. M.; Katritzky, A. R.; Schleyer, P. v. R. *J. Org. Chem.* **2002**, *67*, 1333.
(232) Katritzky, A. R.; Jug, K.; Oniciu, D. C. *Chem. Rev.* **2001**, *101*, 1421. Katritzky, A. R.; Karelson, M.; Sild, S.; Krygowski, T. M.; Jug, K. *J. Org. Chem.* **1998**, *63*, 5228.
(233) Luaña, V.; Martín Pendás, A.; Costales, A.; Carriedo, G. A.; García-Alonso, F. J. *J. Phys. Chem. A* **2001**, *105*, 5280.
(234) Matta, C. F.; Hernández-Trujillo, J. *J. Phys. Chem. A* **2003**, *107*, 7496.
(235) Williams, R. V. *Chem. Rev.* **2001**, *101*, 1185.
(236) Cremer, D.; Kraka, E.; Slee, T. S.; Bader, R. F. W.; Lau, C. D. H.; Nguyendang, T. T.; MacDougall, P. J. *J. Am. Chem. Soc.* **1983**, *105*, 5069.
(237) Werstiuk, N. H.; Wang, Y.-G. *J. Phys. Chem. A* **2003**, *107*, 9434.
(238) Winstein, S. *J. Am. Chem. Soc.* **1959**, *81*, 6524.
(239) Winstein, S. *Q. Rev., Chem. Soc.* **1969**, *23*, 141. Warner, P. M. In *Topics in Nonbenzenoid Aromatic Chemistry*; Nozoe, T., Breslow, R., Hafner, K., Ito, S., Murata, I., Eds.; Hirokawa: Tokyo, Japan, 1976; Vol. 2. Paquette, L. A. *Angew. Chem., Int. Ed. Engl.* **1978**, *17*, 106.
(240) Jorgensen, W. L. *J. Am. Chem. Soc.* **1975**, *97*, 3082.
(241) El-Bergmi, R.; Dobado, J. A.; Portal, D.; Molina Molina, J. *J. Comput. Chem.* **2000**, *21*, 322.
(242) Bremer, M.; Schötz, K.; Schleyer, P. v. R.; Fleischer, U.; Schindler, M.; Kutzelnigg, W.; Koch, W.; Pulay, P. *Angew. Chem., Int. Ed. Engl.* **1989**, *28*, 1042. Schulman, J. M.; Disch, R. L.; Schleyer, P. v. R.; Buhl, M.; Bremer, M.; Koch, W. *J. Am. Chem. Soc.* **1992**, *114*, 7897. Goldstein, M. J.; Hoffmann, R. *J. Am. Chem. Soc.* **1971**, *93*, 6193.
(243) Scott, L. T.; Siegel, J. S. *Tetrahedron* **2001**, *57*, ix.
(244) Haddon, R. C.; Schneemeyer, L. F.; Waszczak, J. V.; Glarum, S. H.; Tycko, R.; Dabbagh, G.; Kortan, A. R.; Muller, A. J.; Mujse, A. M.; Rosseinsky, M. J.; Zahurak, S. M.; Makhija, A. V.; Thiel, F. A.; Raghavachari, K.; Cockayne, E.; Elser, V. *Nature* **1991**, *350*, 46. Krygowski, T. M.; Ciesielski, A. *J. Chem. Inf. Comput. Sci.* **1995**, *35*, 1001.
(245) Haddon, R. C. *Science* **1993**, *261*, 1545. Fowler, P. *Nature* **1991**, *350*, 20.
(246) Poater, J.; Fradera, X.; Duran, M.; Solà, M. *Chem. Eur. J.* **2003**, *9*, 1113.
(247) Melchor Ferrer, S.; Molina Molina, J. *J. Comput. Chem.* **1999**, *20*, 1412.
(248) Taylor, R.; Hare, J. P.; Abdul-Sada, A. K.; Kroto, H. W. *J. Chem. Soc., Chem. Commun.* **1990**, 1423.
(249) Mestres, J.; Duran, M.; Solà, M. *J. Phys. Chem.* **1996**, *100*, 7449.
(250) Akasaka, T.; Mitsuhida, E.; Ando, W.; Kobayashi, K.; Nagase, S. *J. Am. Chem. Soc.* **1994**, *116*, 2627. Balch, A. L.; Lee, J. W.; Olmstead, M. M. *Angew. Chem., Int. Ed. Engl.* **1992**, *31*, 1356. Meier, M. S.; Wang, G. W.; Haddon, R. C.; Brock, C. P.; Lloyd, M. A.; Selegue, J. P. *J. Am. Chem. Soc.* **1998**, *120*, 2337. Bellavia-Lund, C.; Wudl, F. *J. Am. Chem. Soc.* **1997**, *119*, 9937. Thilgen, C.; Herrmann, A.; Diederich, F. *Angew. Chem., Int. Ed. Engl.* **1997**, *36*, 2269.
(251) Taylor, R.; Walton, D. R. M. *Nature* **1993**, *363*, 685.
(252) Poater, J.; Duran, M.; Solà, M. *Int. J. Quantum Chem.* **2004**, *98*, 361.
(253) Giambiagi, M.; de Giambiagi, M. S.; dos Santos Silva, C. D.; de Figueiredo, A. P. *Phys. Chem. Chem. Phys.* **2000**, *2*, 3381.
(254) Giambiagi, M.; de Giambiagi, M. S.; Grempel, D. R.; Heymann, D. *J. Chem. Phys.* **1975**, *72*, 15.
(255) Portella, G.; Poater, J.; Bofill, J. M.; Alemany, P.; Solà, M. *J. Org. Chem.* **2005**, *70*, 2509.
(256) Hammett, L. P. *Chem. Rev.* **1935**, *17*, 125.
(257) Krygowski, T. M.; Ejsmont, K.; Stepién, B. T.; Cyrañski, M. K.; Poater, J.; Solà, M. *J. Org. Chem.* **2004**, *69*, 6634.
(258) Poater, J.; García-Cruz, I.; Illas, F.; Solà, M. *Phys. Chem. Chem. Phys.* **2004**, *6*, 314.
(259) Cyrañski, M. K.; Gilski, M.; Jaskolski, M.; Krygowski, T. M. *J. Org. Chem.* **2003**, *68*, 8607. Box, V. G. S.; Jean-Mary, F. *J. Mol. Model.* **2001**, *7*, 334.
(260) Krygowski, T. M.; Zachara, J. E.; Szatylowicz, H. *J. Org. Chem.* **2004**, *69*, 7038. Krygowski, T. M.; Szatylowicz, H.; Zachara, J. E. *J. Chem. Inf. Comput. Sci.* **2004**, *44*, 2077.
(261) Havenith, R. W. A.; Jiao, H.; Jenneskens, L. W.; van Lenthe, J. H.; Sarobe, M.; Schleyer, P. v. R.; Kataoka, M.; Necula, A.; Scott, L. T. *J. Am. Chem. Soc.* **2002**, *124*, 2363. Havenith, R. W. A.; van Lenthe, J. H.; Dijkstra, F.; Jenneskens, L. W. *J. Phys. Chem. A* **2001**, *105*, 3838. Steiner, E.; Fowler, P. W.; Jenneskens, L. W.; Havenith, R. W. A. *Eur. J. Org. Chem.* **2002**, 163.
(262) Solà, M.; Mestres, J.; Duran, M. *J. Phys. Chem.* **1995**, *99*, 10752.
(263) Kraakman, P. A.; Valk, J. M.; Niederlander, H. A. G.; Brouwer, D. B. E.; Bickelhaupt, F. M.; Dewolf, W. H.; Bickelhaupt, F.; Stam, C. H. *J. Am. Chem. Soc.* **1990**, *112*, 6638. Bodwell, G. J.; Bridson, J. N.; Houghton, T. J.; Kennedy, J. W. J.; Mannion, M. R. *Angew. Chem., Int. Ed. Engl.* **1996**, *35*, 1320. Bodwell, G. J.; Bridson, J. N.; Houghton, T. J.; Kennedy, J. W. J.; Mannion, M. R. *Chem. Eur. J.* **1999**, *5*, 1823. Bodwell, G. J.; Bridson, J. N.; Cyrañski, M. K.; Kennedy, J. W. J.; Krygowski, T. M.; Mannion, M. R.; Miller, D. O. *J. Org. Chem.* **2003**, *68*, 2089.
(264) Jenneskens, L. W.; Vaneenige, E. N.; Louwen, J. N. *New J. Chem.* **1992**, *16*, 775. Grimme, S. *J. Am. Chem. Soc.* **1992**, *114*, 10542. Dijkstra, F.; van Lenthe, J. H. *Int. J. Quantum Chem.* **1999**, *74*, 213.

(265) Zhigalko, M. V.; Shishkin, O. V.; Gorb, L.; Leszczynski, J. *J. Mol. Struct. (THEOCHEM)* **2004**, *693*, 153.
(266) Lazzeretti, P.; Malagoni, M.; Zanasi, R. *Chem. Phys. Lett.* **1994**, *220*, 299. Fowler, P. W.; Steiner, E.; Cadioli, B.; Zanasi, R. *J. Phys. Chem. A* **1998**, *102*, 7297.
(267) Corminboeuf, C.; Heine, T.; Seifert, G.; Schleyer, P. V.; Weber, J. *Phys. Chem. Chem. Phys.* **2004**, *6*, 273.
(268) Steiner, E.; Fowler, P. W.; Jenneskens, L. W. *Angew. Chem., Int. Ed.* **2001**, *40*, 362.
(269) Schleyer, P. v. R.; Manoharan, M.; Jiao, H. J.; Stahl, F. *Org. Lett.* **2001**, *3*, 3643.
(270) Matito, E.; Duran, M.; Solà, M. *J. Chem. Phys.* **2005**, *122*, 014109.
(271) Katritzky, A. R.; Barczynski, P.; Musumarra, G.; Pisano, D.; Szafran, M. *J. Am. Chem. Soc.* **1989**, *111*, 7.
(272) Fuster, F.; Sevin, A.; Silvi, B. *J. Phys. Chem. A* **2000**, *104*, 852.
(273) Fuster, F.; Sevin, A.; Silvi, B. *J. Comput. Chem.* **2000**, *21*, 509.
(274) Chesnut, D. B.; Bartolotti, L. J. *Chem. Phys.* **2000**, *253*, 1.
(275) Santos, J. C.; Andrés, J.; Aizman, A.; Fuentealba, P. *J. Chem. Theor. Comput.* **2005**, *1*, 83.
(276) Hernandez-Trujillo, J.; García-Cruz, I.; Martínez-Magadán, J. M. *Chem. Phys.* **2005**, *308*, 181.
(277) Holleman, A. F. *Recl. Trav. Chim. Pays-Bas* **1906**, *24*, 140. Holleman, A. F. *Chem. Rev.* **1925**, *1*, 187. Holleman, A. F.; Wibaut, J. P. *Organic Chemistry, a Tranlation from the Sixteenth Deutch Edition*; Elsevier: Amsterdam, The Netherlands, 1951. Norman, R. O. C. *Electrophilic Substitution in Benzenoid Compounds*; Elsevier: Amstedam, The Netherlands, 1965.
(278) Coulson, C. A. *Valence*; Clarendon: Oxford, U.K., 1952. Streitwieser, A., Jr. *A Molecular Orbital Theory for Organic Chemists*; Wiley: New York, 1961. Salem, L. *The Molecular Orbital Theory of Conjugated Systems*; W. A. Benjamin: Reading, MA, 1966. Dewar, M. J. S. *Molecular Orbital Theory of Organic Chemistry*; McGraw-Hill: New York, 1968. Epiotis, N. D. *J. Am. Chem. Soc.* **1973**, *95*, 3188. Epiotis, N. D.; Cherry, W. *J. Am. Chem. Soc.* **1976**, *98*, 4361. Epiotis, N. D.; Cherry, W. *J. Am. Chem. Soc.* **1976**, *98*, 4365. Epiotis, N. D.; Cherry, W. *J. Am. Chem. Soc.* **1976**, *98*, 5432.
(279) Bader, R. F. W.; Chang, C. *J. Phys. Chem.* **1989**, *93*, 5095.
(280) Gadre, S. R.; Suresh, C. H. *J. Org. Chem.* **1997**, *62*, 2625. Suresh, C. H.; Gadre, S. R. *J. Am. Chem. Soc.* **1998**, *120*, 7049. Suresh, C. H.; Gadre, S. R. *J. Am. Chem. Soc.* **1998**, *120*, 10276. Suresh, C. H.; Gadre, S. R. *J. Org. Chem.* **1999**, *64*, 2505.
(281) Cubero, E.; Orozco, M.; Luque, F. J. *J. Phys. Chem. A* **1999**, *103*, 315.
(282) Guggenheim, E. A. *J. Chem. Phys.* **1945**, *13*, 253.
(283) Panek, J. J.; Jezierska, A.; Vracko, M. *J. Chem. Inf. Model.* **2005**, *45*, 264.
(284) Santos, J. C.; Tiznado, W.; Contreras, R.; Fuentealba, P. *J. Chem. Phys.* **2004**, *120*, 1670.
(285) Shaik, S. S.; Hiberty, P. C. *J. Am. Chem. Soc.* **1985**, *107*, 3089.
(286) Portella, G.; Poater, J.; Solà, M. *J. Phys. Org. Chem.* **2005**, *18*, 785.
(287) Clar, E. *The Aromatic Sextet*; Wiley: New York, 1972.
(288) Matito, E.; Poater, J.; Duran, M.; Solà, M. *J. Mol. Struct. (THEOCHEM)* **2005**, *727*, 165.
(289) Dewar, M. J. S.; Zoebisch, E. G.; Healy, E. F.; Stewart, J. J. P. *J. Am. Chem. Soc.* **1985**, *107*, 3902.
(290) Becke, A. D. *J. Chem. Phys.* **1993**, *98*, 5648.
(291) Lee, C.; Yang, W.; Parr, R. G. *Phys. Rev. B* **1988**, *37*, 785.
(292) Wang, Y.; Perdew, J. P. *Phys. Rev. B* **1991**, *44*, 13298.
(293) Wolinski, K.; Hilton, J. F.; Pulay, P. *J. Am. Chem. Soc.* **1990**, *112*, 8251.

CR030085X